LBNL-60152

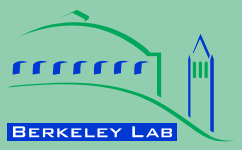

ERNEST ORLANDO LAWRENCE
BERKELEY NATIONAL LABORATORY

Analyzing the Effects of Temporal Wind Patterns on the Value of Wind-Generated Electricity at Different Sites in California and the Northwest

Matthias Fripp and Ryan Wiser

Environmental Energy Technologies Division

June 2006

The work described in this report was funded by the Office of Energy Efficiency and Renewable Energy (Wind & Hydropower Technologies Program) and by the Office of Electricity Delivery and Energy Reliability (Permitting, Siting and Analysis) of the U.S. Department of Energy under Contract No. DE-AC02-05CH11231.

Disclaimer

LBNL-60152

Analyzing the Effects of Temporal Wind Patterns on the Value of Wind-Generated Electricity at Different Sites in California and the Northwest

Prepared for the:

Wind & Hydropower Technologies Program
Office of Energy Efficiency and Renewable Energy
U.S. Department of Energy

and

Permitting, Siting and Analysis
Office of Electricity Delivery and Energy Reliability
U.S. Department of Energy

Principal Authors

Matthias Fripp and Ryan Wiser
Ernest Orlando Lawrence Berkeley National Laboratory
1 Cyclotron Road, MS 90R4000
Berkeley CA 94720-8136

June 2006

The work described in this report was funded by the Office of Energy Efficiency and Renewable Energy (Wind & Hydropower Technologies Program) and by the Office of Electricity Delivery and Energy Reliability (Permitting, Siting and Analysis) of the U.S. Department of Energy under Contract No. DE-AC02-05CH11231.

Acknowledgements

The work described in this report was funded by the Office of Energy Efficiency and Renewable Energy (Wind & Hydropower Technologies Program) and by the Office of Electricity Delivery and Energy Reliability (Permitting, Siting and Analysis) of the U.S. Department of Energy under Contract No. DE-AC02-05CH11231. The authors thank Jack Cadogan and the entire Wind & Hydropower Technologies Program team, as well as Larry Mansueti, for their support of this work. For reviewing drafts of this manuscript and/or providing critical data or insights that made this work possible, we also thank Michael Brower, Michael Milligan, Marc Schwartz, Dennis Elliott, Mark Bolinger, George N. Scott, Stel N. Walker, Heather Rhoads-Weaver, Donna Heimiller, Ray George, Dora Yen Nakafuji, Elliot Mainzer, Orville J. Blumhardt, Kristina E. Rohe, Jeff King, Joel Klein, Ron Nierenberg, Severin Borenstein, Case van Dam, and Kevin Jackson. Of course, any remaining errors or omissions are our own.

Table of Contents

List of Figures and Tables

Executive Summary

INTRODUCTION

Wind power production varies on a diurnal and seasonal basis. In this report, we use wind speed data modeled by TrueWind Solutions, LLC (now AWS Truewind) to assess the effects of wind timing on the value of electric power from potential wind farm locations in California and the Northwest. (Data from this dataset are referred to as "TrueWind data" throughout this report.) The intra-annual wind speed variations reported in the TrueWind datasets have not previously been used in published work, however, so we also compare them to a collection of anemometer wind speed measurements and to a limited set of actual wind farm production data.

The research reported in this paper seeks to answer three specific questions:

1) How large of an effect can the temporal variation of wind power have on the value of wind in different wind resource areas?
2) Which locations are affected most positively or negatively by the seasonal and diurnal timing of wind speeds?
3) How compatible are wind resources in the Northwest and California with wholesale power prices and loads in either region?

The latter question is motivated by the fact that wind power projects in the Northwest could sell their output into California (and vice versa), and that California has an aggressive renewable energy policy that may ultimately yield such imports.

Based on our research, we reach three key conclusions.

- **Temporal patterns have a moderate impact on the wholesale market value of wind power and a larger impact on the capacity factor during peak hours.** The best-timed wind power sites have a wholesale market value that is up to 4 percent higher than the average market price, while the worst-timed sites have a market value that is up to 11 percent below the average market price. The best-timed wind sites could produce as much as 30–40 percent more power during peak hours than they do on average during the year, while the worst timed sites may produce 30–60 percent less power during peak hours.
- **Northwestern markets appear to be well served by Northwestern wind and poorly served by California wind; results are less clear for California markets.** Both the modeled TrueWind data and the anemometer data indicate that many Northwestern wind sites are reasonably well-matched to the Northwest's historically winter-peaking wholesale electricity prices and loads, while most California sites are poorly matched to these prices and loads. However, the TrueWind data indicate that most California and Northwestern wind sites are poorly matched to California's summer-afternoon-peaking prices and loads, while the anemometer data suggest that many of these same sites are well matched to California's wholesale prices and loads.
- **TrueWind and anemometer data agree about wind speeds in most times and places, but disagree about California's summer afternoon wind speeds:** The TrueWind data indicate that wind speeds at sites in California's coastal mountains and some Northwestern locations

dip deeply during summer days and stay low through much of the afternoon. In contrast, the anemometer data indicate that winds at these sites begin to rise during the afternoon and are relatively strong when power is needed most. At other times and locations, the two datasets show good agreement. This disagreement may be due in part to time-varying wind shear between the anemometer heights (20-25m) and the TrueWind reference height (50m or 70m), but may also be due to modeling errors or data collection inconsistencies.

METHODS

We used three wind datasets to estimate the time-varying wind power available from California and Northwest wind sites:

1) **TrueWind:** TrueWind Solutions, LLC (now AWS Truewind) provided modeled wind speeds for every cell on a 200-meter grid in California and a 400-meter grid in the Northwest. Wind speeds were given for every month-hour combination in California and every season-hour in the Northwest.
2) **Anemometers:** We used hourly anemometer data from Kenetech, Inc. (167 sites), the Bonneville Power Administration (6 sites) and the DOE Candidate Site program (7 sites).
3) **Actual Wind Farm Production:** We used historical hourly power production data from the Altamont, Tehachapi and San Gorgonio areas in California and monthly power production data from several more sites in California and the Northwest.

We used the wind data with electricity load and wholesale electricity price series for California and the Northwest to estimate the effects of wind timing on the value of wind-generated electricity at locations throughout California and the Northwest. The effects of timing were measured by two approaches, yielding three key metrics for each location.

- **Capacity Metric:** We calculated the annual average capacity factor for a wind turbine at each location and then the capacity factor for that turbine during the top 10 percent of historical peak-load hours. The difference between these two capacity factors is a loose proxy for the effect of wind timing on the "capacity value" of a wind turbine at any location.
- **Price Metrics:** We estimated the annual wholesale market value of a flat block of power and the annual market value expected from the time-varying wind speeds found at each location (when correlated with time-varying wholesale market prices). The difference between these two values reflects the potential effects of temporal wind patterns on the wholesale market value of power from a wind turbine. These values were calculated using (1) historical wholesale power prices, and (2) forecast wholesale power prices.

Historical loads for California and the Northwest were based on FERC Form 714 filings by electric utilities for 2000–04. Historical wholesale prices for California were the average of the CalPX prices for the NP15 and SP15 hubs for 7/98–6/99, and historical prices for the Northwest were based on the Dow Jones hourly prices for the Mid-C hub for 5/02–4/05. Our forecast price series for California was the average of hourly forecasts for all California hubs for 2006–13, provided by the California Energy Commission. Our price forecast for the Northwest was the average of the Northwest Power and Conservation Council's base-case hourly forecasts for the Mid-C hub for the years 2006–2025.

For some of the analysis that follows, we grouped the anemometers in our dataset into separate "wind resource areas," about 40 km across, in order to estimate the local effects of wind timing in the areas that are most likely to receive wind power development. These areas are shown in Figures ES-1 and ES-2.

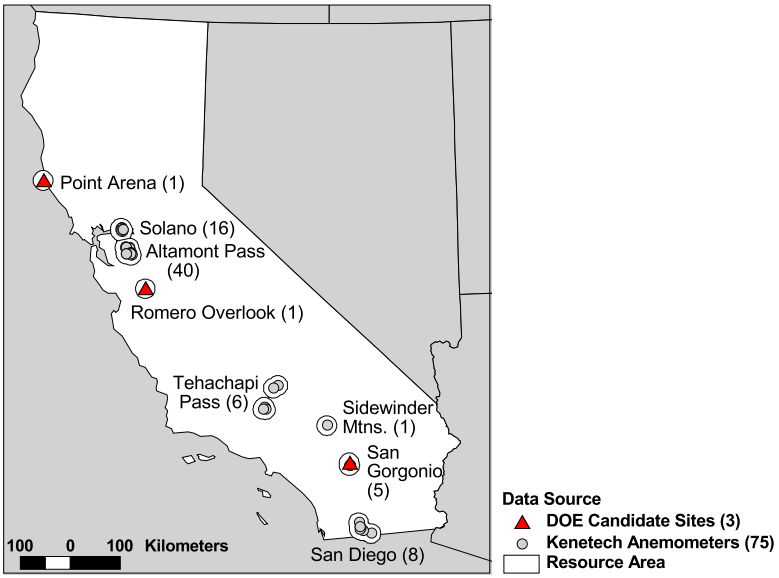

Figure ES-1. Locations of Anemometer Towers and Resource Areas in California

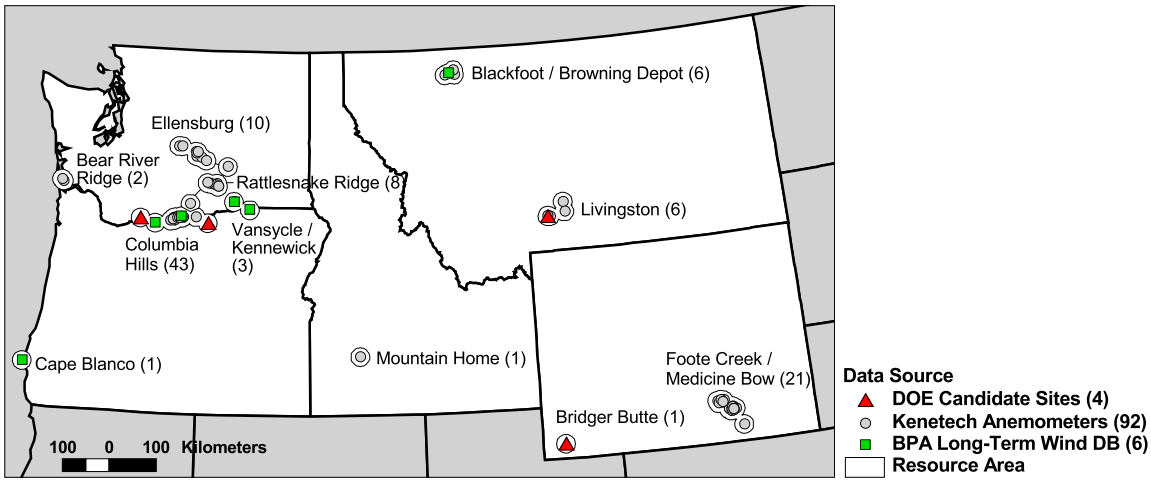

Figure ES-2. Locations of Anemometer Towers and Resource Areas in the Northwest

REGION-WIDE RESULTS FROM TRUEWIND DATA

We found that temporal wind patterns at different locations could have a large effect on the average power output during hours of peak electricity demand, and a smaller but not insignificant effect on the annual wholesale market value of wind power, based on historical and forecast wholesale-market electricity prices.

Figure ES-3 summarizes the findings from the TrueWind data for all grid cells in California and the Northwest with annual average winds equivalent to Class 4 or greater. The central bar of each marker in Figure ES-3 shows the median effect of wind timing on each measure of wind power, based on the TrueWind data. The lower and upper bars show the range of effects between the 10th and 90th percentile of wind sites in each region. It should be noted that these results include many locations that are inaccessible or otherwise unsuitable for wind farm development.

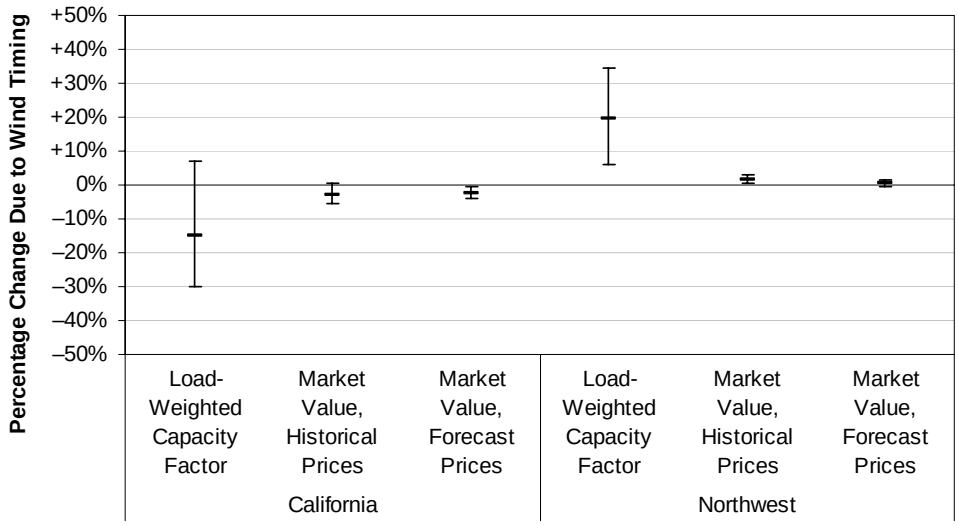

Figure ES-3. Effects of Wind Timing on Load-Weighted Capacity Factor and Annual Market Value at Class 4+ Grid Cells in California and the Northwest (Median, 10th and 90th Percentiles)

The TrueWind data indicate that the best- and worst-timed of the windy California grid cells have *peak-hour capacity factors* that range from 7 percent above to 30 percent below their annual average capacity factors (at the 10th and 90th percentiles), with a median of 15 percent below. Windy locations in the Northwest have peak-hour capacity factors ranging from 6 to 34 percent above their annual average capacity factors, with a median of 20 percent.

According to the TrueWind data, the best-timed California sites have a *wholesale market value* approximately equal to what would be obtained if their power output was completely uncorrelated with electricity demand, while the worst-timed sites would have a market value about 4–6 percent less than this, based on historical or forecast prices. The timing of wind at sites in the Northwest covers a somewhat more negative range than California when forecast prices are used, but yields a wholesale market value ranging from an amount equal to what the wind site would earn with uncorrelated power output, up to about 3 percent more than this, when historical prices are considered. When forecast prices are used, the value of power at Northwestern sites ranges from about 1 percent below to 2 percent above the value of a flat block of power.

Figure ES-4 shows the geographic distribution of the effect of wind timing at Class 4+ cells, according to the TrueWind dataset, when using California wind power with California's historical prices or Northwestern wind power with the Northwest's historical prices. Wind timing

appears to improve the value of power from California's northernmost coast, but reduces the value of power from high-wind locations elsewhere in the state. High-wind locations throughout the Northwest appear to be well-matched to Northwestern power markets.

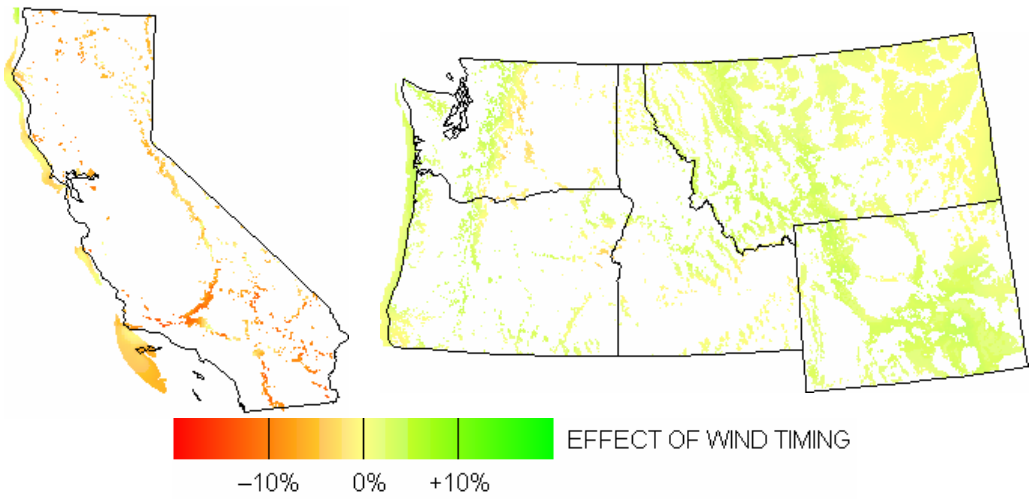

Figure ES-4. Percentage Change in Market Value of Power due to Temporal Wind Patterns at all Class 4+ Grid Cells in California and the Northwest, Based on Local Historical Power Prices

REGION-WIDE RESULTS FROM ANEMOMETER DATA

Figure ES-5 shows the range of each of the three wind value metrics, when using either anemometer measurements or TrueWind data for the cells matching each anemometer tower. Although these findings are not as comprehensive as those shown above, they allow us to compare the results from the TrueWind and anemometer data at similar locations. Anemometers in our dataset are generally concentrated in the most promising areas for wind development, so the results found at these locations may also be more representative of the effects of wind timing in the areas where wind farms are likely to be built.

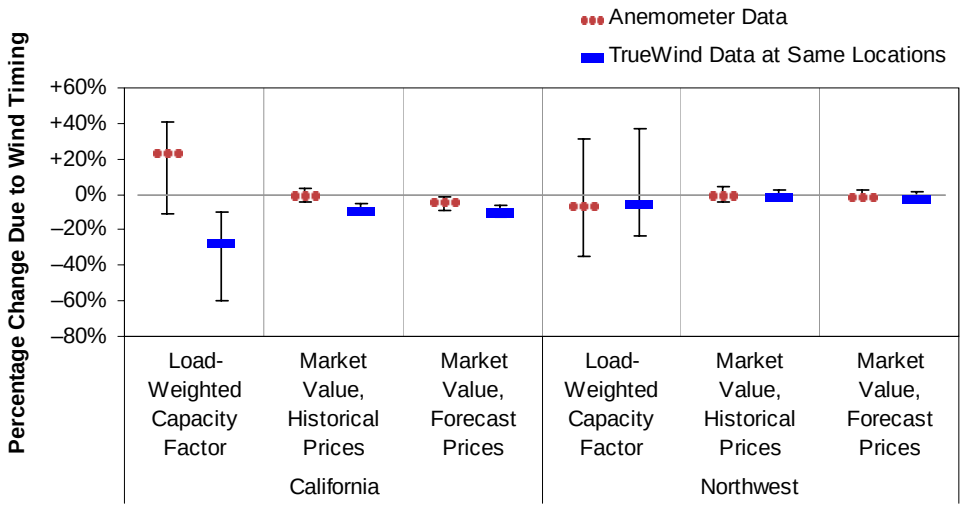

Figure ES-5. Comparison Between Wind-Value Measures Derived from Anemometer Measurements and Measures Derived from TrueWind Data for the Same Locations (Median and 10th–90th Percentile Range)

The TrueWind data suggest that wind timing generally reduces the value of power at California anemometer sites, while the anemometer data suggest that wind timing has a more neutral or positive effect at those same locations. This difference appears to be caused by disagreement about the diurnal timing of summer winds in some California wind resource areas, which is discussed further in the next section. Despite this disagreement, the two datasets generally agree on the size of the effect of wind timing (that is, the difference between the best and worst timed sites).

The two datasets are in better agreement in the Northwest. There, by either measure, wind resources at the anemometer sites appear to be about neutrally matched to historically winter-peaking electrical loads and historical and forecast wholesale market prices.

The TrueWind results for all California Class 4+ grid cells, shown in Figures ES-3 and ES-4, include summer-peaking coastal and mountain locations that make them more optimistic than the results at the anemometer locations used for Figure ES-5. Figure ES-3 also shows better results than Figure ES-5 for load-weighted capacity factors in the Northwest, probably because of the inclusion of winter-peaking mountain sites where anemometers have not been placed and wind resource development is unlikely.

TEMPORAL WIND PATTERNS FROM TRUEWIND, ANEMOMETER AND PRODUCTION DATA

Before we present the effects of wind timing in each of the resource areas defined earlier, we briefly compare the wind patterns reported by our three datasets for these areas. We find that there is generally good agreement between the TrueWind and anemometer data about the times of year when wind speeds peak in each resource area. The two datasets are also in reasonably good agreement about winter-time diurnal profiles in each resource area, which tend to be relatively flat. However, in some resource areas, the two datasets show significant disagreement about summertime diurnal wind profiles. These disagreements can in turn cause significant disagreement about the effect of wind timing on the value of power when summer-peaking load or price series are considered. We note three distinct types of disagreement about summer diurnal wind speed profiles:

1) In a number of resource areas, the TrueWind data show a deeper, longer dip in summer daytime wind speeds than the anemometer data, reducing the amount of power available on summer afternoons (Figure ES-6a). We observe this type of disagreement in two of the eleven Northwestern resource areas (Ellensburg and Rattlesnake Ridge), and four of the eight California resource areas (Solano, Altamont Pass, Romero Overlook and San Gorgonio).
2) In several resource areas, the TrueWind data show summer winds rising steadily from early afternoon until they peak at midnight, while the anemometer data show winds rising from late morning and peaking around 6 pm (Figure ES-6b). This type of disagreement also causes the TrueWind data to report that less power is available to meet summer-afternoon-peaking electricity loads. We noted this effect in the Ellensburg and Rattlesnake Ridge areas in Washington, and in the Tehachapi, Sidewinder and San Diego areas in California.
3) In the Blackfoot and Livingston areas in Montana and the Mountain Home area in Idaho, the weak summertime diurnal profiles from TrueWind and the anemometers are nearly reversed

(Figure ES-6c). In these areas, anemometers show morning lulls and afternoon peaks, while the TrueWind data show morning peaks and afternoon lulls, again reducing the amount of wind power available on summer afternoons.

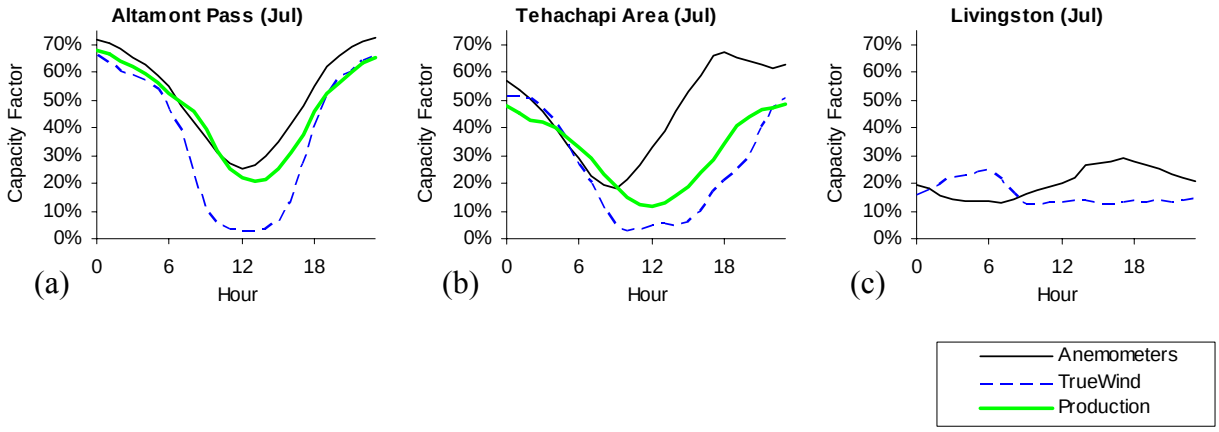

Figure ES-6. Diurnal Average Capacity Factor for Three Resource Areas from Anemometers and TrueWind Data at the Same Grid Cell, and Production Turbines in the Same Region

The historical production data from operating wind projects in the Tehachapi and San Gorgonio areas appear to agree more with the TrueWind data, while the historical production data for Altamont Pass more closely resemble the anemometer data. However, these comparisons are of limited value in resolving the disagreement between the TrueWind and anemometer data, because the wind turbines in these locations are mounted at relatively low tower heights.

Some of the difference in temporal wind speed patterns between the anemometers and TrueWind data may be due to temporal variations in wind shear which result from surface heating or strong near-surface flows on summer days. These processes could increase power production at lower levels during the day and reduce it at night, relative to the upper-level winds. The height of the turbines at wind farms in California is often between the anemometer heights (20-30 m) and the TrueWind reference height (50 m in the Northwest and 70 m in California), so the intermediate estimates of the effects of wind timing from the wind farm production data are consistent with this hypothesis. However, much of the difference could also be due to errors in the anemometer or TrueWind datasets. More anemometer or production data from tall towers are needed before we can judge whether the TrueWind data provide an accurate picture of the effects of wind timing on the value of power at most wind resource sites.

EFFECTS OF WIND TIMING IN EACH RESOURCE AREA

In the body of the report, we show the effects of wind timing using historical electricity loads and historical and forecast wholesale market prices for both California and the Northwest, for each of the specified wind resource areas. For brevity, here we discuss only the results found using historical wholesale prices for California and the Northwest. California's historical wholesale prices peak on summer afternoons, and our results using this series are similar to those found using California's historical loads or forecast prices, which also peak on summer afternoons. Variations in load-weighted capacity factor are about seven times greater than

variations in market value, but the relative standing of different resource areas remains the same. The Northwest's historical wholesale prices generally peak on winter mornings and evenings, and this data series yields similar results to those found using the Northwest's historical electricity loads or forecast electricity prices.

Figure ES-7 shows the effects of wind timing on the value of wind power from each of the resource areas where anemometers were placed, when considering historical California wholesale power prices. The red and blue markers indicate the median effects among all anemometer locations in each resource area, as calculated using either anemometer data or TrueWind data at the same sites. For the Altamont, Tehachapi and San Gorgonio resource areas, we also show the effects calculated using the total output from all wind farms in each region. California's historical wholesale power prices peak strongly on summer afternoons. Consequently, the TrueWind and anemometer data show significant disagreement about the effects of wind timing in the same places where they disagree about summer afternoon wind speeds, particularly in California's major existing wind resource areas. Where available, the actual historical power production data yield results that are intermediate between those found using the other two datasets.

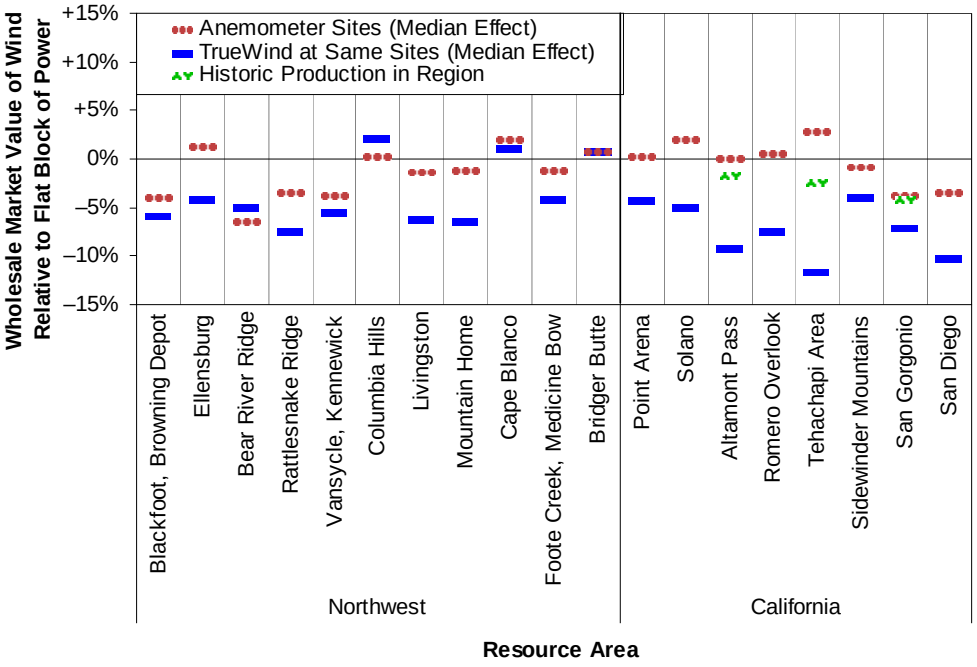

Figure ES-7. Median Effects of Timing on Market Value at Anemometer Sites in Each Resource Area, Based on Historical California Prices

According to the anemometer data shown in Figure ES-7, about a third of the Northwestern resource areas and half of the California resource areas are positively matched to California's summer-afternoon-peaking historical prices. However, TrueWind data at the same locations suggests that only a quarter of the Northwestern resource areas and no California areas are positively matched to California's historical prices. If both the anemometer and TrueWind data are correct, and the differences are due to their different elevations, then it is possible that the

timing of power production will worsen as new wind farms use taller towers, offsetting some of the gains due to improved capacity factors.

Figure ES-8 shows the effects of temporal wind patterns on the value of wind power from each resource area, using the Northwest's winter-peaking historical wholesale prices. Values calculated using this price series are much less sensitive to summer daytime wind speeds, so there is good agreement between the anemometer and TrueWind datasets. Seven or eight out of eleven Northwestern resource areas appear to be at least somewhat positively matched to historical Northwestern wholesale prices, while only 1–3 of the eight California sites show a weak positive match.

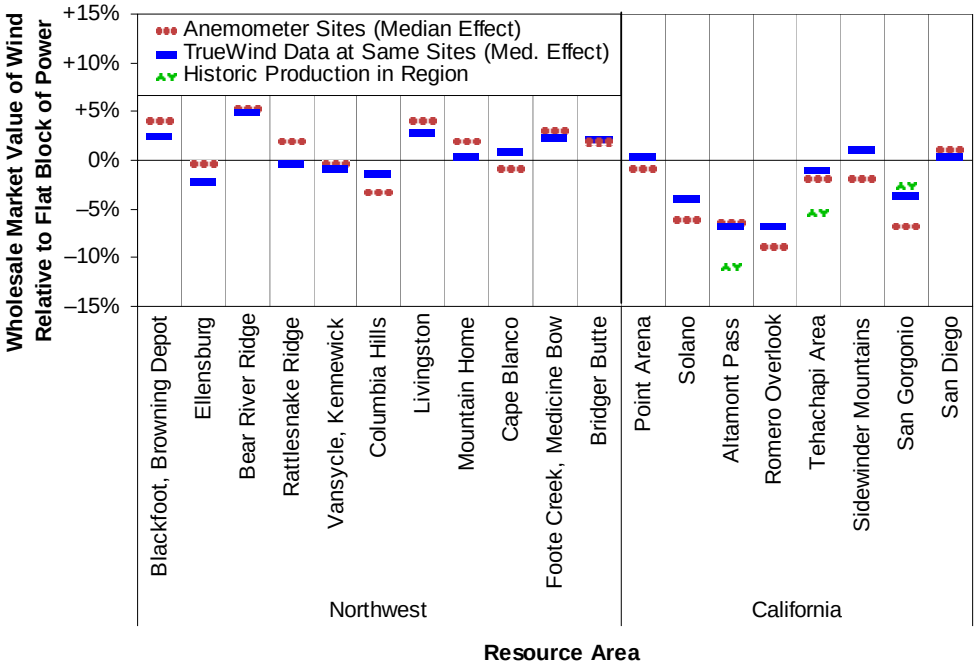

Figure ES-8. Median Effects of Timing on Market Value at Anemometer Sites in Each Resource Area, Based on Historical Northwestern Prices

DATA LIMITATIONS

Several factors may reduce the accuracy of our estimates of turbine-height wind speeds from the TrueWind, anemometer and production datasets. These factors could reduce the quality of fit between the datasets, and make it difficult to say which dataset gives a more accurate picture of hub-height wind patterns.

- **Modeling Uncertainty.** The TrueWind wind-speed estimates and diurnal profiles are based on a computerized atmospheric model, which is subject to uncertainty due to limitations in its resolution and the number of atmospheric processes it can incorporate.
- **Wind Shear.** We estimated wind speeds at a 70 m hub height from anemometer measurements taken at lower elevations by way of a relatively simple power law relationship, with fixed exponents of 0.09 during the day and 0.20 at night at all locations. This

approximation neglects the fact that wind shear can change with time of year and terrain. We also applied no correction to the available wind farm production data, which came from a variety of heights.

- **Limitations of Historical Data.** TrueWind estimated wind speeds by sampling from a 15-year period to estimate long-term average wind speed and wind power at each grid cell. However, our anemometer and wind farm production data come from specific historical periods, and cover differing lengths of time at each site, so they may not reflect the same meteorological conditions as the TrueWind dataset. This concern is reduced by the fact that we use only month-hour or season-hour averages of wind data for our analysis.
- **Anemometer Location.** The locations reported for anemometers in our dataset may be incorrect by a few kilometers in some cases, causing them to be compared to the wrong TrueWind grid cell.
- **Effective Ground Level Differences.** The wind speeds reported by TrueWind were given at heights of 50 or 70 meters above "effective ground level." In dense forest, this is relative to the canopy height, which may be a significant distance above the true ground level. We did not correct these effective heights to true heights before comparing them to observations.

1 Introduction

Improved modeling capabilities have led in recent years to a dramatic increase in planners' ability to estimate wind power production at locations throughout the United States (Nielsen *et al.* 2002). A significant use of this new capability has been to produce high-resolution maps showing the annual average power density of wind, or web-enabled databases that allow users to look up localized estimates of average wind speeds (see, *e.g.,* Brower 2002a; Brower 2002b; TrueWind 2002). These reporting methods are useful for identifying areas with the greatest average potential for wind power production during the year. However, they neglect the timing of when wind is most likely to blow at each location, during the day and year, a factor that may affect the attractiveness of a site for wind power development.

In this report, we make new use of modeled estimates of the time variation of wind speeds at locations throughout California and the Northwest, to investigate the possible effects of temporal wind patterns on the value of wind power in each of these regions. We report our results both in terms of the amount of energy that might be supplied from each site during the top 10 percent of load hours, and in terms of the effects of wind timing on the potential market value of wind-generated electricity due to wholesale market prices that fluctuate by hour and month.

We seek to answer three specific questions:

1) How large of an effect can the temporal variation of wind power have on the value of wind in different wind resource areas?
2) Which locations are affected most positively or negatively by the seasonal and diurnal timing of wind speeds?
3) How compatible are wind resources in the Northwest and California with wholesale power prices and loads in either region?

Much of our analysis was conducted using temporal wind speeds modeled by TrueWind Solutions, LLC (now AWS Truewind) for California and the Northwestern United States. (This company and the data they supplied are referred to simply as "TrueWind" or "the TrueWind data" throughout this report.) TrueWind's modeled wind speeds have usually been reported and used on an annual average basis, but TrueWind also produces monthly or seasonal diurnal wind profiles. Ours is the first attempt to use these more detailed temporal wind speed estimates in public domain research.

Relevant and publicly available anemometer wind speed measurements currently cover only a limited geographical area and time range. The model results from TrueWind allow us to analyze wind resources across the complete map of large regions of the United States. They also reflect meteorological conditions sampled from a fifteen year period, which could make them more suitable than short-term hour-by-hour wind speed observations for estimating the expected wind speed for each hour of a "typical" year. However, the main use of the TrueWind data to-date has been to map annual average wind speeds, and the only validation of the TrueWind estimates that we are aware of has been on this time scale.

Because TrueWind's temporal wind speed estimates have not previously been validated, and their reliability is uncertain, we also used a large database of public domain anemometer data to test the suitability of the TrueWind data for this research. In addition, we compared the TrueWind and anemometer datasets to a much smaller database of actual wind power production. We found some agreement between these three datasets on the temporal and spatial variation of wind speeds, and on the size of the effects of timing on the value of wind power. This provided us some confidence in using the larger TrueWind dataset for our analysis. As discussed in Sections 4 and 5 and Appendix A, however, we were unable to resolve some (significant) differences between these datasets, and more work will be necessary to understand the reliability of the TrueWind temporal data.

The rest of this report is organized as follows:

- **Section 2** highlights the wind speed and electricity load and price data used for our analysis, as well as our techniques for estimating electricity output based on wind speeds for each site, month and hour. We also describe the limitations of our data series, especially the TrueWind modeled wind speeds and the anemometer-based observational wind speeds.
- **Section 3** describes our methods for analyzing the effects of wind timing on the value of power from different locations, and presents the results of this work in detail, relying entirely on the TrueWind modeled wind speed dataset. We show the effects of temporal wind patterns on wind project capacity factors in the top 10 percent of load hours, and on the wholesale market value of wind-generated electricity, using load and wholesale price data from California and the Northwest. Our analysis includes sites in all wind power classes and at all locations across California and the Northwest.
- **Section 4** compares the findings from the TrueWind dataset with similar analyses performed using anemometers from California and the Northwest and hourly power production from wind farms in California. This analysis includes data from 78 anemometers in California, and 102 anemometers in the Northwest, as well as average power output from wind farms in the Altamont, Tehachapi and San Gorgonio areas.
- **Section 5** divides the variability of wind power output into seasonal and diurnal components, in order to assess the effects of each type of variation on the value of wind power. We also compare the monthly and diurnal data from the TrueWind, anemometer and actual wind power production datasets, in order to better understand the disagreements among them.
- **Section 6** concludes the body of the report, and summarizes our key findings about the effects of temporal patterns on the value of wind power, as well as our preliminary efforts to validate the use of TrueWind data for this type of work.

Finally, **Appendix A** describes in more detail our work to compare the temporal wind speed patterns recorded in the TrueWind data with measurements from anemometers. Unlike the work in Section 4, the appendix focuses on a comparison of wind speeds at each anemometer site, rather than comparing the results of the wind-value analysis.

2 Data Series Used for this Analysis

In this section we discuss the data series we used for our analysis, and the calculations and assumptions we used to develop estimates of time-varying wind power production throughout California and the Northwest. We begin by discussing the time-scale and averaging process used for the data in our analysis (Section 2.1). We then describe the three wind speed datasets used in the later analysis: TrueWind wind speed estimates, observed anemometer measurements, and actual wind power project output (Section 2.2). We next describe our treatment of wind shear, which can have a significant effect on estimates of the time variation of wind speeds at anemometer height (Section 2.3). Section 2.4 discusses the system we used for clustering anemometer and TrueWind data into geographically distinct resource areas. In Section 2.5, we summarize the limitations to each of the datasets we used, and the difficulties encountered in comparing the datasets. We then summarize our methods for translating wind speeds to wind power output (Section 2.6). Finally, we identify the sources for the electricity load and price data series used for the Northwest and California (Section 2.7).

2.1 Averaging of Wind Speeds and Electricity Data

We performed all of our analysis using wind speeds and electricity data that were averaged for each combination of month and hour or season and hour. We generally refer to these combinations – *e.g.,* 6 p.m. in June, or 8 p.m. in summer – as "intervals" throughout this report, although they do not actually represent contiguous periods of time. We averaged data over these periods, rather than using 8760 separate hours of the year, for two main reasons:

- TrueWind provided diurnal profiles that were averaged over months or seasons, because they believe that reporting modeled wind data at any finer temporal resolution would be scientifically unjustified. Given that the TrueWind data are reported on a season-hour or month-hour basis, there was no precision to be gained by comparing that data to a series of prices, loads, or observed wind speeds with a finer temporal resolution.
- In most cases, insufficient historical or forecast data were available to make estimates of the "typical" wind speed, electricity load, or price in each of the 8760 hours of the year. We nonetheless believe that using averages for each month-hour or season-hour interval allows us to capture much of the important seasonal and diurnal variation in wind speeds and electricity demand.

The averaged values for wind power production and electricity price and load represent the expected value of each of these variables for each interval. We then combined these values to produce expected values for market value or load-weighted capacity factor at each site. Averages combined in this way will produce the same results as an hour-by-hour combination of the same variables if and only if the variables are not actually correlated on a finer time scale than that at which the averages were taken. Thus, in using month-hour or season-hour averages, we are implicitly assuming that wind speeds and electricity demand and prices are not substantially

correlated on an hour-by-hour basis, beyond the correlation captured by their month-hour or season-hour averages.[1]

We performed our wind speed comparisons between the TrueWind and anemometer data (Appendix A) on a month-hour basis for California and a season-hour basis for the Northwest. However, when comparing the annual values for wind power at each grid cell (Sections 3.2 and 3.3), we replicated the season-hour wind speeds from the Northwestern TrueWind data onto a month-hour basis, in order to make our calculations more consistent between California and the Northwest, and so that we could incorporate the small month-to-month variations in air density into the Northwestern electrical power calculations (Section 2.6).

2.2 Wind Speed Data Sets

2.2.1 TrueWind Modeled Wind Speeds

The main wind speed datasets that we used for this project were produced by TrueWind Solutions, LLC (now AWS Truewind) for the California Energy Commission and a group of sponsors in the Northwest (Brower 2002a; Brower 2002b). (This company and the data they supplied are referred to simply as "TrueWind" or "the TrueWind data" throughout this report.) TrueWind uses a mesoscale atmospheric model to simulate wind conditions on a 2-3 km grid for 366 days selected randomly from 15 years of weather data. They then feed this mesoscale data into a basic wind flow model which estimates wind speeds on a 200-400 m grid, based on detailed land cover and terrain data. This combination provides finer spatial resolution than most other wind models. Most or all previous applications of the TrueWind model data have used the annual or seasonal average wind speed for each grid cell. We believe ours is the first published work to use wind speeds on a finer temporal scale from the TrueWind model.

2.2.1.1 California

For California, TrueWind produced several data series that were useful for our research. Each of these series contains one data point for each cell on a grid across the state. These grids are on two spatial scales: one contains cells exactly 200 meters apart north-south and east-west on a Universal Transverse Mercator (UTM) projection; the other uses a polar projection and has cells about 8 km apart. We used the following TrueWind data for California:

- annual average wind speeds (70 m elevation, 200 m grid);
- shape factor for Weibull distribution of wind speeds for each season (50 m elevation, 200 m grid);
- cell elevation (200 m grid); and
- average wind speed for each month-hour combination, *e.g.,* the average speed for 4-5 pm in June (70 m elevation, 8 km grid).

[1] This assumption may be invalid; for example, there is some evidence that the calmest days in summer are also the ones with the greatest air conditioning demand in California (Jackson 2002). However, without several years of simultaneous hourly wind and electricity data, we were unable to test this assumption.

Using these data, we calculated month-hour wind speeds for each cell on the 200 m grid as follows. First, for each cell on the 8 km grid, we converted the average month-hour wind speeds into weighting factors by dividing them by the average of the full year's worth of month-hour wind speeds for that cell. This produced a set of diurnal weights for each 8 km cell with an average of one for all month-hour combinations. For each cell on the 200 m grid, we then selected the nearest 8 km cell and multiplied the annual average wind speed for the 200 m cell by the month-hour weights for the 8 km cell. This produced a month-hour average wind speed series for each cell on the 200 m grid.[2]

2.2.1.2 Northwest

TrueWind also prepared data for the Northwest on grids with two different spatial scales: a 400 m grid and a 10 km grid. Both of these grids are evenly spaced on a UTM projection, and they extend across all of Washington, Oregon, Idaho, Montana and Wyoming. We used the following TrueWind data series for the Northwest:

- average wind speeds for each season (50 m elevation, 400 m grid);
- shape factor for Weibull distribution of wind speeds for each season (50 m elevation, 400 m grid);
- cell elevation (400 m grid); and
- weights for the wind speed for each hour of the day in each season, indexed against the seasonal average, *e.g.,* the ratio between the wind speed at 4-5 pm in summer and the average wind speed for all hours of the day in the summer (50 m elevation, 10 km grid).

We calculated season-hour wind speeds for each cell on the 400 m grid as follows. We multiplied the average wind speed for each season for each cell on the 400 m grid by the season-hour weights for the same season for the nearest 10 km cell to obtain the average wind speed at 50 m elevation for each season-hour combination for that 400 m cell. We then used a power law relationship to estimate the corresponding wind speed at 70 m elevation. This calculation used an exponent of 0.09 during the day and 0.20 at night, as discussed in Section 2.3.

2.2.1.3 Land Use Restrictions

Many of the areas covered by the TrueWind datasets – such as mountain ridges, national parks or other environmentally sensitive areas – cannot or should not be developed for wind power. However, in order to simplify our analysis and make the most complete possible estimate of the range of effects of wind timing, much of our analysis is based on data from all of these cells, or from simple subsets such as the windiest cells. This should be borne in mind when considering these broad-ranging assessments. In some cases, we have addressed land-use and environmental concerns by limiting our analysis to areas within 20 km of existing anemometer sites, as discussed in Sections 2.4 and 3.2.2.4.

[2] For example, TrueWind estimated an annual average wind speed of 6.54 m/s at the 200 m cell at (37.729º N, 121.648º W), and had a weighting factor of 0.891 for 3 pm (UTC) in January for the 8km cell closest to this location (about 2.25 km northwest), yielding a mean speed of 5.83 m/s for this 200 m cell during this interval.

2.2.1.4 Weibull Distribution Assumptions

To estimate the average wind power production for each month-hour or season-hour for each grid cell, we needed information about the shape of the probability distribution of wind speeds within each month- or season-hour. We began by assuming that the wind speeds in each month- or season-hour followed a Weibull distribution, with the same shape factor at 70 meter elevation as at 50 meter elevation, and with the same shape factor for all month-hours during each season (as these seasonal shape factors are reported by TrueWind). These were simplifying assumptions that reflected the paucity of data on fine time-scale variations in wind speeds.[3] As an alternative to this approach, we also calculated the single Weibull shape factor for all the month- or season-hours within each season that would be consistent with both the full-season shape factor and the variation in average wind speed among all the month- or season-hours, as reported by TrueWind.[4] We tested this approach using our anemometer database and found that it gave a significantly better estimate of the wind power production in each month- or season-hour than would other techniques, such as using the full-season shape factor for each month- or season-hour, or assuming a constant shape factor of 2 (a Rayleigh distribution). We therefore adopted this approach for the remainder of this report.

We did not formally validate the Weibull shape factors supplied by TrueWind. However, at one stage in our analysis, we calculated power output using the TrueWind month-hourly average wind speeds with two different estimates of the variability among the hours included in that month-hour, and compared the results. The first estimate of variability was the Weibull distribution described above. The second estimate was based directly on the anemometer data from the same location – i.e., instead of using a Weibull distribution for speeds during each month-hour, we used the set of measured hourly speeds for that month-hour, scaled to have the same average as the TrueWind estimate. In most cases, the second, "real" distribution of wind speeds yielded no substantial difference in power production from the Weibull distribution. However, in San Gorgonio, measured wind speeds were much steadier on summer nights than the TrueWind shape factors suggested. That is, wind speeds measured by anemometers held steady in the optimal range for a wind turbine, while the TrueWind Weibull distribution had about the same mean wind speed but included many more hours when the wind speed was above or below the optimal range for the turbine. Consequently, we found much higher power production during these times when we used the "real" variability of wind speeds instead of the TrueWind Weibull shape factor. This analysis suggests that our use of the TrueWind Weibull shape factors may introduce errors in our analysis on summer nights in San Gorgonio or similar

[3] These assumptions neglect the effect of diurnal variations in the wind regime, which could cause the Weibull shape factor to change with elevation and time. However, we did not have enough information to estimate these effects.

[4] The TrueWind dataset provided a single Weibull shape factor for each grid cell for each season, as well as average wind speeds for that grid cell for each month- or season-hour during that season. We assumed that wind speeds during each month- or season-hour within each season were also Weibull distributed, and that they all had the same shape factor (not necessarily equal to the full-season shape factor). We then calculated the unknown month-hour shape factor as the single shape factor that could be combined with the set of month- or season-hour average wind speeds and yield a full-season wind speed distribution consistent with the known seasonal shape factor. That is, we assumed that wind speeds followed a Weibull distribution within each month- or season-hour, and that the union of all month- or season-hour distributions must produce a full-season distribution with the same variance as the already known seasonal distribution. We then calculated the single month- or season-hour shape factor that would yield a full-season wind speed distribution with the appropriate variance.

areas where anemometers were not placed, but is not likely to contribute significant error at other locations and times.

2.2.2 Anemometer-Based Wind Speeds

The TrueWind data discussed above are geographically comprehensive and show a great deal of promise for analyzing wind performance across the full map of California and the Northwest. However, these datasets have not previously been validated for use in work like ours. Consequently we built a dataset of wind speeds measured via anemometers in order to double-check the results of the TrueWind data.

We collected hourly wind speed measurements from several publicly available sources. The data used for our validation analysis were originally collected by Kenetech, the Department of Energy Candidate Site program, and the Bonneville Power Administration.[5]

- **Kenetech**: The Kenetech wind company collected wind data at a large number of sites in the 1980s and 1990s, which entered the public domain after their bankruptcy. The National Renewable Energy Laboratory (NREL) is working to make these data available to the general public. Kenetech stored the observations in a proprietary, binary data format, and metadata for each site – such as tower height, location, and time zone – were recorded inconsistently or not at all. NREL is reading paper records and working with former Kenetech engineers to correct some of these problems. We obtained a preliminary dataset from NREL, and performed further processing on it to obtain better metadata.[6] For this

[5] We identified four other potential sources of anemometer-based wind data that we did not use for this project. The Energy Resources Research Laboratory has shorter-term wind speed data for a large number of sites in addition to the BPA Long Term Wind Data Base, but these data were not available during our research schedule. The California Energy Commission published wind resource reports for perhaps two dozen California locations in paper form in the 1980s. We have not identified a digital source for these data, but these reports could be collected and digitized for further analysis. The National Weather Service has collected long-term, hourly wind speed measurements at a number of locations, mostly at airports, while the California Department of Water Resources collects similar data in agricultural areas. These measurements are generally taken at a 10-meter elevation, so estimates of turbine-height wind speeds at these locations would be very sensitive to assumptions about wind shear; however, they could be useful for identifying seasonal wind patterns at a greater variety of locations.

[6] NREL has converted Kenetech's proprietary data format into more modern ASCII files. However, this work is not yet complete, and the site descriptions and time series data we received from NREL were not linked in a machine-readable manner. We found it easiest to build our database from Kenetech's binary files, even though this duplicated some of NREL's work. Data types and units (*e.g.,* wind speed, mph) for each data series were fairly clearly described in the Kenetech data files, but we had to parse individual site names and instrument heights for each data series from Kenetech's parameter description field (*e.g.,* "SITE 3 - 50 FT WIND SPEED"), since Kenetech had provided no dedicated field for these purposes. Kenetech made no digital record of site locations, so NREL staff have built a table of site locations based on paper records and consultations with Kenetech engineers. We supplemented this table by looking up locations of sites in California and the Northwest where NREL had not reported latitude or longitude coordinates, but had recorded geographical names or legal locations (township/range/section). If sites had no latitude or longitude data but had the same location name as other sites in the database, we assigned the average latitude and longitude of the other sites to the unlabeled sites. Where both legal coordinates and latitude and longitude were reported for the same site, we compared the two. We then corrected the latitudes and longitudes of several sites where there was a discrepancy greater than 10 km (NREL staff had also noted that the latitude was incorrect for these sites). Finally, we imported all the Kenetech and NREL data into a single database of site descriptions and wind time series, and removed values from the time series which did not match Kenetech's official error markers, but which were clearly invalid (mostly out-of-range values).

report, we used data from 75 Kenetech sites in California and 92 Kenetech sites in the Northwest. Kenetech collected 1-3 years of data for each of these sites, with most of the data recorded from 1991 to 1994. Instruments were placed at 5-40 m elevation above the ground in the Northwest, and 14-30 m elevation in California.

- **U.S. DOE:** The U.S. Department of Energy Candidate Site wind measurement program collected data from promising wind sites in 1977-82. We used data from this program for 3 sites in California and 4 sites in the Northwest. There are 2-6 years of data for each site, generally collected at an elevation of 45.7 m (150 ft).

- **BPA:** The Bonneville Power Administration has collected wind data for several sites in the Northwest continuously since the late-1970s and mid-1980s. We obtained their dataset, extending until the end of 2003, from the Energy Resources Research Laboratory at Oregon State University. We used data from 6 Northwest sites. Measurements in this dataset were taken at elevations ranging from 15 to 60 m.

For towers with multiple anemometers, we checked each calendar month when data was recorded, and chose the highest instrument that had at least 200 valid hourly observations in that month (generally, the highest anemometer installed on each tower met this criterion for every month it was installed). We then retrieved all the wind speed measurements from each of these gauges for each month. Almost all of these measurements were taken at a height below 70 m, the standard wind tower height used for this project. We therefore estimated the wind speed in each hour at 70 m height by using the power law relationship $v_{70}=v_h \bullet (70/h)^{\alpha}$, where h is the height of the instrument in meters, v_h is the wind speed measured by that instrument, v_{70} is the estimated wind speed at 70 m, and α is an exponent varying between 0.09 during the day and 0.20 at night (see Section 2.3). We did not use data from four anemometers in California for which no height was specified. Once we had assembled our wind observation dataset, we calculated the 70-m mean wind speed for each month-hour (California) or season-hour (Northwest) interval at each site.

We ignored any anemometer-based data series that failed to cover all 12 months of the year. However, we did not give any special treatment to observation series that covered a non-integer number of years: for example, site number 2 had observations from October 1992 to February 1994, so our final averages included data from two Decembers (1992 and 1993), but only one June (1993). We also did not renormalize the wind speeds to match long-term climatological patterns. Such an effort could substantially change the average capacity factor for each wind site, but would have only a secondary effect on the intra-annual timing effects we studied.

In total, there were 106 sites in California and 164 sites in the Northwest with at least one month of observations, but only 78 in California and 102 in the Northwest with data from all twelve months of the year.[7] The partial-year data series may contain useful additional information about

[7] The Kenetech dataset included information from several additional Northwestern anemometer towers which we did not use. Specifically, data series from ten towers in Medicine Bow, WY, were reported twice, and the anemometer at Diablo Dam, WA, had low average wind speeds and was sharply mismatched with the corresponding TrueWind cell.

regional wind patterns, but we were concerned that they would introduce a bias toward certain months and sites in our analysis, so we excluded these data from our analysis.

2.2.3 Wind Farm Production Data

Actual wind power production data, on an hourly basis, are rarely available publicly. Nonetheless, we were able to supplement the TrueWind and anemometer datasets with a limited amount of historical production data from several (larger) wind resource areas. Although these production data cannot be used to easily estimate prevailing wind speeds or the power production from any one single site, they nevertheless provide a useful benchmark for the performance of wind farms in several important regions.

We obtained monthly average power production values from a number of individual wind farms in California and the Northwest during 2001-2004, based on filings by wind farm operators with the Federal Energy Regulatory Commission and the Energy Information Administration (Bolinger 2005). We consolidated these values to estimate monthly average capacity factors for the Vansycle, Columbia Hills, Foote Creek, Bridger Butte and Solano resource areas. Table 1 shows the total rated capacity for wind farms in each of these areas.

Table 1. Rated Capacity of Wind Farms for which Monthly Production Data was Available

Wind Resource Area	Rated Capacity, 2004
Vansycle	430 MW
Columbia Hills	24 MW
Foote Creek	133 MW
Bridger Butte	144 MW
Solano	162 MW

We also obtained hourly average production data for 2002 for the Altamont, Tehachapi and San Gorgonio wind resource areas in California from the National Renewable Energy Laboratory (Milligan 2003). We did not receive information on the rated capacity of the wind farms that contributed to these outputs, so we estimated the total capacity by finding the maximum power output for each resource area during any hour of the year. These values are shown in Table 2. We then divided the hourly production in each area by the maximum production for the year to obtain hourly capacity factors and month-hour average capacity factors for each resource area.

Table 2. Maximum Power Output from each California Wind Resource Area

Wind Resource Area	Maximum Power Output, 2002
Altamont Pass	435 MW
San Gorgonio	306 MW
Tehachapi	569 MW

We assume implicitly in our analysis that variations in the capacity factor in each wind resource area were due entirely to variation in wind speeds in that area. It is possible that some of this variation was actually caused by equipment failure or maintenance, but we were unable to obtain

information on the size and duration of wind farm outages, making it impossible to account for this effect precisely. However, given that the wind resource areas generally contain hundreds of individual turbines, it appears likely that localized outages would "average out," rather than significantly biasing a region's total output during any period. Consequently, we believe it is reasonable to assume that the time-varying capacity factors in each resource area are driven primarily by variations in wind speed.

It deserves note that the data from California's three major wind resource areas are primarily based on older wind technology installed at heights that are far lower than typical hub-heights for wind projects today (and also much lower than TrueWind's wind speed estimates). Monthly output data from the Northwest and the Solano area, however, are based on present technology, and are therefore more comparable to TrueWind estimates.

2.3 Wind Shear

Much of the wind speed data available to us were reported for heights other than the 70-meter turbine level used for this report. This includes the Northwestern wind speeds from the TrueWind model, reported at 50 meters, and virtually all of the anemometer data. In order to compare these datasets to each other and to estimate the effect of wind timing at our reference hub height, it was necessary to adjust these data based on an estimate of the wind shear (change in wind speed) between the level of the original data and the 70-meter turbine height.

It is common practice to use a power law model to estimate wind speeds at one location based on measurements taken at a different elevation. This is an empirical approach, with no firm theoretical basis, but appears to fit the observed behavior in many cases (Gipe 2004: 39-45). The power law model assumes wind speeds at different heights are related by the equation,

$$v_h = v_{h_0}\left(\frac{h}{h_0}\right)^{\alpha},$$

where h is the turbine height, h_0 is a height for which the wind speed is known, v_h and v_{h0} are the wind speeds at these heights, and α is a "wind shear exponent," between 0 and 1, which is greater for sites with stronger wind shear.

A wind shear exponent of 1/7 is often used to conservatively adjust annual average wind speeds from lower level anemometers up to turbine height). This exponent often gives good results for neutrally stable air, or for long-term average wind speeds at a site (Gipe 2004: 39-45; Peterson and Hennessey 1978). However, the appropriate wind shear exponent varies significantly from day to night in many locations, as atmospheric conditions oscillate between stable and unstable states. During the day, solar heating of the ground warms the lower air levels, leading to turbulent mixing of the lower atmosphere. This mixing can transfer fast-moving air down from upper to lower levels, so that relatively consistent wind speeds are found from near the ground up to levels above wind turbine heights. In these unstable conditions, a lower wind shear exponent usually applies. At night, temperatures near the ground can drop, forming a temperature inversion which prevents vertical mixing. In these stable conditions, upper-level winds become decoupled from lower-level winds and a higher wind shear exponent applies

(Sisterson and Frenzen 1978). As a result of temporally varying wind shear, the timing of maximum and minimum winds aloft may differ markedly from the timing of wind at lower elevations (Archer and Jacobson 2003).

Wind shear in West Coast mountain passes may be especially low – or even negative – during summer days, due to the complex terrain which shapes the wind there. A layer of dense marine air builds up during the day west of these passes until it is high enough to pass through. Then a shallow flow is formed through the pass, which is accelerated by gravity as it moves down the eastern slope. As a result, winds near the ground may be faster than winds at higher levels (Brower 2005; Gipe 2004: 150-1).

In order to develop an appropriate wind-shear methodology for our analysis, we first reviewed a number of studies of wind shear under a variety of conditions. In most of these studies, we found power law exponents in the range of 0.07–0.13 during the day and 0.19–0.36 at night. Wind shear in these studies was usually fairly consistent during the day and night, with 3–4 hour transition periods beginning at dawn and a couple of hours before sunset (Alawaji *et al.* 1996; Emeis 2001; Farrugia 2003; Kirchhoff and Kaminsky 1983; Mahrt 1981; Martner and Marwitz 1982; OWPI 2003, 2004; Perez *et al.* 2005; Rehman and Al-Abbadi 2005; Sisterson 1983; Smith and Jurotich 2004; Smith *et al.* 2002).

We also estimated wind shear from the anemometer towers in our dataset where simultaneous measurements were taken at two or more levels. This analysis included some anemometer towers that were not used for our main research because they did not provide a full year of data, and excluded about half of the towers that were used for our main research, because they had anemometers at only one level. In particular, we were not able to perform this analysis for towers in the major California passes, because they each contained only one anemometer. Consequently, we cannot be confident that conditions at these towers will prevail for all the towers used in our main research. This analysis yielded daytime wind shear exponents of 0.09–0.15 and nighttime exponents of 0.17–0.21. The differences between the wind shear exponents from our anemometer database and those from other studies could be due to tower height, or to the necessarily arbitrary selection of wind shear studies or anemometer sites.

Based on these two reviews, we adopted a wind shear methodology for this report that uses a power law exponent of 0.09 during the day and 0.20 at night. The exponent changes linearly from the night value to the day value during the first three hours after dawn, and changes from the day to night value between two hours before sunset and one hour after sunset.

We compared this day/night wind shear approach to several other possible approaches by estimating upper-level speeds from lower-level speeds in our anemometer dataset. We found that our chosen approach worked significantly better than an approach using a constant 0.14 exponent, and slightly better than a more complicated approach that estimated a time-varying wind shear based on typical irradiance and cloud cover at each location and time. We found our approach performed slightly worse on this test than approaches that adjusted the daytime wind shear exponent based on the sun's declination angle (time of year) or angle above the horizon (time of year and time of day). However, we wanted to keep the temporal influences of our wind

shear model as simple as possible, and we decided that the marginal improvement from these latter approaches did not justify their extra complexity.

We also note that the day and night wind shear exponents that we adopted are consistent with what we would obtain if we used the EPA's regulatory modeling guidelines for rural locations and assumed moderate wind speeds (3–5 m/s), moderately sunny days (class B–C stability), and partly cloudy nights (class D–E stability) (EPA 2002: ch. 6).

It is important to note that the wind shear approach we adopted was not custom-tailored to any specific geographic location. In particular, we did not give special treatment to the wind conditions in West Coast passes, so our approach may overestimate summer daytime wind shear (and upper level anemometer-based wind speeds) in these areas.

2.4 Resource Areas

To facilitate our analysis, we grouped anemometer sites into "resource areas," which can be seen in Figures 1 and 2. We assigned anemometer towers to resource areas as follows. We first identified areas where anemometers were clustered within a radius of 30 km or so, by inspection of the map of anemometer locations. In south-central Washington and along the Washington Oregon border, it was not completely clear which sites to group into separate resource areas. There, we first identified the four most sharply defined clusters of sites (Ellensburg, Rattlesnake Ridge, Columbia Hills and Vansycle/Kennewick). This left several unassigned sites that fell between these areas. We compared the temporal pattern of wind speeds at each of these unassigned sites to the wind speeds in the neighboring clusters and assigned each site to the neighboring resource area with the most similar wind pattern. In the Tehachapi area, we could have defined two different resource areas based on the geographical clustering of the anemometer sites, but we found that the neighboring clusters had very similar wind regimes. So we instead defined a single resource area with anemometers from a relatively widespread region, as shown in Figure 1.

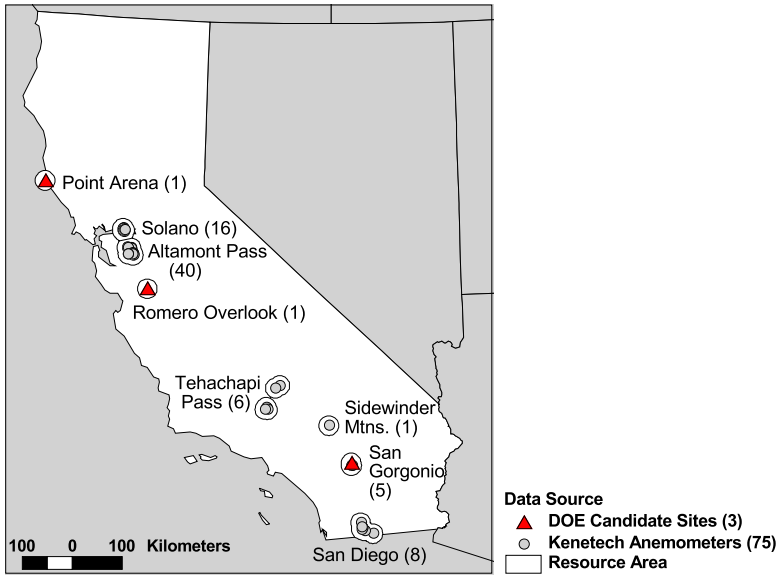

Figure 1. Locations of Anemometer Towers and Resource Areas in California

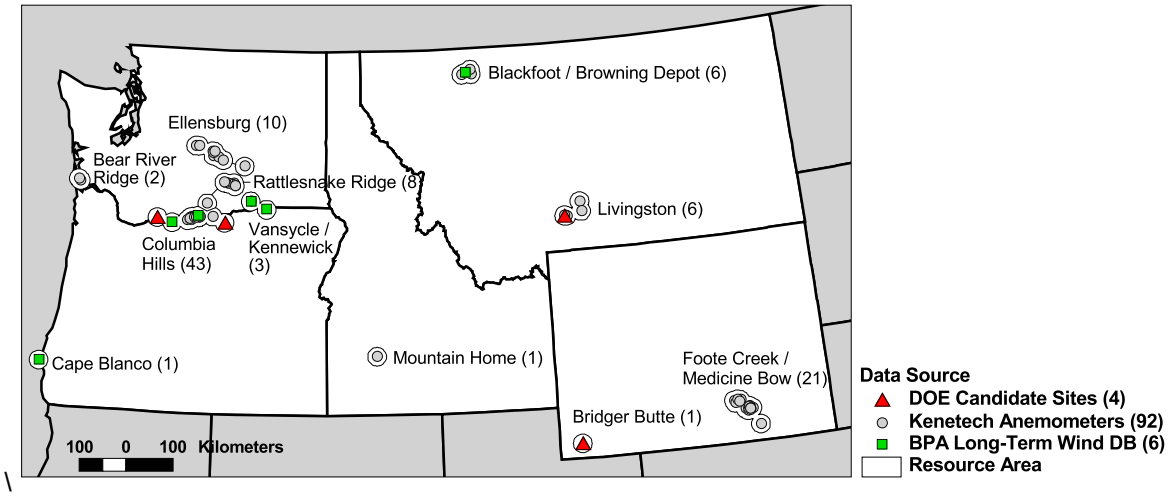

Figure 2. Locations of Anemometer Towers and Resource Areas in the Northwest

In later sections, we also use these resource areas to categorize the TrueWind data in two ways:

1) When comparing TrueWind and anemometer data, we often group the results by resource area. In these cases, we use TrueWind data from the single grid cell closest to each anemometer tower and then take the median value for various measures among all anemometer sites and matching TrueWind cells in each resource area. When used this way, individual TrueWind cells are assigned to exactly the same resource area as the corresponding anemometer tower. This is the case in Sections 4 and 5, and Appendix A.

2) When reporting wind value measures derived only from the TrueWind data, it was sometimes useful to limit our discussion to the areas where wind farms are most likely to be developed. We defined such areas as all grid cells with Class 4 or greater capacity factors,

located within 20 km of an existing anemometer site. We describe these as grid cells "near known resource areas," and assigned each of these cells to the same resource area as the closest anemometer tower. We used this definition of resource areas when reporting TrueWind results in Section 3. The borders of these areas are shown in Figures 1 and 2.

2.5 Data Limitations

A number of factors may reduce the accuracy of the TrueWind, anemometer or actual production data as estimators of wind speeds or power output at the 70-meter reference height used for our analysis. Consequently, throughout this report, we compare wind speed measurements and analytical results based on all three of these datasets. Where results from different datasets agree, we may be able to place greater confidence in the common findings. However, when these datasets disagree, insufficient information is available to identify any one of them as unequivocally the best estimator of the power output in which we are interested.

We list here a number of factors affecting the accuracy of hub-height power estimates based on the TrueWind, anemometer and production datasets, as well as the quality of fit between these datasets:

- **Modeling Uncertainty.** The TrueWind wind speed estimates and diurnal profiles are based on a computerized mesoscale atmospheric model with a grid scale of about 2 km, with a second stage designed to improve treatment of finer-scale terrain features. Although this approach is state-of-the-art, it remains subject to significant uncertainty, because of limitations in the number of forces that can be modeled and the spatial and temporal scale at which analysis can be conducted. As discussed in Section A.7, limited resolution may specifically introduce significant errors to the TrueWind results for Tehachapi, San Gorgonio, Livingston and Mountain Home regions, and may cause problems in other areas as well.

- **Wind Shear.** An important limitation to the quality of our estimates of turbine-height wind speeds comes from our treatment of wind shear. None of the anemometer wind speed measurements were made at a height of 70 m, the elevation for which we performed our analysis. We estimated wind speeds at 70 m from anemometer measurements or TrueWind Northwestern estimates made at lower elevations by way of a relatively simple power law relationship, with the same day and night exponents at all locations. This approach is an approximation at best, and neglects the fact that wind shear can change with time of year and roughness of terrain. If the correct exponent could vary by a factor of 2 in either direction, then our assumption may have introduced errors of up to 20 percent in the estimate of the observed wind speed at various times and locations. Using separate day and night exponents appears to provide more accurate results than a single exponent at all times, but limited analysis suggests that this could still be a significant source of disagreement between TrueWind and the anemometer data.

  Wind shear introduces uncertainty in any estimate of upper level wind speeds from lower-level anemometer data, and since wind shear can vary over time, it also introduces uncertainty about the temporal pattern of wind speeds above the anemometer height. These

difficulties could be partly overcome by any technique that gives a better estimate of the time and spatial variation in wind shear (*e.g.,* using anemometers at multiple levels on the same towers). However, they can never be completely overcome, except by using anemometer data from the turbine hub height (70 m for our analysis), which is not readily available.

- **Wind Farm Technology, Location and Turbine Height.** In most cases historical data from wind farms was reported as the average power output across a large geographical region, with little or no information about the technology, location or height of individual turbines. This introduces three potential problems:

  - Wind farm data can only be compared to other datasets in terms of power output, not wind speed. These comparisons may be hindered by the fact that many operating wind farms use different turbine technology than our reference system.

  - Wind farm production data for each resource area must be compared to TrueWind or anemometer data on an aggregated basis, rather than comparing the power output at individual turbine locations. Further, the TrueWind and anemometer locations selected for this comparison may not exactly match the locations where the actual production took place.

  - We were unable to adjust the power output found at the (often unknown) heights of the wind farm towers in order to estimate the power output that would be likely at our 70 m reference elevation. Instead, we used the lower-elevation capacity factors without correction. This problem is particularly pronounced for California locations, where older turbines have been installed on relatively short towers. It may not be significant for the Northwest, where newer production turbines have been placed close to our 70 m reference height.

- **Anemometer Location.** TrueWind has worked with NREL and several consulting meteorologists to validate their annual average wind speeds against measured wind speeds. As part of that process, TrueWind adjusted the reported location of anemometer sites so that they were aligned to similar terrain features (*e.g.,* ridgelines) included in the TrueWind model, which sometimes required corrections of a few kilometers. There are likely to be similar mismatches between the locations of sites in our observation database and the terrain features in the TrueWind model. In addition, we know locations for some anemometer sites only within a few kilometers, and we consistently had differences of a hundred meters or so between our geographic projection system and TrueWind's. We did not attempt to correct the location data we received for individual anemometer sites to align them more closely with terrain features in the TrueWind database, so it is possible that anemometer sites that are actually on top of ridges have been matched with TrueWind model cells which correspond to other types of terrain (*e.g.,* nearby but further downslope, or possibly at a random location, depending on the magnitude of error). Wind patterns can vary dramatically from one type of terrain to another, so these problems could cause TrueWind's data to appear more mismatched to real conditions than they actually are.[8,9]

[8] There were 7 Kenetech sites in the Northwest and 8 Kenetech sites in California for which we assigned approximate latitude and longitude values, based on location names, as described in footnote 6. We estimate that

- **Date Range of Anemometer and Production Data.** It is possible that the anemometer measurements at any given site or actual power production in any resource area were recorded during a time with particularly high or low wind speeds, or an otherwise atypical pattern of wind speeds (*e.g.,* some of the meteorological towers only collected data for a single year, which may have been an abnormal year). If this is the case, the anemometer or production data may be less "typical" of long-term conditions than the TrueWind data. Anemometer and production data may cover only one year in some cases, and may cover different years at different sites. Consequently, it is also possible that the spatial distribution of high and low average wind speeds in our dataset does not match the spatial pattern that would be found in any real calendar year. On the other hand, our averaging of anemometer and production values for each month-hour is likely to reduce the effect of short-term variations in wind speed, and the diurnal patterns for each month may vary little from year to year, even if the annual or monthly average wind speeds vary. As a result, this issue may not contribute much to disagreement between the TrueWind, anemometer and production datasets, or to disagreement on the effects of wind timing on the value of power at individual locations.

- **Effective Ground Level Differences.** The wind speeds reported by TrueWind were given at heights of 50 or 70 meters above "effective ground level." In dense forest, this is relative to the canopy height, which may be a significant distance above the true ground level. We did not correct these effective heights to true heights before comparing them to observations, which could make the TrueWind speeds artificially high in heavily vegetated areas.

- **Overemphasis on Existing Resource Areas.** Our comparisons are made only at the sites for which we have data. As such, they are weighted toward the regions for which we have the most data, and say nothing directly about the regions for which we do not have any measurements. TrueWind data can only be compared to hourly historical power production in three regions in California. The anemometer datasets include wind data from most of the promising wind areas in California and the Northwest, so to some extent the anemometer-based comparisons rate the TrueWind data based on its performance in the areas of most interest. However, the representation of wind regions in our database is idiosyncratic, so our analysis may or may not accurately reflect the importance of each region to wind power developers. For example, 40 of the 78 California anemometer sites are in Altamont Pass, so about half of the region-wide ratings for the TrueWind data in Appendix A come from how well they match wind speeds in this limited region. This may also be a significant issue in the Northwest, where 41 of the 102 sites used for this analysis are in the Columbia Hills region.

---

these approximations are correct to within about 10 km. The fit between the TrueWind and observation data was worse at these sites than at other sites in the dataset. For example, the mean absolute error (MAE) for the California sites with approximate locations was 2.3 m/s, compared to 1.6 m/s for the sites with exact locations. In the Northwest, the MAEs were 2.5 m/s for the approximate locations and 1.5 m/s for the exact locations.

[9] We do not have a list of the anemometer sites originally used to validate TrueWind's annual average wind speeds. If any of the sites that we used for validation were previously used to correct the TrueWind data, it is possible that we could find an artificially high correlation between TrueWind's wind speeds and the annual averages at our observation sites. However, we think it is unlikely that many sites were used for both validation efforts, and TrueWind used data from individual sites too indirectly to produce much false correlation.

Further research would be valuable using lower-level anemometer data from the National Weather Service or the California Department of Water Resources to identify seasonal and possibly diurnal wind patterns at a wider variety of locations (see footnote 5).

2.6 Estimating Wind Power from Wind Speeds

We used the power curve from the GE 1.5s wind turbine to estimate the power output for each grid cell for each month-hour combination, based on the corresponding average wind speed from TrueWind, and for each chronological hour at each anemometer site.

For consistency, we used the same turbine for our analysis at all locations. Since the power output from any turbine is a nonlinear function of wind speed, other turbines could yield different temporal patterns of power output: for example, a turbine optimized for lower wind speeds than the GE 1.5s would produce more power than the 1.5s during low wind periods, but less power during high wind periods. Wind farm developers choose the turbine that will give optimal total power output in a particular local wind regime; to the extent that the timing of power output affects project viability, it is possible that they could select particular turbine models that optimize the timing of their power output as well. We did not explore this possibility in our work.

We were supplied with a table showing the power output for the GE 1.5s turbine for wind speeds ranging from 0 to 25 m/s at standard temperature and pressure (1.225 kg/m^3 air density) as well as additional power curves for lower air densities, corresponding to higher elevations or temperatures (Milligan 2004). We found that the power curve for any air density could be reproduced by using the power curve for standard temperature and pressure, and scaling the wind speed according to the difference between the two air densities.[10]

To facilitate our wind power calculations, we then fit the standard-density power curve with a piecewise polynomial function.[11] This approach allowed us to reproduce the power curve for the GE 1.5s at all wind speeds and air densities, interpolating smoothly between the discrete, published values. The R^2 goodness-of-fit between our polynomial and the power tables for all wind speeds and air densities is 0.99996, indicating that this approach produced power output estimates that were virtually identical to those in the published power curves.

The air density for each month-hour combination at each location was estimated from the elevation of that location and the average temperature for that month and hour according to the properties of the standard atmosphere. We calculated air density (ρ) according to the formula

[10] The power density of wind (in W/m^2) is given by $P = \frac{1}{2}\rho v^3$, where ρ is the air density (kg/m^3) and v is the wind speed (m/s). Setting $P_{sea\ level} = P_{local}$, we obtain the sea-level wind speed with the same power density as a given local wind speed: $v_{sea\ level} = (\rho_{local} / \rho_{sea\ level})^{\frac{1}{3}} \cdot v_{local}$.

[11] This function consisted of one polynomial segment (showing the turbine output at speeds between the cut-in and rated speeds) and three linear segments (zero power output below the cut-in speed of 4 m/s, 1.5 MW output above the rated speed of approximately 13 m/s, and zero power above the cut-out speed of 25 m/s).

$$\rho = \frac{\rho_0}{R_d(T+\beta z)}\left(1+\frac{\beta z}{T}\right)^{1-\frac{g}{R_d\beta}},$$

where ρ_0 is the density of air at standard temperature and pressure, β is the temperature lapse rate for the standard atmosphere (6.5°C/km), z is the elevation of the turbine above sea level, R_d is the gas constant for dry air, and g is the force of gravity.

The elevation used in this calculation was the average grid cell elevation provided with the TrueWind dataset. Temperatures for each grid cell for each month and hour were estimated by interpolating between observation stations in the U.S. Historical Climatology Network (Karl *et al.* 1990), and then fitting monthly high and low temperatures to a diurnal profile that peaked in the afternoon and fell to the minimum temperature from late evening until dawn.[12]

For the TrueWind data, we assumed that the wind speeds for each grid cell during each month-hour combination were distributed according to a Weibull distribution, with mean wind speed and shape factor as discussed in Section 2.2.1. We were then able to directly estimate the average power output for each cell, month and hour by calculating the average value of our piecewise polynomial power curve when applied to the Weibull distributed wind speeds for that time and location.[13] This value was then used as the basis for all the power-value calculations discussed later in this report.

---

[12] We used the monthly high and low temperatures recorded for 1971–2000 to get a long-term average of the monthly high and low temperatures for each station in the climatology network. We then averaged the temperatures of all stations within 200 km of each coarse grid cell, weighting the values by the inverse square of the distance from the grid cell to the station, and using a 6.5°C/km lapse rate to correct for elevation. The large averaging distance was used to ensure that each grid cell would be within range of at least a few temperature stations, but the steep weighting ensures that nearby stations dominate the average temperature calculation for any cell. The timing of the daily temperature profile is scaled according to the number of hours of daylight per day at each location in each month. It starts at the minimum temperature at dawn, then follows a sinusoidal pattern, rising to the maximum temperature one third of the way through the afternoon, and then drops to the minimum temperature by one third of the number of daylight hours (about 4 hours) after sunset. It remains at the minimum temperature until dawn.

[13] The mean value of a piecewise polynomial function of a Weibull-distributed random variable can be calculated as the sum of several incomplete gamma functions as follows:

First, we define the power curve as a function of the wind speed:

$$\mathrm{P}(v) = \begin{cases} 0, & v < v_{in} \\ \mathrm{P}_1(v), & v_{in} \le v < v_r \\ \mathrm{P}_{\max}, & v_r \le v < v_{out} \end{cases}$$

where v_{in} is the cut-in speed of the turbine, v_r is the rated wind speed of the turbine (the wind speed at which it begins to produce its maximum power output), and v_{out} is the cut-out speed of the turbine (above which it produces no power), $\mathrm{P}_1(v)$ is the power curve function between the cut-in and rated speed, and $\mathrm{P}_{\max}$ is the amount of power produced by the turbine at its rated speed.

Then, the mean value of the power output function is

$$E[P(V)] = \int_{-\infty}^{\infty} P(v)f(v)dv = \int_{v_{in}}^{v_r} P_1(v)f(v)dv + \int_{v_r}^{v_{out}} P_{max}f(v)dv$$

where V is the randomly varying wind speed and $f(v)$ is the probability density for this variable.

For the anemometer data, we assumed that the wind speed was constant during each chronological hour, and calculated the power output for that hour by feeding the average wind speed directly into the polynomial power curve for the wind turbine. We then averaged the power output values for all the relevant chronological hours to obtain the average power output for each month-hour at that site.[14]

In both cases, we assumed that a total of 12 percent of power was lost at all locations and times, due to electrical and control system losses, blade contamination, weather, wake effects, turbulence, and turbine outages (Milligan 2004).

When $P_1(v)$ is a polynomial, we have

$$E[P(V)] = \int_{v_{in}}^{v_r}\left(\sum_{i=0}^{n} a_i v^i\right) f(v)dv + \int_{v_r}^{v_{out}} P_{max} f(v)dv = \sum_{i=0}^{n} a_i \int_{v_{in}}^{v_r} v^i f(v)dv + P_{max}\int_{v_r}^{v_{out}} f(v)dv$$

where a_i are the coefficients of the polynomial (which has degree *n)*.

When V is Weibull-distributed, it can be shown that

$$a_i \int_{v_{in}}^{v_r} v^i f(v)dv = a_i \int_{v_{in}}^{v_r} v^i \frac{k}{c}\left(\frac{v}{c}\right)^{k-1} e^{-\left(\frac{v}{c}\right)^k} dv = a_i c^i \left[\Gamma\left(\frac{i}{k}+1, \left[\frac{v_{in}}{c}\right]^k\right) - \Gamma\left(\frac{i}{k}+1, \left[\frac{v_r}{c}\right]^k\right)\right]$$

and

$$P_{max}\int_{v_r}^{v_{out}} f(v)dv = P_{max}\left[e^{-\left(\frac{v_r}{c}\right)^k} - e^{-\left(\frac{v_{out}}{c}\right)^k}\right],$$

where k is the shape factor and c is the scale factor for the distribution, and $\Gamma(\alpha_1, \alpha_2)$ is the incomplete gamma function. So, the average power output is given by

$$E[P(V)] = \sum_{i=0}^{n} a_i c^i \left[\Gamma\left(\frac{i}{k}+1, \left[\frac{v_{in}}{c}\right]^k\right) - \Gamma\left(\frac{i}{k}+1, \left[\frac{v_r}{c}\right]^k\right)\right] + P_{max}\left[e^{-\left(\frac{v_r}{c}\right)^k} - e^{-\left(\frac{v_{out}}{c}\right)^k}\right].$$

We defined a single function in the C computer language that performed the following steps to calculate the average power output for any cell, month, and hour, based on the average wind speed, Weibull shape factor, elevation, and temperature for that place and time:

1. calculate the air density based on the temperature and elevation, and then convert the average wind speed to the equivalent sea-level wind speed;
2. calculate the scale factor (*c*) for the Weibull distribution, based on the shape factor and sea-level wind speed; and
3. calculate the mean power output, using the formula above, with the appropriate parameters for the GE 1.5s turbine (a_0–a_6, v_{in}, v_r, v_{out}, *and* P_{max}).

This function allowed us to quickly calculate the electric power output values needed for the rest of our analysis.

[14] The speeds reported for each hour at each anemometer are the average value for that hour. In many cases, standard deviations of the wind speed during the hour were also reported. Although speeds varied during each chronological hour, we found that the variation was relatively narrow, and our results showed little difference whether we assumed constant speeds for each hour or assumed a Weibull distribution of wind speeds during the hour, with the specified standard deviation. Variability within each hour was much smaller than the variability during the whole year, and most of the temporal variation in wind speeds is reflected in the variation of the hourly average wind speeds.

2.7 Electricity Price and Load Data

The fundamental purpose of this report is to correlate temporal wind patterns with various wind value metrics, including both "market value" and "capacity value" proxies. Market value proxies are derived from correlations between wind timing and historical or forecast wholesale power prices in California and the Northwest. The capacity value proxy is derived from estimates of wind output during the top 10 percent of load hours, based on historical load in California and the Northwest.

All prices used in this report are in nominal, current-year terms. We made no adjustment for inflation, or economic discounting. This approach should have little direct effect on our results, since they are generally reported as percent changes in revenue, rather than in dollar-and-cents terms. However, if the timing of peak prices changes in the later years of any particular multi-year price series, this approach may give somewhat disproportionate weight to those later years when all the years are averaged together to create a single, typical price series.

2.7.1 Northwest Power Prices

For our analysis of power values in the Northwest, we used historical and forecast wholesale power prices from the Mid-Columbia (Mid-C) trading hub. Due to transmission interconnections, wholesale power prices in parts of Idaho and Wyoming may actually be linked more closely to southwestern markets than to the Mid-C hub. However, we used the Mid-C hub for the whole region in order to perform a more uniform analysis, and to therefore better reflect the general impact of wind timing on wholesale market value.

For historical prices at the Mid-C hub, we used month-hour averages of the Dow Jones hourly wholesale power prices from May 2002 through April 2005 (BPA 2005).

Our price forecast series for the Northwest was the average of the Northwest Power and Conservation Council's hourly forecasts for the Mid-C hub for the years 2006–2025, prepared using the base case assumptions for that agency's Fifth Power Plan (King 2005).

We averaged each of these series for each month and hour to obtain the historical and forecast price series for our analysis. As shown in Figure 3, the historical price series is relatively flat seasonally and diurnally, with a modest winter peak. The price forecast shows increasing summertime prices, producing a second peak in August. The forecast also shows stronger diurnal variation throughout the year.

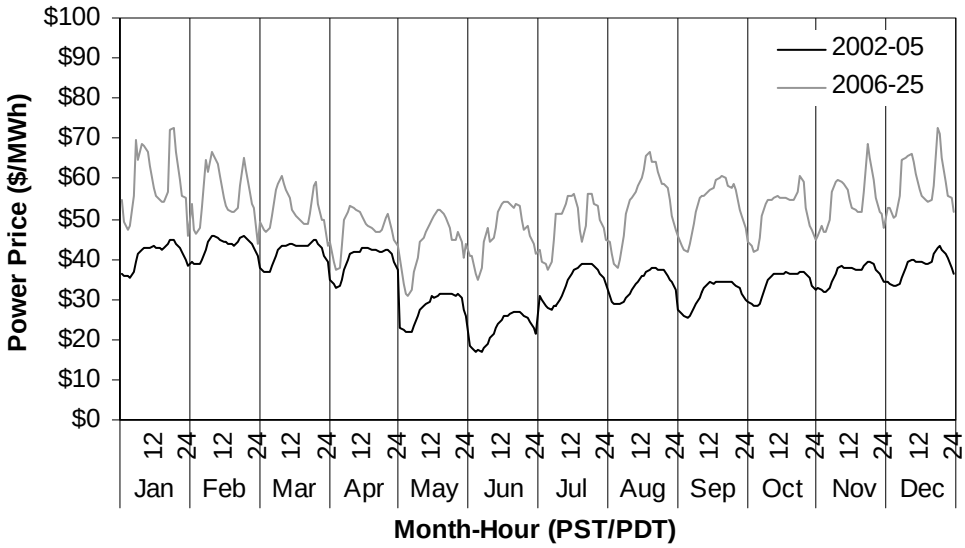

Figure 3. Historical and Forecast Power Prices for the Northwest

2.7.2 California Power Prices

Our historical price series for California was the simple average of the day-ahead hourly zonal prices published by the California Power Exchange for the NP15 and SP15 hubs between July 1998 and June 1999. This period was chosen because it provided a full year of market data before the California power crisis of 2000–01 and the subsequent restriction of wholesale markets. The day-ahead zonal price is the marginal price set by the Power Exchange after accepting the lowest-priced bids in its day-ahead auctions, within the constraints of the transmission system (UCEI 2004). We used the average of the two hubs for all wind sites, rather than dividing the state into separate northern and southern markets, so that the results from all sites would be referenced to a common set of market conditions.

Our forecast price series for California was the average of hourly forecasts for all California hubs for 2006–13, provided by the California Energy Commission. This forecast was part of the baseline case for the CEC's 2003 Electricity and Natural Gas Assessment Report. In this forecast, monthly average power prices for each hub come from Henwood's MarketSym electricity market model. They are averaged together for the whole state, and then diurnal shapes for each month come from the simple average of the day-ahead NP15 and SP15 hourly prices from October 1998 to September 1999 (Klein 2004; Gopal *et al.* 2003).

As shown in Figure 4, the price forecast has a lower monthly variation than the historical prices, but as a result of the methodology used (described above) the diurnal component of both price series are similar.

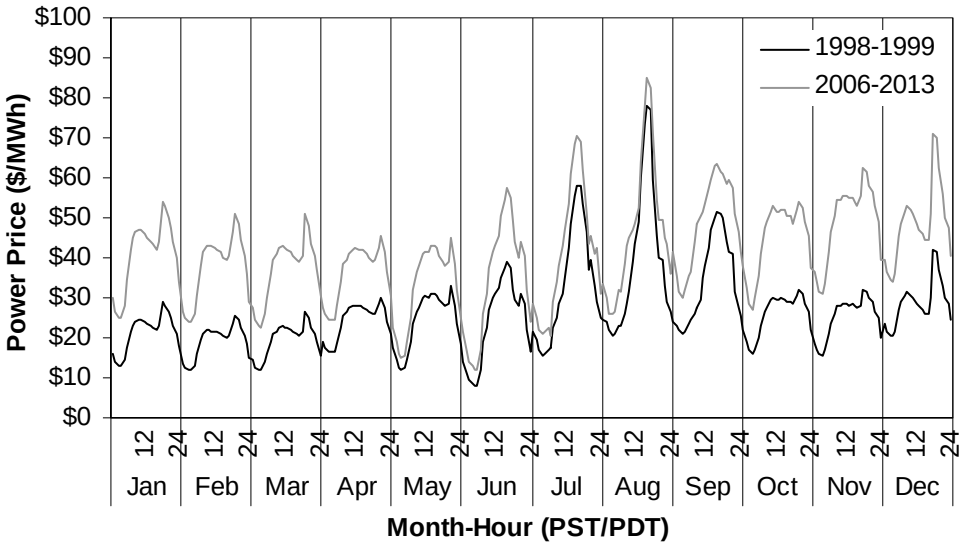

Figure 4. Historical and Forecast Power Prices for California

2.7.3 Long-Run Equilibrium Prices Not Used

Both the historical and forecast prices shown in Figures 3 and 4 show a similar degree of temporal variability. The highest prices of the year in the Northwest (on a month-hour basis) are 30–40 percent higher than the annual average, while the peak California prices are three times as high as the annual average. Borenstein (2005) indicates that these prices reflect conditions where most or all customers pay a flat rate for electricity throughout the year, and part of their bills are used to purchase generation "capacity" to ensure that peak power demands are met. A more economically efficient approach would be to use "energy-only" tariffs, where prices are allowed to rise during hours of peak demand. Under this system, peak-hour electricity prices would reflect the long-run equilibrium between the value of power to customers and the cost of additional generation plants. Although this system would produce lower prices on average throughout the year, peak-hour prices would likely be significantly higher than those shown in Figures 3 and 4. Space and time constraints prevented us from using estimated long-run equilibrium prices for our analysis, but we would expect these to increase the effect of wind timing on the market value of wind power beyond what we show in this report.

2.7.4 Historical Loads for California and the Northwest

Historical electricity loads for both California and the Northwest were based on the total demand reported in FERC Form 714 filings for all electric control areas within each region for each hour for 2000 through 2004[15] (FERC 2005). Figure 5 shows that Northwestern loads have historically peaked in the winter months, while California loads have had a clear summer-afternoon peak.

[15] California loads were calculated as the sum of the hourly loads reported for the following service areas: California Independent System Operator, Los Angeles Department of Water and Power, Sacramento Municipal Utility District, and Imperial Irrigation District. Northwest loads were reported by Avista Corp., Bonneville Power Administration, PUD No. 1 of Chelan County, PUD No. 1 of Douglas County, PUD No. 2 of Grant County, Puget Sound Energy, Seattle Department of Lighting, Tacoma Power, PacifiCorp, Portland General Electric, Idaho Power Company, and

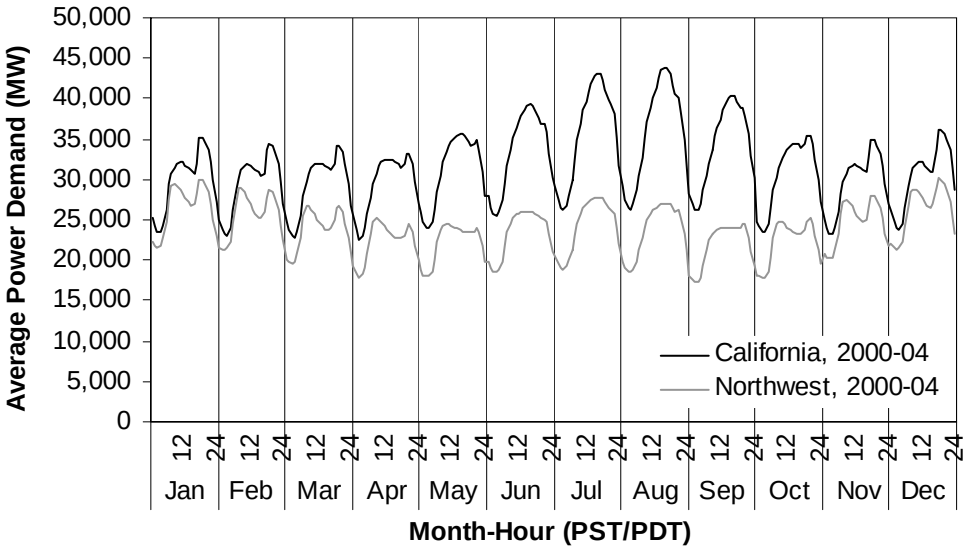

Figure 5. Historical Electricity Demand in California and the Northwest

NorthWestern Energy (formerly Montana Power Company). The FERC reports from the Western Area Power Administration (Rocky Mountain Region) cover large parts of Wyoming as well as other regions outside our area of analysis. These reports were excluded from our load calculations for the Northwest, because it was impossible to disaggregate the areas within our study region from those outside. These filings included data from a number of smaller entities serving parts of our study area, including Basin Electric Power Cooperative, Black Hills Power and Light Company; Cheyenne Light, Fuel & Power Company; Tri-State Generation & Transmission Association, Inc.; and Wyoming Municipal Power Agency.

3 Effects of Wind Timing on the Value of Wind Power, using TrueWind Data

In this section we use the TrueWind modeled data set to estimate the effects of wind timing on the value of wind power at each cell on the TrueWind grid. In Section 3.1 we describe the capacity- and price-based approaches we used to estimate the effects of wind timing at each grid cell, and summarize our findings based on these two approaches. In Section 3.2 we describe the capacity-based approach and results in greater detail, and in Section 3.3 we do the same for the price-based approach. Finally, in Section 3.4, we compare the results found via the capacity- and price-based approaches. All of the analysis in Section 3 is performed using the TrueWind modeled data. Later, in Section 4, we compare the results found from the TrueWind data with estimates of the effects of wind timing based on anemometer and actual wind production data.

3.1 Background and Summary

We used the TrueWind wind power data and electricity load and price series discussed in Section 2 to estimate the effects of wind timing on the value of wind-generated electricity at each grid cell in California and the Northwest. The effects of timing were measured by two approaches, yielding three key metrics for each cell:

- ***Capacity Metric:*** the difference between the annual average capacity factor and the capacity factor during the top 10 percent of peak load hours (based on historical loads).

- ***Price Metrics:*** the difference between annual wholesale market value of wind power with unvarying power output from each turbine and the annual market value expected with the time-varying wind speeds found at that turbine location, using: (1) historical wholesale power prices, and (2) forecast wholesale power prices.

These effects are mapped and tabulated in detail in the sections below. To summarize, we found that temporal wind patterns at different locations had large effects on the average power output during hours of peak electricity demand, and smaller but still substantial effects on the annual wholesale market value of that wind generation based on historical and forecast wholesale market prices. Figure 6 summarizes these findings, showing the median effect of wind timing on each measure of power value among all good (Class 4+) wind locations in California and the Northwest (central bar of each marker), as well as the range of effects between the 10th and 90th percentile of wind sites (lower and upper bars).[16]

[16] Here we assume that California wind projects sell into the California market, and that Northwestern projects sell into the Northwest market. Differences in timing between California and Northwest power markets are more significant than the differences in timing between many of the wind sites, so this is an important assumption.

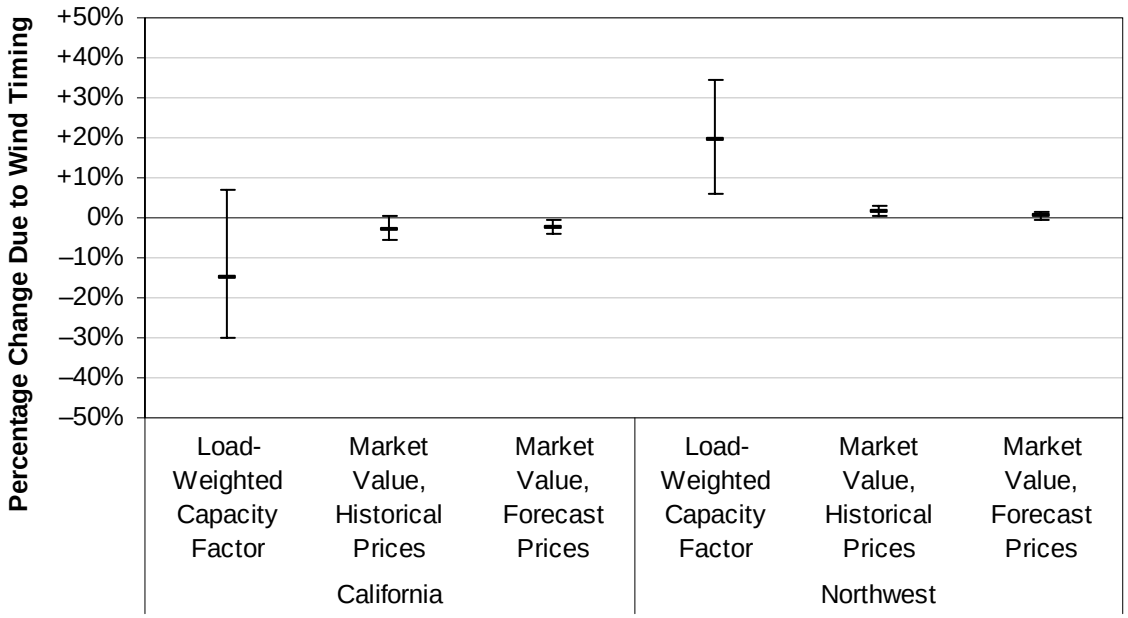

Figure 6. Effects of Wind Timing on Load-Weighted Capacity Factor and Annual Market Value at Class 4+ Grid Cells in California and the Northwest (Median, 10th and 90th Percentiles)

According to the TrueWind data, the best- and worst-timed of the windy California grid cells have capacity factors in the top 10 percent of load hours that range from 7 percent above to 30 percent below their annual average capacity factors, with a median value of 15 percent below the annual average. Northwest wind sites appear well suited for Northwestern load: windy locations in the Northwest have peak-hour capacity factors ranging from 6 to 34 percent above their annual capacity factors, with a median of 20 percent (Section 3.2.2).

The best-timed California sites have a wholesale market value approximately equal to what would be obtained if their power output was completely uncorrelated with wholesale electricity prices, while the worst sites have a market value about 4–6 percent less than this based on historical or forecast prices. Sites in the Northwest are somewhat better matched to their power markets, with a wholesale market value ranging from an amount equal to what they would earn with uncorrelated power output, up to about 2–3 percent more than this, using historical or forecast prices (Section 3.3.2).

The difference in power production (25-40%) between the best- and worst-timed grid cells during the hours of peak electricity demand is approximately equivalent to the difference in power production between wind sites two or three power classes apart. So, for example, the best-timed Class 3 sites could produce about as much power as the worst-timed Class 6 sites during the hours of peak electricity demand. However, when the year-round value of power is considered, using wholesale market prices, the best-timed sites have a market value only about 2–6 percent better than the worst-timed sites. By this measure, the timing of wind appears to increase the market value of wind power by the equivalent of about a quarter of a wind power class between the worst- and best-timed sites, so that even the worst-timed Class 4 wind sites would have a greater market value than the best-timed Class 3 sites.

The results presented in this section are based on analysis using the wind speed estimates provided by TrueWind. As will be discussed in Section 4, these results differ in some cases from what would be found using anemometer data for the same locations (or from actual wind power production data). Overall, TrueWind and the anemometers are in good agreement on the difference in the relative value of power between sites with winds well matched or poorly matched to electricity demand, and they are in partial agreement about which locations have the best and worst wind timing. However, the TrueWind data suggest that wind timing generally decreases the value of wind power in California, while the anemometer data suggest that wind timing has a more neutral effect on the value of wind power in California. This disagreement is difficult to resolve, and may be based on inaccuracy in either or both data sources. It is possible that wind timing at turbine hub height (where TrueWind's estimates were made) is worse than wind timing at lower elevations (where anemometer measurements were taken), due to variations in wind shear during the day and year. If this is the case, then the TrueWind data may provide a more accurate picture than the anemometers of the effects of wind timing on new commercial-scale turbines. However, until more anemometer data (or actual production data) at high elevations are available, we are unable to say conclusively which data source is more reliable. The TrueWind and anemometer data are compared in more detail in Appendix A.

There are, however, some issues that we were not able to address within the scope of this report. First, we treat all of California as a single market for electricity, and do the same for the Northwest. This allows us to judge the value of power from all wind sites within each study area by a common standard. However, it neglects constraints on the capacity of the transmission system to deliver power from the best-timed locations to the major centers of demand. Second, our chief measures for the value of wind power are the capacity factor during peak load hours, and the time-varying wholesale price of electricity. This simplified approach forgoes a more detailed analysis of the effect of wind timing and variability on the system integration costs and capacity value of wind power.

3.2 Capacity-Based Measures of Wind Value

We used the potential capacity factor of a wind turbine at each cell on the TrueWind grid during the top 10 percent of hours of peak electricity demand as a simplified measure of the contribution that a wind turbine at that location could make to the reliable operation of the electricity system. The difference between the peak-hours capacity factor and the annual average capacity factor at each location provides an idea of how the temporal patterns of the wind affect the potential capacity contribution of wind projects at each location.

3.2.1 Methods

3.2.1.1 Annual Average Capacity Factor

One of the most common measures of the electricity production from a wind turbine at any location is the annual average capacity factor. We calculated the annual capacity factor for our reference turbine at each grid cell based on the potential power output for every month and hour, using the TrueWind data, as discussed in Section 2.6.

Elliott *et al.* (1986) introduced the "wind power class" system, which is widely used to report the overall wind resource potential at different locations. In this system, each location is assigned a class from 1 to 7, based on the average power density of the wind at a 10 meter elevation above the ground (Elliott *et al.* 1986, Guey-Lee 2001).

Unfortunately, the wind class for a location cannot be related directly to the power output from a wind turbine at that location,[17] making wind power classes somewhat problematic for comparing the performance of wind turbines at different locations and times. To work around this difficulty, while still maintaining the useful wind class system of categorization, we identified equivalent wind classes for several ranges of capacity factors for the GE 1.5s wind turbine.

9Table 3 shows the annual capacity factors that the GE 1.5s turbine would achieve if mounted at 70m above ground, at a location with standard temperature and pressure (15°C, at sea-level), with a wind speed that scales up from the 10-meter level according to a power law with 1/7 as the wind shear exponent, and with the standard power losses that we assume for our analysis. Wind sites with Class 4 or higher winds, corresponding to a capacity factor greater than about 0.316 for our reference turbine, are typically considered the most commercially viable (Elliott and Schwartz 1993), but progress is being made toward profitable development of Class 3 wind sites (corresponding to a capacity factor of 0.262–0.316 for our reference turbine)

Throughout this report, when we refer to the "equivalent wind class" for any location, we mean the standard wind class shown in 9Table 3 that would yield the same capacity factor as the particular wind regime found at that location.

[17] This is true for two key reasons: (1) the average wind power density at elevations more than 10 meters above the ground may be different at two sites with the same average wind power density at a 10 meter elevation (*i.e.,* they may have different wind shears), and (2) the distribution of wind speeds may differ between locations with the same average power density, so that the same model of turbine could produce different amounts of electrical power at two wind sites with the same average wind power density.

9Table 3. Capacity Factor of GE 1.5s Turbine in Various Wind Power Classes

	(1)	(2)	(3)	(4)
Wind Power Class	**Wind Power Density, 10m Elev. (W/m^2)**	**Average Wind Speed, 10m Elev. (m/s)**	**Average Wind Speed, 70m Elev. (m/s)**	**GE 1.5s Capacity Factor**
Class 1	0–100	0.0–4.4	0.0–5.8	0.000–0.193
Class 2	100–150	4.4–5.0	5.8–6.7	0.193–0.262
Class 3	150–200	5.0–5.6	6.7–7.3	0.262–0.316
Class 4	200–250	5.6–6.0	7.3–7.9	0.316–0.359
Class 5	250–300	6.0–6.4	7.9–8.4	0.359–0.393
Class 6	300–400	6.4–7.0	8.4–9.2	0.393–0.446
Class 7	400–1000	7.0–9.5	9.2–12.5	0.446–0.564

Notes: Column (1) is the definition for each wind power class, given by Elliott et al. (1986). Column (2) is derived from (1) using simple physics and assuming standard temperature and pressure. Column (3) is derived from (2), using a power law relation with wind shear exponent 1/7 ($[70/10]^{1/7}=1.32$). Column (4) is based on (3), assuming a Rayleigh distribution of wind speeds, standard temperature and pressure, and using the GE 1.5s power curve, with 12 percent losses.

3.2.1.2 Load-Weighted Capacity Factor

Power planners often need to estimate the contribution that a new generator can make to the reliable supply of electricity on the grid. The most rigorous technique for doing this is to use a formal adequacy analysis, in which the new generator is added to a simulated version of the system's existing portfolio of generators, and then the system's time-varying load is increased incrementally until the overall reliability of the power system is equal to what it was before the generator was added. The additional year-round demand that can be safely added along with the new generator determines the "estimated load carrying capacity" (ELCC) of the generator. This is the most widely accepted way to estimate the capacity contribution from wind generators, but it requires complete details about the system's existing generator portfolio, as well as computing resources that would make it prohibitive for estimating the capacity contribution from wind power located at millions of different grid cells. (See, *e.g.,* Kahn 1991, Kirby *et al*. 2003, Milligan 2002).

The load-weighted capacity factor is a simplified measure of the capacity contribution of a wind turbine. In many power systems, most of the risk of a power shortfall is concentrated during the few hours with the greatest electricity demand. Milligan and Porter (2005) note that the capacity factor of a wind plant during the top 10 percent of load hours can be within a few percentage points of the ELCC for that plant, and remains about the same if a larger number of hours are used. Kirby *et al.* (2003, pp. 25-26), drawing on the same research, also identify the capacity factor during the top 10 percent of system load hours as a simplified proxy for the ELCC of a plant. However, they note several concerns about this approach:

1) This method appears generally to underestimate the ELCC of a plant;
2) It is unclear whether one should choose the hours with the greatest system load, or the hours with the greatest risk of shortfall (which may not be the same);

3) It is unclear how many hours should be used for this analysis; and
4) Intermittent plants may make a useful contribution to system reliability during other hours, when the system is not near its peak load.

Though we acknowledge the imperfections in this approach, absent a reasonable alternative, we calculated a load-weighted capacity factor for each location by estimating the capacity factor during only the top 10 percent of month-hours of the electricity load series.[18] Since there are 288 month-hours in the year, we estimated the capacity factor at each grid cell during the 29 month-hours when electricity demand is highest. Table 4 shows when these 29 hours occur for the two load series we use for our analysis, based on electricity demand in 2000–2004 (see Section 2.7.4). As shown, historically, California has been a summer-peaking area, whereas the Northwest has been predominantly winter-peaking.

Table 4. Top Ten Percent of Month-Hours for Electricity Demand in California and the Northwest (2000–2004)

	California														Northwest													
Hour (PDT/ PST)	7	8	9	10	11	12	13	14	15	16	17	18	19	20	7	8	9	10	11	12	13	14	15	16	17	18	19	20
June								■	■	■																		
July					■	■	■	■	■	■	■	■	■	■									■	■				
Aug.					■	■	■	■	■	■	■	■	■	■														
Sep.							■	■	■	■	■	■																
Oct.																												
Nov.																									■	■		
Dec.															■	■	■	■						■	■	■	■	■
Jan.															■	■	■	■	■					■	■	■	■	■
Feb.															■	■	■								■	■	■	

3.2.1.3 Difference Between Annual Capacity Factor and Load-Weighted Capacity Factor

We next compared the load-weighted capacity factor and annual average capacity factor at each grid cell, assuming that Northwest wind is sold into the Northwest and that California wind is sold into California. This gives a sense of whether the capacity contribution from wind turbines at each grid cell would exceed or fall short of their annual energy contribution. This, in turn, reflects the effect of wind timing on the ability of each location to contribute to a reliable electric supply.

The fractional difference (f) between the load-weighted capacity factor and the annual average capacity factor is defined by the equation

[18] We used the top 10 percent of hours instead of some other number because this was compatible with the discussion in Milligan and Porter (2005) and Kirby *et al*. (2003). This also appears to be short enough to capture the truly critical periods, while being long enough to smooth over idiosyncratic behavior that might appear during a smaller number of hours.

$$f = \frac{CF_{peak} - CF_{year}}{CF_{year}} = \frac{CF_{peak}}{CF_{year}} - 1,$$

where CF_{year} is the annual average capacity factor and CF_{peak} is the capacity factor during the hours of greatest electricity demand. For example, a site with a load-weighted capacity factor of 0.25 and an annual average capacity factor of 0.30 would have a fractional difference of –16.7 percent, indicating that the site produced 16.7 percent less power during peak demand hours than it did on average during the year.

We also estimated the fractional change in capacity factor when California loads are served by Northwestern wind and vice-versa to test whether one state's loads might best be served with in-state or out-of-state wind resources

3.2.2 Results

3.2.2.1 Annual Average Capacity Factor

Table 5 shows the percentage of cells on the California and Northwest TrueWind grids with capacity factors equivalent to the performance of our reference turbine in each of the standard wind classes. This table is based on an estimate of potential wind power production at every location in California or the Northwest, using the TrueWind data. The cells have not been screened based on other factors that could affect project viability, such as physical accessibility or proximity to transmission lines.

Table 5. Capacity Factor and Equivalent Wind Class for GE 1.5s Wind Turbine at Locations on the TrueWind Grid

Capacity Factor	Equivalent Wind Power Class	Percent of Grid Cells in California	Percent of Grid Cells in the Northwest
0.000–0.193	Class 1	83.6	54.1
0.193–0.262	Class 2	9.0	20.3
0.262–0.316	Class 3	3.4	15.2
0.316–0.359	Class 4	1.7	7.2
0.359–0.393	Class 5	1.1	1.9
0.393–0.446	Class 6	1.2	0.9
0.446–0.564	Class 7	0.0	0.3

Figures 7 and 8 show the distribution of these cells across California and the Northwest.[19] In these maps, orange or red cells indicate capacity factors below 0.316, while green indicates cells with capacity factors greater than 0.316. These maps are similar to maps of wind power density created directly from the TrueWind data, but they show the average performance of our specific reference turbine, rather than the average power available in the wind.

[19] These maps have a relatively low resolution (about ten times coarser than the TrueWind data), and good wind areas are often much narrower than the pixels used here. To highlight the windiest regions, each pixel in these maps shows information for the windiest TrueWind cell in the corresponding region, rather than the average of the 100 or so TrueWind cells in that area.

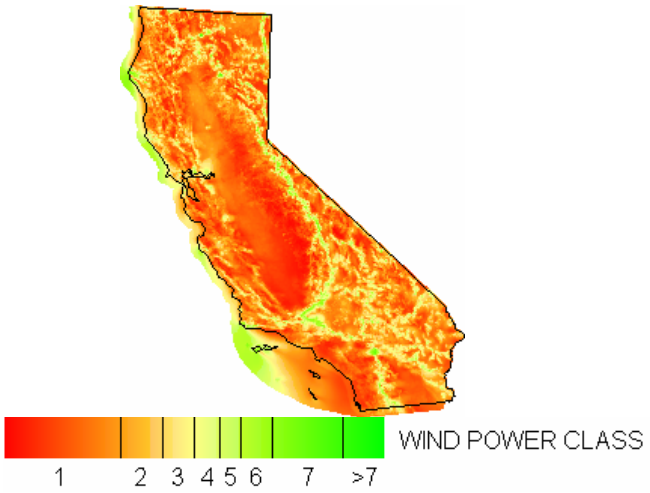

Figure 7. Annual Average Capacity Factor for Grid Cells in California

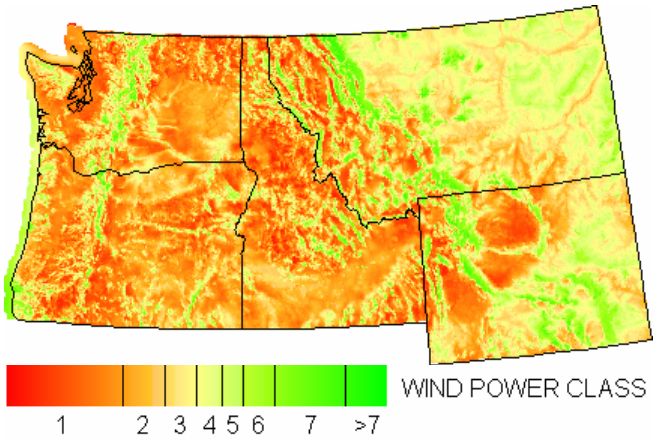

Figure 8. Annual Average Capacity Factor for Grid Cells in the Northwest

From Figure 7, we can see that areas with Class 4 or better capacity factors in California are highly concentrated in certain coastal regions, along the Sierra Nevada mountain range, and in the southeastern part of the state. In the Northwest (Figure 8), good wind resources are found in a greater percentage of the grid cells than in California, and are also more widely dispersed. The windiest areas are found along mountain ranges and the coast, and in the hilly areas of eastern Montana and Wyoming.

3.2.2.2 Effect of Wind Timing on Load-Weighted Capacity Factor

Figure 9 and Table 6 show the fractional difference between the load-weighted capacity factor and the annual average capacity factor at grid cells in California and the Northwest, using the TrueWind data. The results are shown separately for three sets of cells:

1) all grid cells in California or the Northwest ("All Classes");
2) only those grid cells with annual average capacity factors greater than 0.316, equivalent to a Class 4 or better wind site ("Class 4+"); and

3) Class 4+ cells within 20 km of the anemometer sites, which we used as markers for some of the major potential wind resource areas in each region ("Near Anem.").

According to the TrueWind data, there is a wide range of impacts in California: during the top 10 percent of peak demand hours, the middle 80 percent of Class 4+ grid cells produce between 30 percent below and 7 percent above their annual average power output. In the Northwest, output from the Class 4+ grid cells during peak load hours is in a more positive and slightly narrower range; the middle 80 percent of these cells produce between 6 percent and 34 percent above their annual average output during peak hours. In both California and the Northwest, the peak-hour output at Class 4+ grid cells near some of the known resource areas was more variable than at the Class 4+ cells throughout the entire region, indicating that disproportionately many of the best- and worst-timed TrueWind grid cells are near the known resource areas. Overall, about 93 percent of all California grid cells had load-weighted capacity factors worse than their annual average, while only 9 percent of Northwestern cells had load-weighted capacity factors worse than their annual average.

Both Northwestern wind and electricity loads generally peak in the winter, while California wind and loads peak in the summer. However, the match between the wind and electricity demand appears to be better in the Northwest, based on the TrueWind data. According to the TrueWind model, California wind speeds rise too late on summer days to create a close match between wind production and summer-afternoon peak load. However, as will be discussed in Section 4, the available anemometer data disagree with the TrueWind model on the effects of wind timing in California, and suggest that California wind is better matched to California loads than Northwest wind is to Northwest loads. As already noted, it is not clear which data source is more correct.

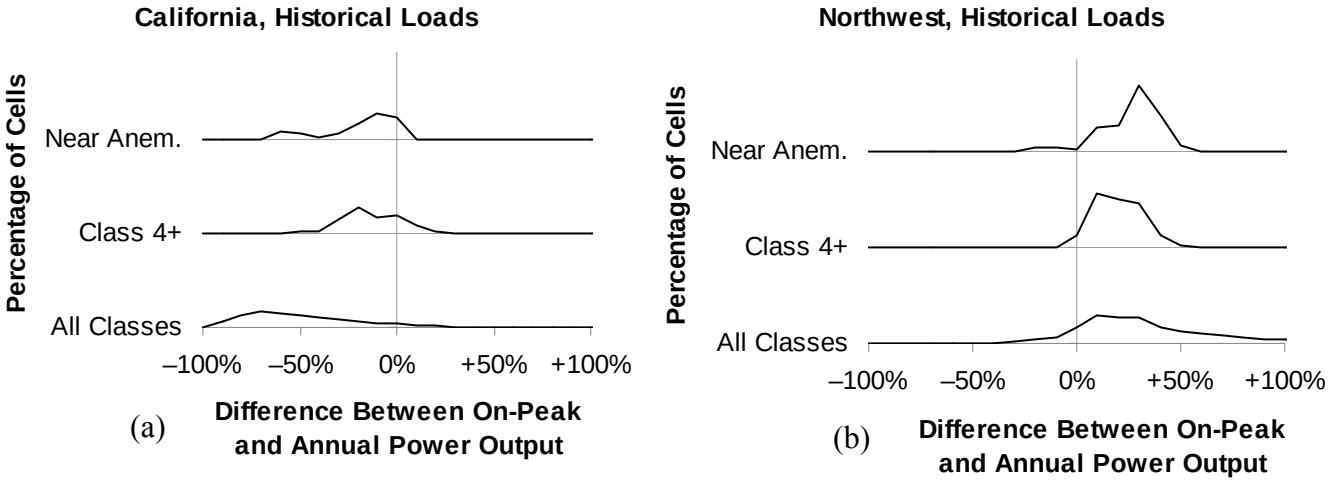

Figure 9. Effect of Wind Timing on Load-Weighted Capacity Factor for Grid Cells in California and the Northwest

Table 6. Effect of Wind Timing on Load-Weighted Capacity Factor in California and the Northwest

	Percentage Difference Between Load-Weighted and Annual Capacity Factor					
	California			Northwest		
	All Grid Cells	Class 4+ Grid Cells	Class 4+ Grid Cells Near Ane-mometers	All Grid Cells	Class 4+ Grid Cells	Class 4+ Grid Cells Near Ane-mometers
10th Percentile	–81.6%	–30.2%	–55.7%	+0.7%	+6.0%	+7.1%
Median	–55.2%	–14.8%	–12.9%	+27.5%	+19.7%	+28.4%
90th Percentile	–9.1%	+7.0%	+0.4%	+79.2%	+34.3%	+41.4%

Figure 10 shows the effect of wind timing on the load-weighted capacity factor for cells in each of the seven wind classes. Generally, the peak-hours performance varies more widely from the annual average performance among sites with lower annual wind speeds, and more narrowly at sites with higher wind speeds. This figure also shows that the match between TrueWind wind speeds and historical loads in California is worse than in the Northwest for all wind classes, although timing seems to have a more positive impact in California at windier sites.

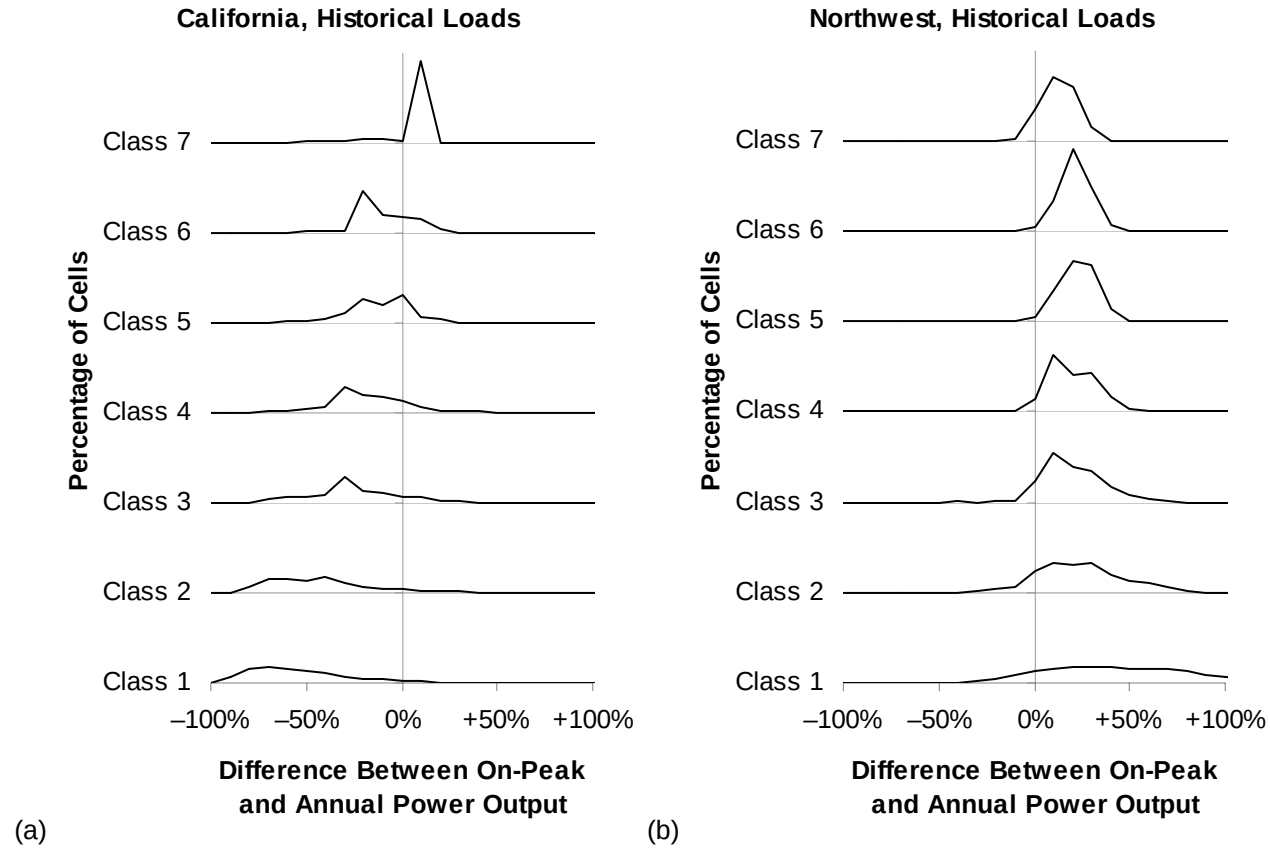

Figure 10. Effect of Wind Timing on Load-Weighted Capacity Factor for Grid Cells in Each Wind Class in California and the Northwest

Figure 11 illustrates the geographic distribution of the effect of wind timing in California. Figure 11a shows the effect of wind timing on the load-weighted capacity factor at all grid cells in the state, while Figure 11b shows only those cells with average capacity factors greater than 0.316 (Class 4+). As might be expected from the previous discussion, capacity factors during peak hours are worse than the annual average in most areas of the state. However, grid cells along the Pacific coast and in parts of the Sierra mountains are found to perform about the same during peak demand hours as they do at other times of year, and small areas in the northwest corner of the state and in Inyo County (east-central California) have peak-hour capacity factors significantly greater than their annual average capacity factors.

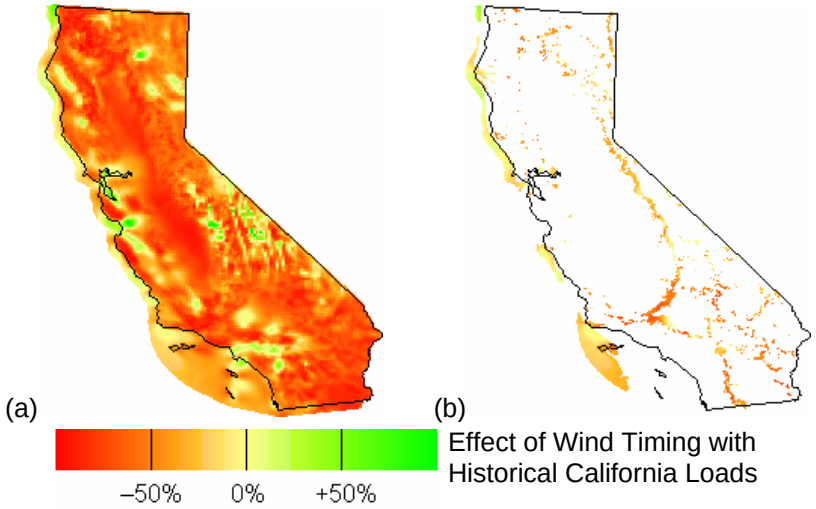

Figure 11. Fractional Difference Between Annual Average Capacity Factor and Load Weighted Capacity Factor at All Grid Cells (a) and Class 4+ Cells (b) in California

California's major wind passes have summer-peaking winds, so it may be surprising that the timing of wind – according to TrueWind estimates – is found to reduce project capacity factors during peak hours in these locations. As we show later, there are significant differences between the TrueWind estimates of temporal wind profiles in California's major wind passes and our anemometer-based wind speed measurements, with the anemometer-based measurements suggesting a more positive temporal profile. These differences are explored in Section 5.

Figure 12 shows the effect of wind timing on the load-weighted capacity factor at grid cells in the Northwest, based on the TrueWind data. Most Northwestern grid cells do as well or better during peak load hours as they do on average during the year. This is probably due to the fact that winds in the Northwest come predominantly during the winter, which is when loads have also historically peaked. Wind sites along the Pacific coast, the western slope of the Cascade Range, near the Idaho/Montana border, in western Montana and in central Wyoming are particularly well matched to historical peak loads. Only a few good sites in central Washington and near the Oregon/Idaho border have peak-hour capacity factors worse than their annual averages.

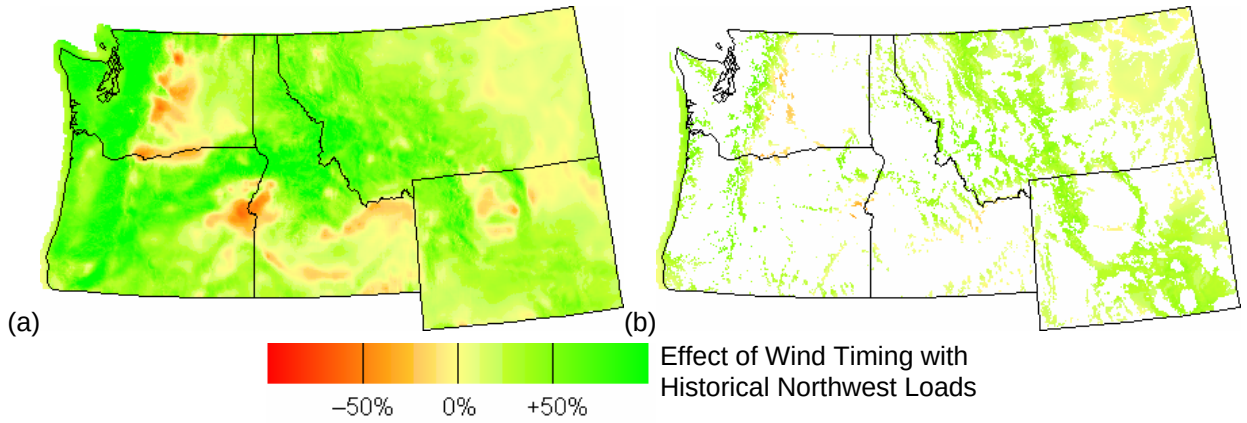

Figure 12. Fractional Difference Between Annual Average Capacity Factor and Load Weighted Capacity Factor at All Grid Cells (a) and Class 4+ Cells (b) in the Northwest

3.2.2.3 Value of Northwest Wind Power in California, and Vice-Versa

We also investigated the possibility that wind power in the Northwest might be better matched to California's electricity load than California wind power is, or that California wind power might be more useful in the Northwest than in California. We did this by recalculating the effect of wind timing on the load-weighted capacity factor, assuming Northwest wind power was used in California, and California wind power was used in the Northwest. The results of this analysis are shown in columns 2 and 4 of Table 7, along with the results presented earlier for wind power that does not cross regional borders (columns 1 and 3).

Table 7. Effect of Wind Timing on Load-Weighted Capacity Factor in California and the Northwest, Using Peak Hours from the Opposite Region

	Percentage Difference Between Load-Weighted and Annual Capacity Factor, Class 4+ Cells			
Wind Power Flow	California ↓ California	Northwest ↓ California	California ↓ Northwest	Northwest ↓ Northwest
10th Percentile	–30.2%	–49.0%	–14.5%	+6.0%
Median	–14.8%	–32.8%	–3.2%	+19.7%
90th Percentile	+7.0%	–13.9%	+10.2%	+34.3%

Comparing the four columns of Table 7, we find that the load-weighted capacity factors are more dependent on the electricity load series than on the wind resource being considered. Both California and Northwestern wind appear better matched to Northwestern loads than to California loads. However, this difference is much more pronounced for Northwestern wind than for California wind. As a result, the Northwest's winter-peaking loads are best matched by Northwestern wind power, while California's summer-peaking loads are best matched by California wind power.

3.2.2.4 Effects of Wind Timing Near Known Resource Areas

The results reported earlier in this section are primarily based on an analysis of all cells on the California or Northwestern TrueWind grid, or all cells with annual average wind power equivalent to Class 4 or higher. However, many areas included in such a broad analysis are unlikely to be developed, particularly those in environmentally sensitive areas or remote areas with inaccessible terrain. For example, many of the Class 4+ cells in California are along ridge tops in the Sierra Mountains, which are not commercially viable sites despite their high average wind speeds. In this section, we limit our analysis to areas of the TrueWind grid that are within 20 km of existing anemometer sites, as discussed in Section 2.4 and shown in Figures 1 and 2. This allows us to assess the effects of wind timing in the areas that are likely most promising for wind power development. We should note, however, that the areas that could be subject to wind development may in some cases be only a small subset of the cells in each of these resource areas; they may also consist of narrow corridors or passes that are too small even to be clearly resolved by the TrueWind model.

Figure 13 shows the range of effects that wind timing has on the load-weighted capacity factor when using historical California loads, at Class 4+ cells in each of the major wind resource areas that we identified. The plot shows the median effect and the range between the 10th and 90th percentiles of cells in each resource area. Given the limited geographic extent of these areas, timing has a surprisingly wide range of effects within each area, often coming close to the range of effects found in the whole state or multi-state region. According to the TrueWind data, wind speeds at most known resource areas have a somewhat negative match to historical California loads. Within each region, some resource areas appear better matched to California loads than others. For example, wind in the northern California areas and around San Gorgonio appears better matched to California demands than wind in the other southern California areas. Wind from the Columbia Hills area in Washington and the Cape Blanco area in Oregon also appears well matched to historical California loads.

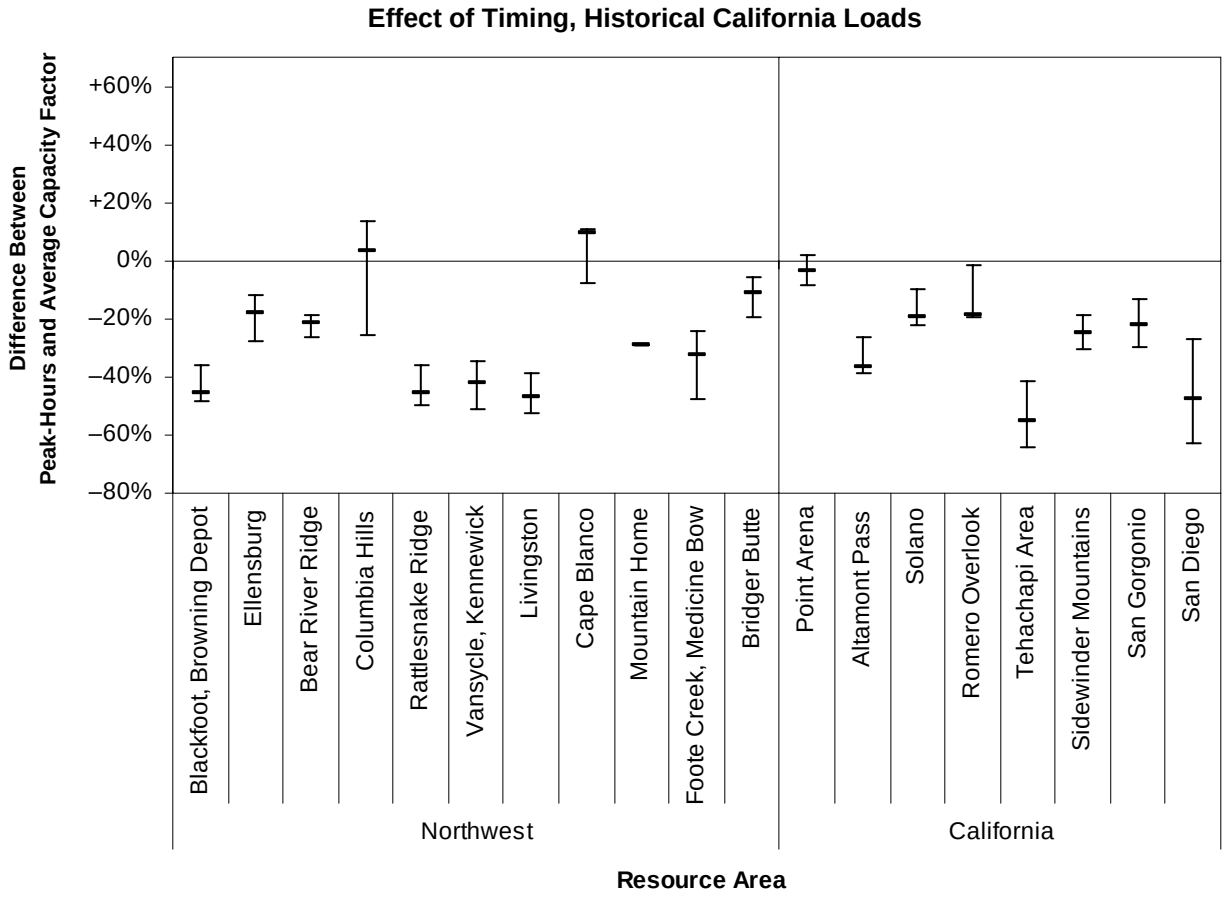

Figure 13. Effect of Wind Timing on Load-Weighted Capacity Factor at Class 4+ Grid Cells Near Individual Wind Resource Areas, Using Historical California Loads (Median and 10th–90th Percentile Range)

Figure 14 shows the effect of wind timing on the load-weighted capacity factor at Class 4+ grid cells near each of the anemometer sites, when using historical Northwestern loads. As with California loads, the range of effects is quite wide, even within limited geographical areas. Northwestern demand appears to be best served by wind power from the Bear River Ridge area in Washington, Browning Depot and Livingston in Montana, and the Medicine Bow area in Wyoming. Wind near the southern California anemometers also seems to be relatively well matched to Northwestern demand, at least compared to Altamont, Solano, and Romero Overlook.

Comparing Figure 14 to Figure 13 we see that wind power from the Columbia Hills (WA), Altamont Pass (CA) and Romero Overlook (CA) areas may be better matched to historical California loads than to historical Northwestern loads. Winds in southern California and most other areas of the Northwest appear to match the Northwest's historical loads better than California's.

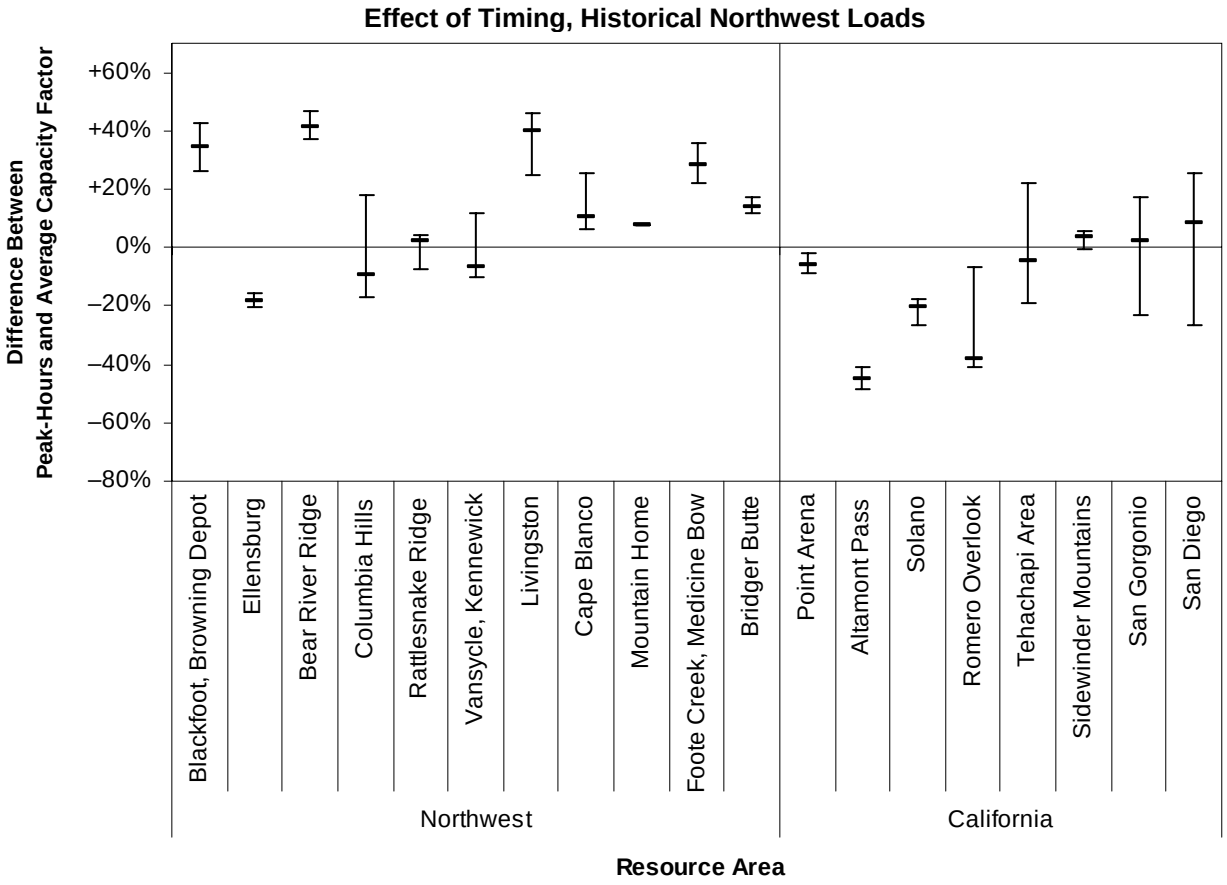

Figure 14. Effect of Wind Timing on Load-Weighted Capacity Factor at Class 4+ Grid Cells Near Individual Wind Resource Areas, Using Historical Northwestern Loads (Median and 10th–90th Percentile Range)

3.3 Price-Based Measures of Wind Value

Another useful metric of the value of different wind sites relates to the correlation of wind output with historical or expected wholesale market prices. This section addresses those correlations. As in the previous section, we first discuss the methods used to assess the wholesale market value of wind production at different sites, and then report results.

3.3.1 Methods

To evaluate the comparative impact of wind timing on the wholesale market value of wind power production at each cell on the TrueWind grid, we compared the wholesale value of wind under two scenarios: one in which wind production does not vary with time and is a price-taker on the wholesale market, and another where wind production does vary with time and wind remains a price taker. In reality, wind farms are unlikely to be "price takers" in wholesale markets, because developers typically arrange long-term power sales agreements. However, this method gives a simple estimate of how valuable power from each location will be for the system as a whole, relative to a flat block of power. To the extent that long-term and short-term markets

tend to balance, these estimates may also give some information about the real revenues available to wind farm developers at each location.

3.3.1.1 Annual Market Value with Unvarying Power Output

We first estimated the total market value of the power that could be produced at each grid cell if the timing of the power output from the wind turbines were uncorrelated with wholesale market prices. This is the value that would be achieved by a turbine with unvarying year-round power output, or power output that varies independently of market prices. Such a turbine would effectively have a market value equal to the annual average market price multiplied by its total power output for the year. These average annual prices – the sources of which were discussed in Section 2 – are shown in Table 8.

Table 8. Historical and Forecast Annual Average Power Prices for California and the Northwest

	California	**Northwest**
Historical Average Price (nominal)	$26.6/MWh	$35.3/MWh
Forecast Average Price (nominal)	$41.6/MWh	$52.2/MWh

3.3.1.2 Annual Market Value with Time-Varying Power and Price

We next estimated the annual market value for each TrueWind grid cell when the temporal variation of wind power output and wholesale market prices are both considered. We performed this analysis for all cells on the TrueWind grid, with both historical market prices and prices forecast for 2006 onward.

Total market value was calculated by multiplying the power production estimate for each month-hour at each location by the average wholesale electricity price for the same month-hour, then by the number of days in that month, and then summing over the year.

We also calculated the average wholesale price for all power produced at each site. This is simply the total annual market value divided by the annual power output.

Sites with particularly good wind timing will have market values above those expected for an equally good site with invariant wind speeds, so they will realize average prices above the market-wide average prices shown in Table 8. Those with worse timing will have lower market values, leading to average prices that are below the system average.

3.3.1.3 Difference Between Time-Variant and Time-Invariant Market Value

To quantify the effect of wind timing on the market value of power from each location, we calculated the fractional difference between the annual value with time-varying power

production and the annual value with invariant or otherwise uncorrelated power production.[20] The fractional difference (*f*) in market value at each site is defined by the equation

$$f = \frac{v_{\text{var}} - v_{inv}}{v_{inv}} = \frac{v_{\text{var}}}{v_{inv}} - 1,$$

where v_{inv} is the market value with invariant power output and v_{var} is the value with time-varying output and prices. This fractional difference also shows the fractional change in realized wholesale prices at each site. That is, the average power price at each site will deviate from the annual average price for the whole power system by the same fraction as the time-varying market value at each site differs from the time-invariant value.[21]

3.3.2 Results

3.3.2.1 Effect of Wind Timing on Wholesale Market Value

Figures 15 and 16 show the range of effects of wind timing on the wholesale value of power, for TrueWind grid cells in California and the Northwest, based on historical and forecast prices. Table 9 shows the same information in tabular form, for Class 4 and better grid cells. The timing of wind reduces wholesale values by about zero to 6 percent at wind sites in California, using historical prices, or zero to 4 percent according to forecast prices. Market values at sites in the Northwest appear to be unaffected or improved by up to about 3 percent by the correspondence of wind timing with historical power prices. When Northwest wholesale prices forecast for 2006–25 are used instead, temporal wind patterns reduce market values by about 1 percent at the worst-timed Northwest sites, and increase market values by about 2 percent at the best-timed sites. Using either historical or forecast prices, the timing of wind at Class 4+ sites within 20 km of existing anemometers appears to be slightly worse than generally found for Class 4+ sites throughout California, and slightly better than the general range for Class 4+ sites in the Northwest.

[20] We neglect the fact that power output that is invariant during the year could contribute more to system reliability than power output that varies independently of power prices. This analysis only considers the expected wholesale market value of power, which is the same for invariant or independently varying power.

[21] Meyer and Luther (2004) use a similar technique for hourly solar power output in Germany in 2001. However, they report the ratio between the value of time-variant power and time-invariant power (v_{var}/v_{inv}), rather than the fractional difference between the two.

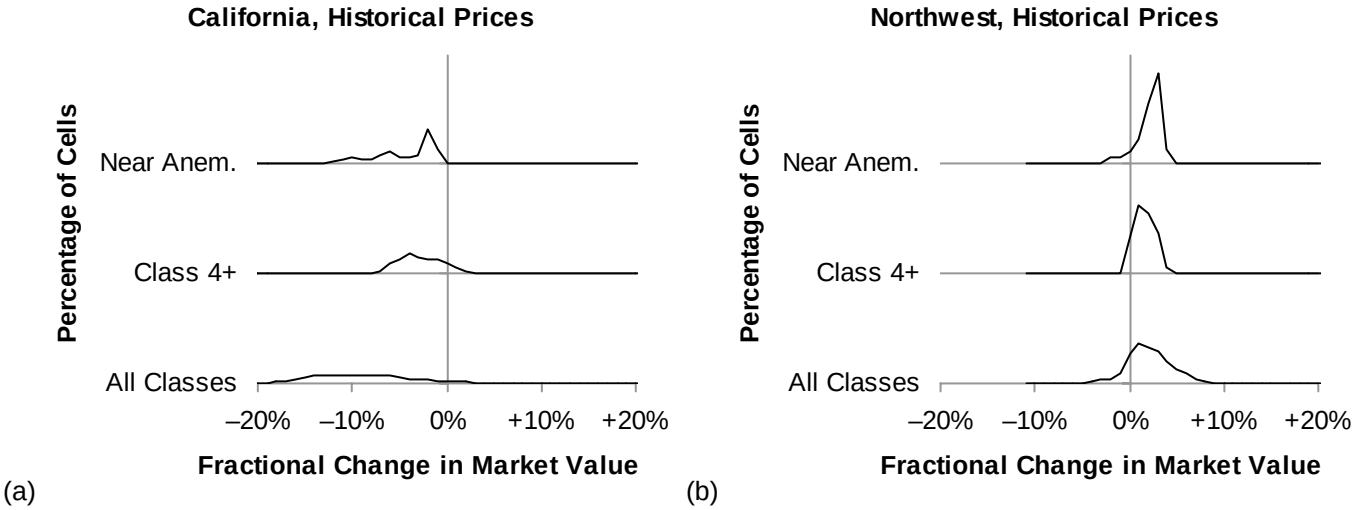

Figure 15. Effect of Wind Timing on Market Value for Grid Cells in California and the Northwest, Using Historical Power Prices

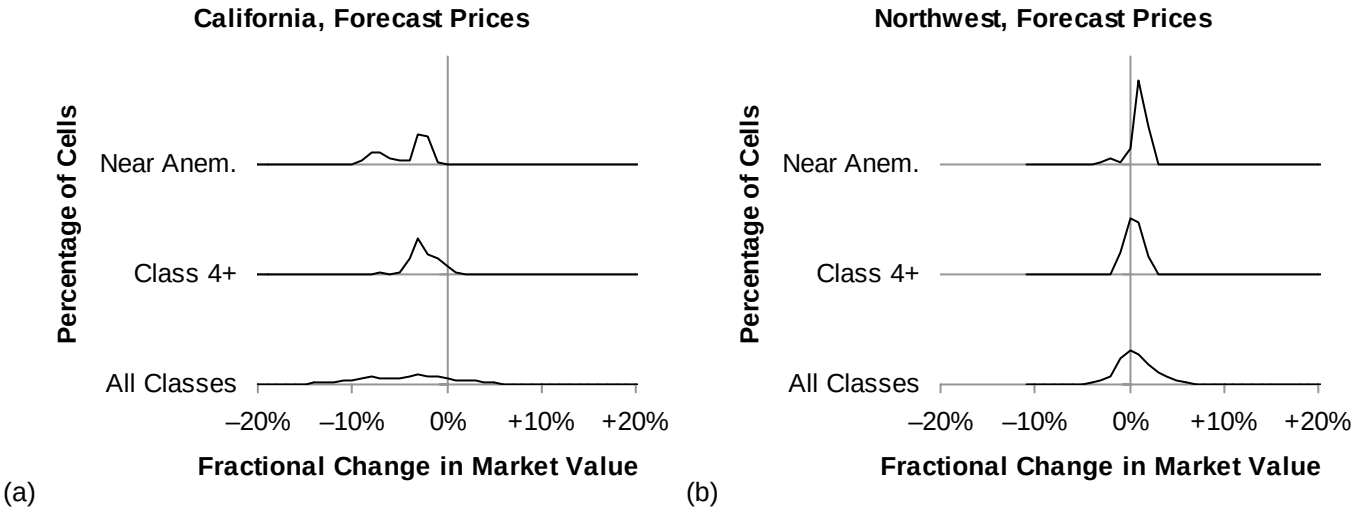

Figure 16. Effect of Wind Timing on Market Value for Grid Cells in California (a) and the Northwest (b), Using Forecast Power Prices

Table 9. Percentage Change in Market Value of Power Due to Wind Timing at Class 4+ Grid Cells in California and the Northwest, with Historical and Forecast Power Prices

Effect of Wind Timing on Market Value (%)	With Historical Prices		With Forecast Prices	
	California	Northwest	California	Northwest
10th Percentile	–5.7%	+0.3%	–3.8%	–0.6%
Median	–3.2%	+1.5%	–2.7%	+0.4%
90th Percentile	+0.3%	+2.9%	–0.3%	+1.6%

In general, sites with winds that are one wind power class apart would be expected to have annual market values that differ by about 15 percent, based on the difference in their annual average capacity factor. Consequently, the differences in market value between the best- and

worst-timed sites in our analysis are equivalent to a change of about one-quarter of a wind power class.

Table 10 shows the effects of wind timing on the average price that could be received for power from grid cells with Class 4 or greater wind speeds, assuming that wind power is sold into a local wholesale market. The difference in average power price between the best and worst sites is around $1.00–$1.50 per megawatt-hour, which is about 2–6 percent of the system average prices shown in Table 8.

Table 10. Change in Effective Price of Power Due to Wind Timing, Class 4+ Grid Cells

Effect of Wind Timing on Market Value ($/MWh, nominal)	With Historical Prices		With Forecast Prices	
	California	Northwest	California	Northwest
10th Percentile	–$1.5 / MWh	+$0.1 / MWh	–$1.6 / MWh	–$0.3 / MWh
Median	–$0.9 / MWh	+$0.5 / MWh	–$1.1 / MWh	+$0.2 / MWh
90th Percentile	+$0.1 / MWh	+$1.0 / MWh	–$0.1 / MWh	+$0.8 / MWh

Figures 17 and 18 show that the effects of wind timing are more narrowly distributed at windier sites. In California, it is also generally more positive at windier sites, using either historical or forecast prices.

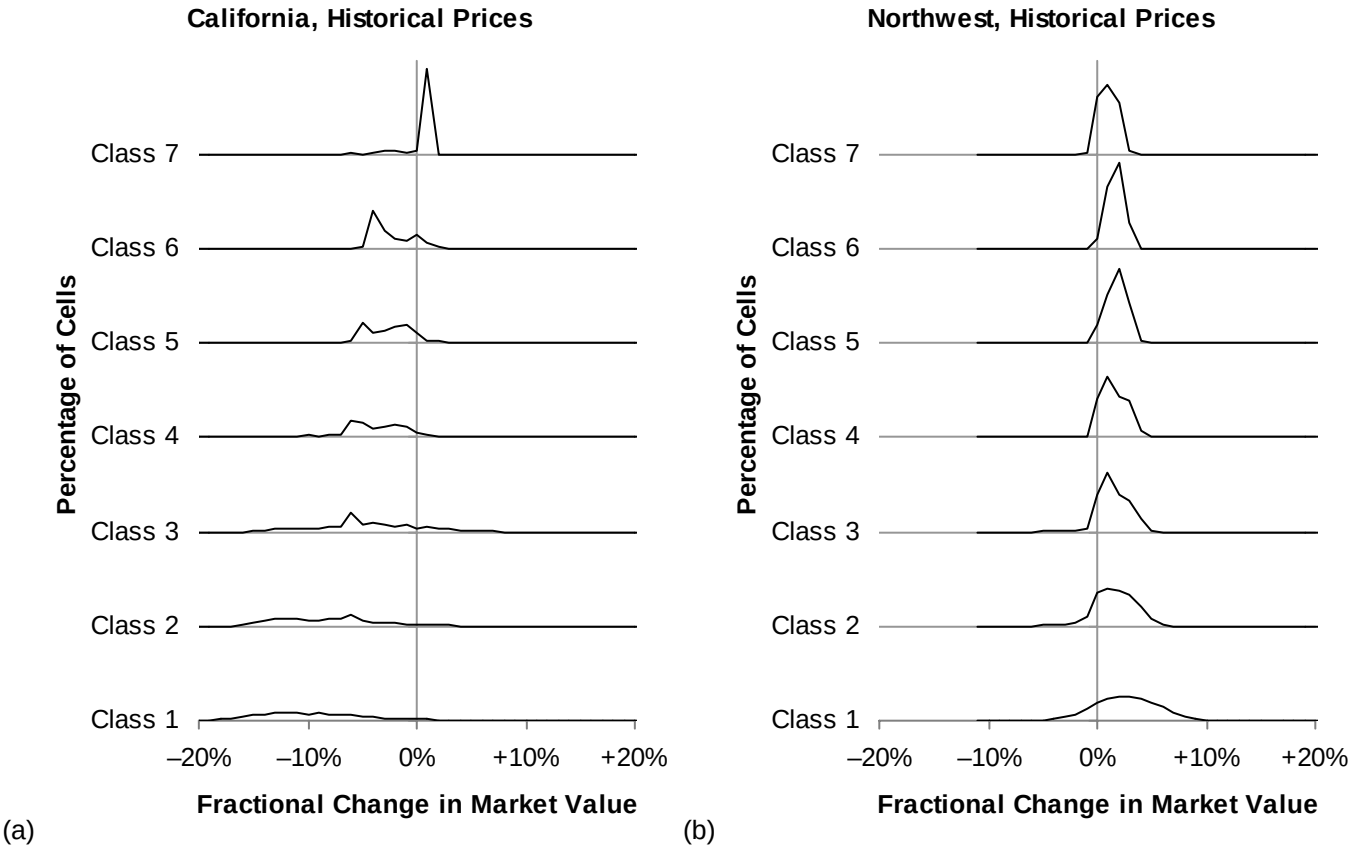

Figure 17. Effect of Wind Timing on Market Value for Grid Cells in Each Wind Class in California (a) and the Northwest (b), Using Historical Power Prices

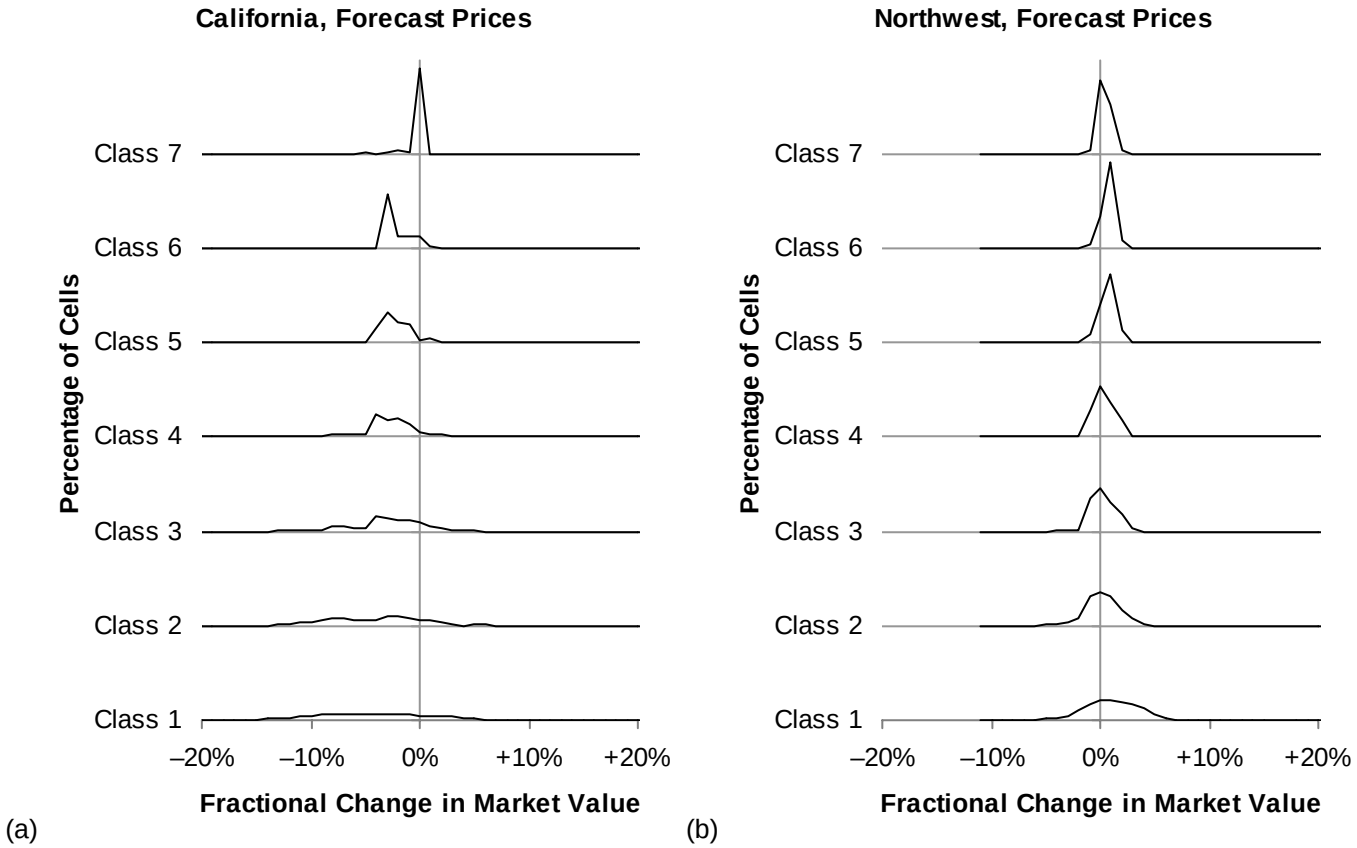

Figure 18. Effect of Wind Timing on Market Value for Grid Cells in Each Wind Class in California (a) and the Northwest (b), Using Forecast Power Prices

Figure 19a shows in map form the fractional change in the market value of power at each location on the California TrueWind grid due to wind timing, based on historical prices. From this figure, we can see that California has some sharply defined regions where wind timing could boost market values by as much as 10 percent, based on historical prices. However, most of these locations have average wind speeds below Class 4. The value of wind power at locations on the northernmost coast of California is improved due to the coincidence of its expected electricity production with historical power prices, but almost all other high-wind regions in the state (Figure 19b) appear to have temporal patterns that are neutral or somewhat poorly matched to wholesale market prices, based on the TrueWind data set.

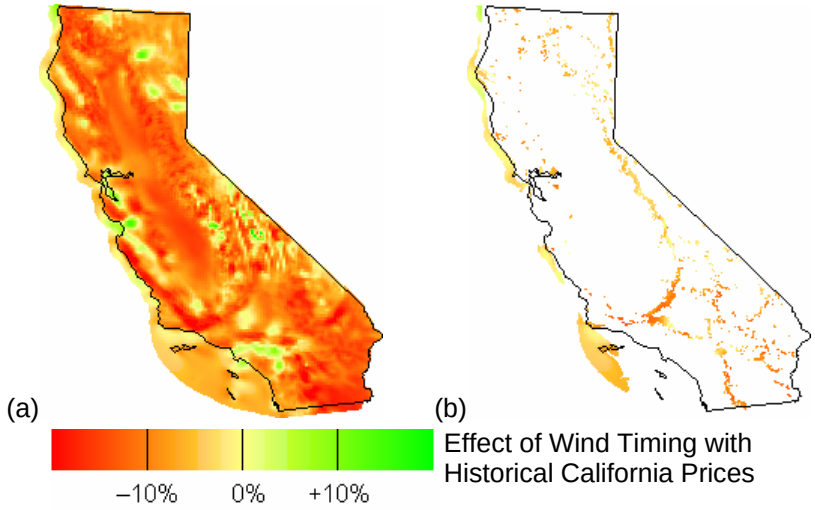

Figure 19. Percentage Change in Market Value of Power due to Temporal Wind Patterns at All Grid Cells (a) and Class 4+ Grid Cells (b) in California, Based on Historical Power Prices

When prices forecast for 2006–13 are used, the effect of wind timing generally improves throughout the state (Figure 20); the effect of timing at many sites moves from negative to neutral, but the overall pattern of which regions have the best or worst timing remains largely the same.

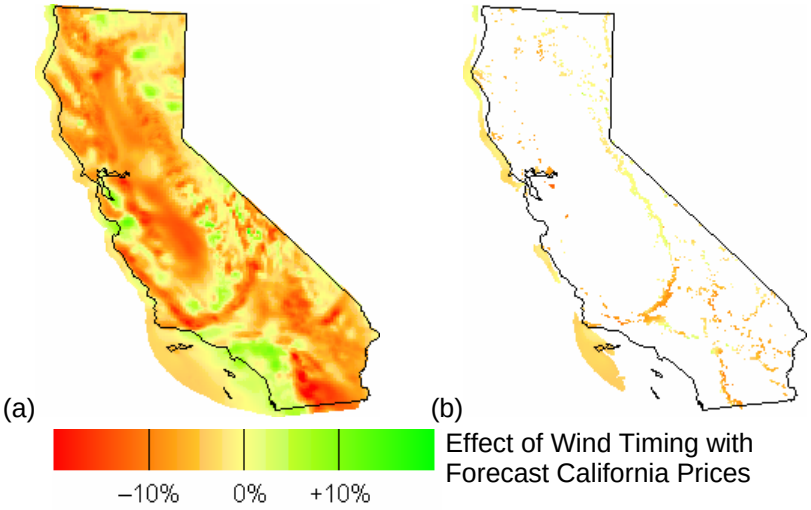

Figure 20. Percentage Change in Market Value of Power due to Temporal Wind Patterns at All Grid Cells (a) and Class 4+ Grid Cells (b) in California, Based on Forecast Power Prices

The historical and forecast wholesale power price series for California use nearly the same diurnal profiles for each month, so the improved effect of wind timing when using the forecast series is mostly explained by the time of year (rather than times of day) when power prices are high. The historical prices had especially strong peaks in July through September, while the forecast calls for prices that are more evenly distributed throughout the year. The TrueWind wind speeds in most of California are better matched to the flatter forecast than to the strongly summer-peaking historical prices. However, as will be shown in Section 3.3.2.3, the value of

wind is reduced somewhat when forecast prices are applied to the output from the local areas around well-known wind resource areas in northern California (Point Arena, Altamont, Solano and Point Romero).

As with the load-weighted capacity factor results discussed in Section 3.2.2.2, and as discussed further in Section 5, these results are different from those found via anemometer data and conventional wisdom for the summer-peaking California passes. As discussed in Section 4 and Appendix A, it is possible that the TrueWind data provide a more accurate picture than the anemometers, but this disagreement cannot be resolved conclusively without more turbine-height wind speed measurements.

Figures 21 and 22 show the fractional change in market value due to the timing of the wind in each grid cell in the Northwest. When historical prices are used (Figure 21), the timing of wind appears to significantly improve the value of power from cells dispersed throughout the Northwest, including along the coast of northwestern Washington, along the west side of the Cascade Range in Washington and Oregon, near the mouth of the Columbia River, in central Idaho, southwestern Montana, and throughout Wyoming.

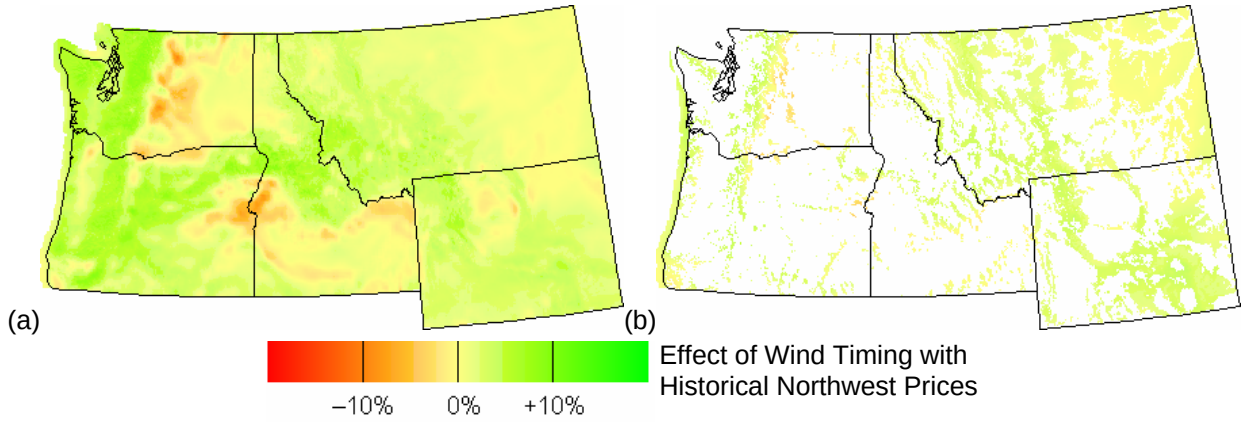

Figure 21. Percentage Change in Market Value of Power due to Temporal Wind Patterns at All Grid Cells (a) and Class 4+ Grid Cells (b) in the Northwest, Based on Historical Power Prices

When average prices forecast for 2006-2025 are used for this analysis (Figure 22), the effects of wind timing follow the same general geographic pattern, but become somewhat less positive. This change appears to be due to the fact that the forecast price series is more summer-peaked than historical prices, and the Northwest's predominantly winter-peaking winds are more poorly matched with this price series.

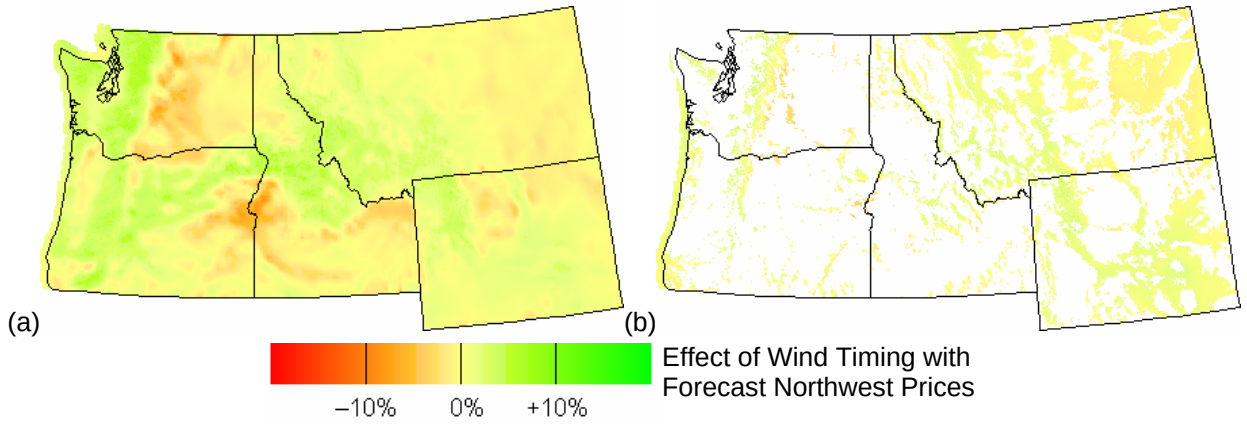

Figure 22. Percentage Change in Market Value of Power due to Temporal Wind Patterns at All Grid Cells (a) and Class 4+ Grid Cells (b) in the Northwest, Based on Forecast Power Prices

3.3.2.2 Value of Northwest Wind Power for California, and Vice-Versa

We also investigated the possibility that wind power in the Northwest might be better matched to California's electricity prices than California wind power is, or that the Northwest might make better use of California wind power than local wind power. To do this, we recalculated the effects of wind timing on the market value of power, assuming the Northwest imported wind power from California, and vice-versa. The results of this analysis are shown in Table 11, along with values for in-state sales, reproduced from Table 9.

Table 11. Percentage Change in Market Value of Power Due to Wind Timing at Class 4+ Grid Cells in California and the Northwest, with Power Prices from the Opposite Region

	With Historical Prices				With Forecast Prices			
Wind Power Flow	CA ↓ CA	NW ↓ CA	CA ↓ NW	NW ↓ NW	CA ↓ CA	NW ↓ CA	CA ↓ NW	NW ↓ NW
10th Perc.	–5.7%	–6.7%	–1.3%	+0.3%	–3.8%	–3.1%	–2.2%	–0.6%
Median	–3.2%	–4.8%	–0.5%	+1.5%	–2.7%	–1.5%	–1.5%	+0.4%
90th Perc.	+0.3%	–1.2%	+0.8%	+2.9%	–0.3%	+1.5%	0.0%	+1.6%

From Table 11, it appears that California's historical wholesale power prices are slightly better served by California wind, while the Northwest's historical prices are better served by Northwestern wind. However, when forecast prices are used, both regions appear to be better-served by Northwestern wind. Moreover, the choice of price series makes a bigger difference to market value than the location of the wind farm: wind output from either region appears better matched to Northwestern prices than California prices, using either historical or forecast market conditions. Within each region, the effects of timing also vary significantly among different resource areas, as will be shown in the next section.

3.3.2.3 Effects of Wind Timing Near Known Resource Areas

Historical California Prices. Figure 23 shows the effect of wind timing on the wholesale market value of wind-generated electricity at Class 4+ cells near anemometer sites in California

and the Northwest, using California's historical power prices. The pattern is much the same as for the load-weighted capacity factors in Figure 13, although the size of the effect is about one seventh as great. Based on the TrueWind data, timing has a wide range of effects within each area, sometimes similar to the range of effects found in the whole state or region. The Columbia Hills, Cape Blanco and Bridger Butte areas in the Northwest appear better matched to California's historical power prices than any of the California areas. Among California resource areas, Point Arena, San Gorgonio and the Sidewinder Mountains appear to be best matched to the state's historical prices.

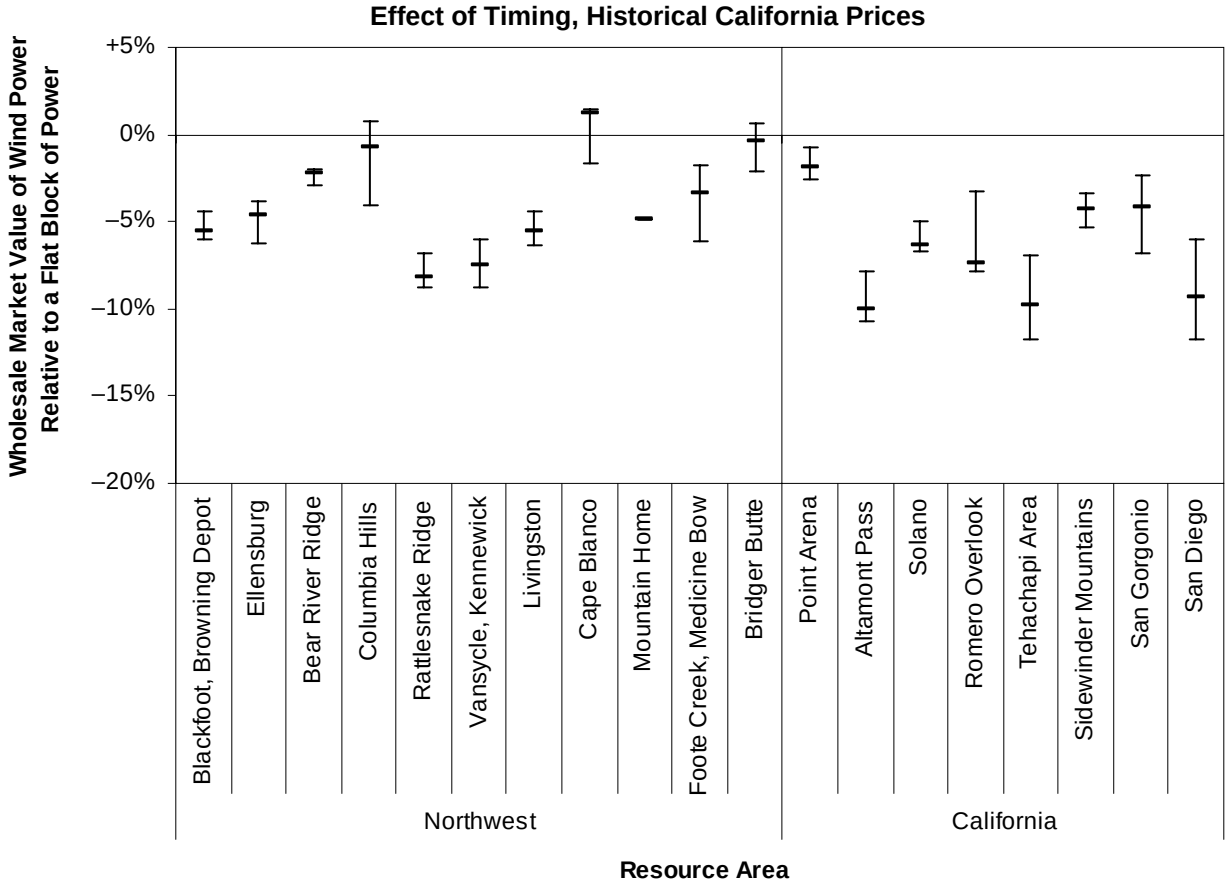

Figure 23. Effect of Wind Timing on Market Value of Power in Individual Resource Areas, Based on Historical California Prices (Median and 10th–90th Percentile Range)

Forecast California Prices. Figure 24 shows the same information as Figure 23, but considers the forecast price series for California instead of historical prices. When California's flatter forecast prices are used, the effect of timing becomes a little more positive than when historical California prices are used, particularly for Northwestern sites. The relative standing of most resource areas is approximately the same with either California price series, but the Bear River Ridge and Browning Depot areas get an extra boost when using the forecast prices. The northern California resource areas perform slightly worse with forecast prices than with historical prices, while the southern California areas perform better with forecast than historical prices.

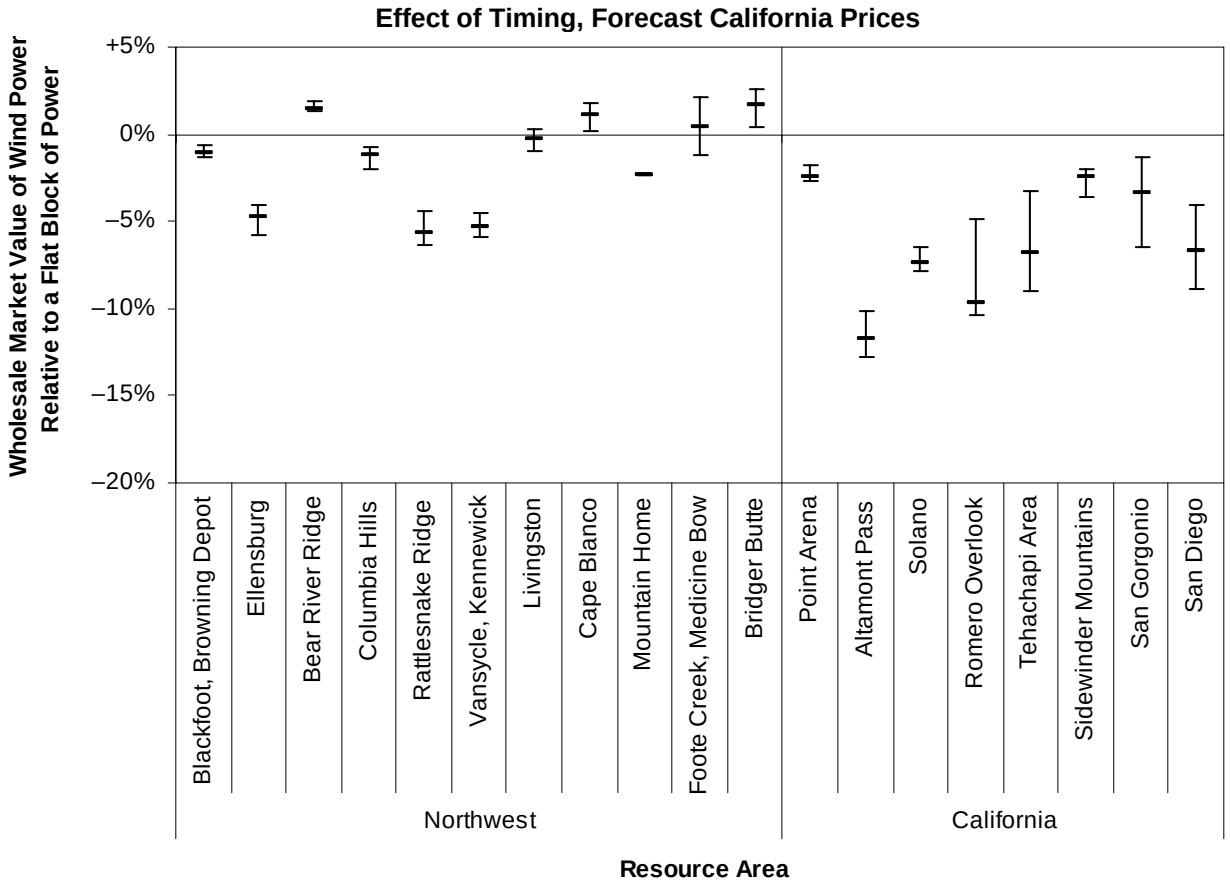

Figure 24. Effect of Wind Timing on Market Value of Power in Individual Resource Areas, Based on Forecast California Prices (Median and 10th–90th Percentile Range)

Historical Northwest Prices. Figure 25 shows the effect of wind timing on the value of power at Class 4+ grid cells in each of the previously noted resource areas, based on the Northwest's historical wholesale power prices. The pattern is similar to that found for the load-weighted capacity factor (Figure 14), although the size of the effect is not as dramatic. As with the load-weighted capacity factor, the Browning Depot, Bear River Ridge, Livingston and Medicine Bow areas appear to have wind output that is well correlated with Northwestern market prices, but Bridger Butte is also in a similar range. Grid cells near Ellensburg, the Columbia Hills, Vansycle and Rattlesnake Ridge have lower market values than equally windy sites in other parts of the Northwest; all of these except Rattlesnake Ridge also had load-weighted capacity factors lower than their annual average capacity factor. According to the TrueWind data, California resource areas are generally worse matched to the Northwest's historical prices than are the Northwestern resource areas. Among the California sites, those in southern California seem best matched to the Northwest's historical power prices, matching them about as well as would a flat block of power.

Comparing Figure 25 to Figure 23, it appears that winds in the Columbia Hills and Cape Blanco resource areas are slightly better matched to variations in California's historical power prices than to Northwestern power prices; all the other resource areas we identified in California and the Northwest are better matched to the Northwest's historical prices than to California's.

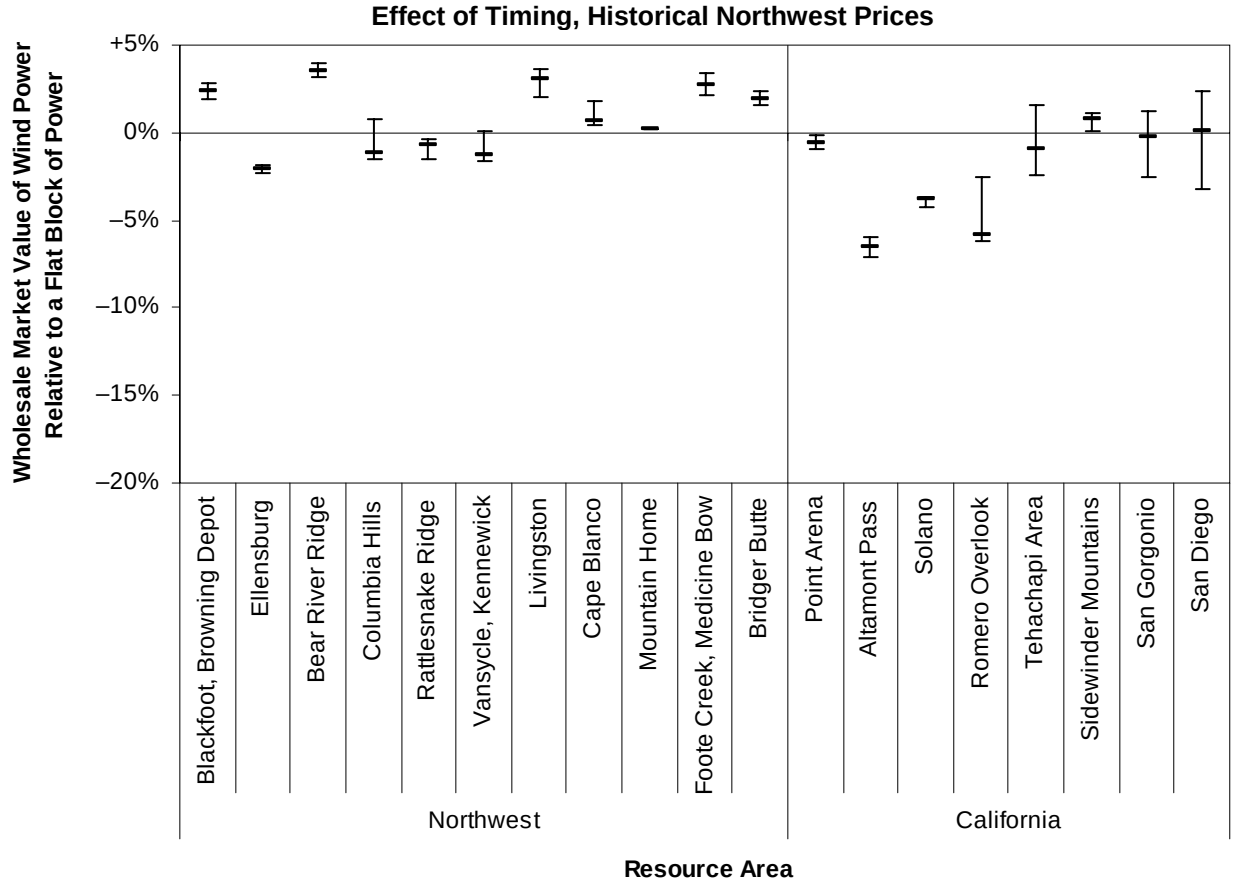

Figure 25. Effect of Wind Timing on Market Value of Power in Individual Resource Areas, Based on Historical Northwest Prices (Median and 10th–90th Percentile Range)

Forecast Northwest Prices. When the Northwest's forecast prices are used (Figure 26), the effect of wind timing is similar to what we found with historical Northwest prices. The relative standing of individual resource areas remains basically unchanged, but the effect of wind timing is slightly worse at most locations and slightly better at Altamont Pass, Solano and Romero Overlook in northern California. The improvement at these three locations appears to be due to relatively higher prices in June in the forecast series, as compared to historical prices.

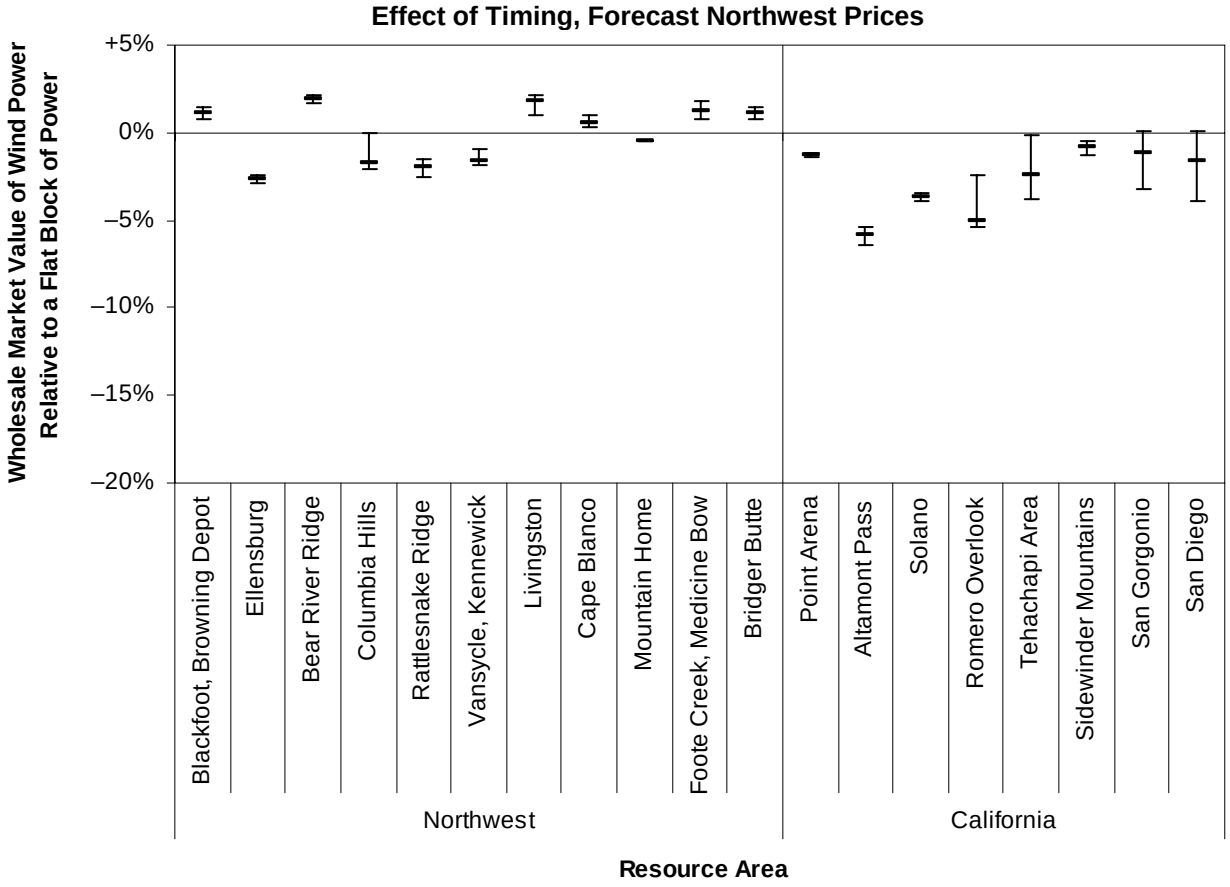

Figure 26. Effect of Wind Timing on Market Value of Power in Individual Resource Areas, Based on Forecast Northwest Prices (Median and 10th–90th Percentile Range)

3.4 Comparison of Capacity- and Market Value-Based Wind Value Metrics

Figure 27 reproduces earlier figures that show (a) the fractional change in load-weighted capacity factor and (b) the fractional change in market value as a result of wind timing, for grid cells in California, using historical loads and prices. The two maps are strikingly similar, indicating that these two measures are good predictors for each other. The coefficient of determination (R^2) for these two measures, across all grid cells, is 87 percent.

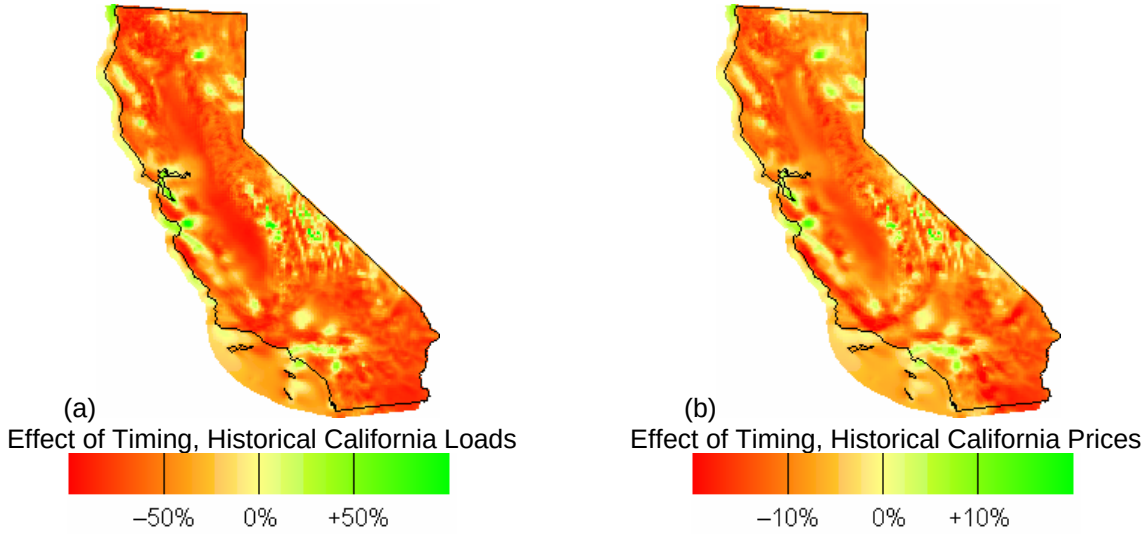

Figure 27. Fractional Changes in Peak-Hours Capacity Factor (a) and Market Value (b) Due to Wind Timing in California, Using Historical Load and Prices

Figure 28 shows the same two measures for the Northwest. The agreement between the load-based and price-based measures is also very good here, with an R^2 value of 84 percent.

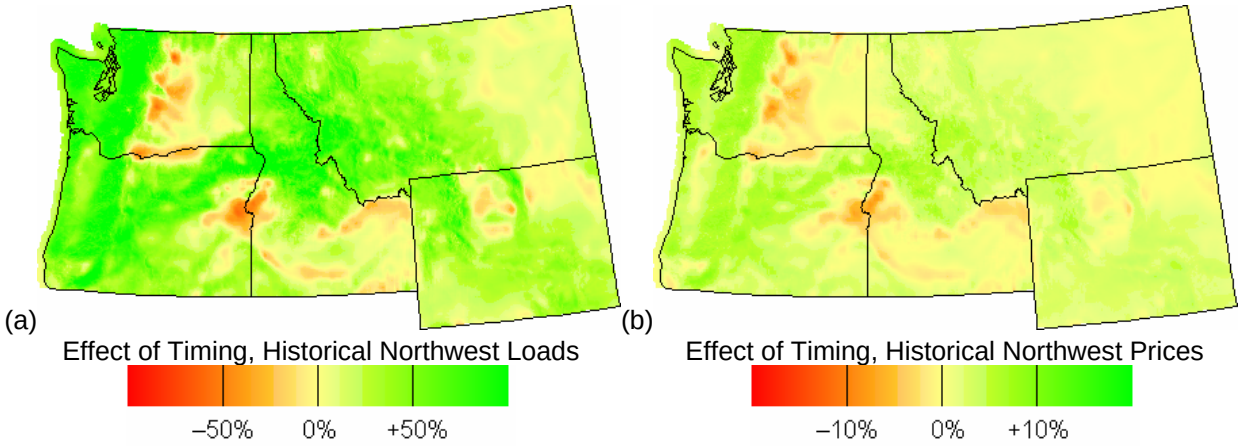

Figure 28. Fractional Changes in Peak-Hours Capacity Factor (a) and Market Value (b) Due to Wind Timing in the Northwest, Using Historical Load and Prices

4 Comparison of Results for TrueWind, Anemometer and Production Data

4.1 Background

The TrueWind modeled wind speeds are the most geographically comprehensive dataset of time-varying wind speeds available for California and the Northwest, making them ideal for the analysis in Section 3. However, the intra-annual wind speeds from TrueWind have not previously been used in published work, and have received little validation against real-world conditions. In Appendix A, we therefore compare the wind *speeds* reported in the TrueWind and anemometer datasets and discuss factors that could cause these datasets to disagree. In this section, we compare the previously presented TrueWind-based *value* estimates with results from similar analyses using both anemometer data (102 anemometers in the Northwest, and 78 anemometers in California) and limited data on actual wind plant output (from the three major California wind resource passes).

In Section 2.5 and Appendix A we describe a number of factors that make it difficult to resolve disagreements between these three datasets. The same factors also make it difficult to draw conclusions when the three datasets disagree about the effect of temporal wind speeds on the value of power at different locations, the subject of this section. When the three datasets produce similar estimates of the effect of wind timing on the value of power, we may be able to place some confidence in our findings, but when they disagree, it is not clear which result is more realistic. Further analysis, using higher-elevation anemometer data, additional wind power production data, or a more precise treatment of wind shear, is needed to identify the source of these disagreements.

For this section, we calculated many of the wind-value measures discussed earlier using both wind speed measurements from anemometer towers and TrueWind data from the nearest point to each anemometer tower on the TrueWind grid. We also performed these calculations with month-hour average power production data from *operating* wind farms in the Altamont, San Gorgonio and Tehachapi areas. The actual wind power production data might be expected to resolve disagreements between the TrueWind and anemometer data. However, much of this power production came from older turbines with towers shorter than our reference height; it is therefore not clear whether the production data are more representative of upper-level conditions than the anemometers. (Estimates of seasonal and diurnal power production from these datasets for each wind resource area are shown in Section 5.)

4.2 Region-Wide Effects of Wind Timing

Figure 29 shows the range of effects of wind timing on wholesale market value are load-weighted capacity factor, when using either anemometer measurements or TrueWind data for the same locations. The central bar for each measure represents the median effect of wind timing among all anemometer sites (or associated TrueWind cells), and the lower and upper bars represent the size of the effect at the tenth and ninetieth percentiles. (Median and 10th–90th Percentile Range)

Table 12 shows the same information numerically.

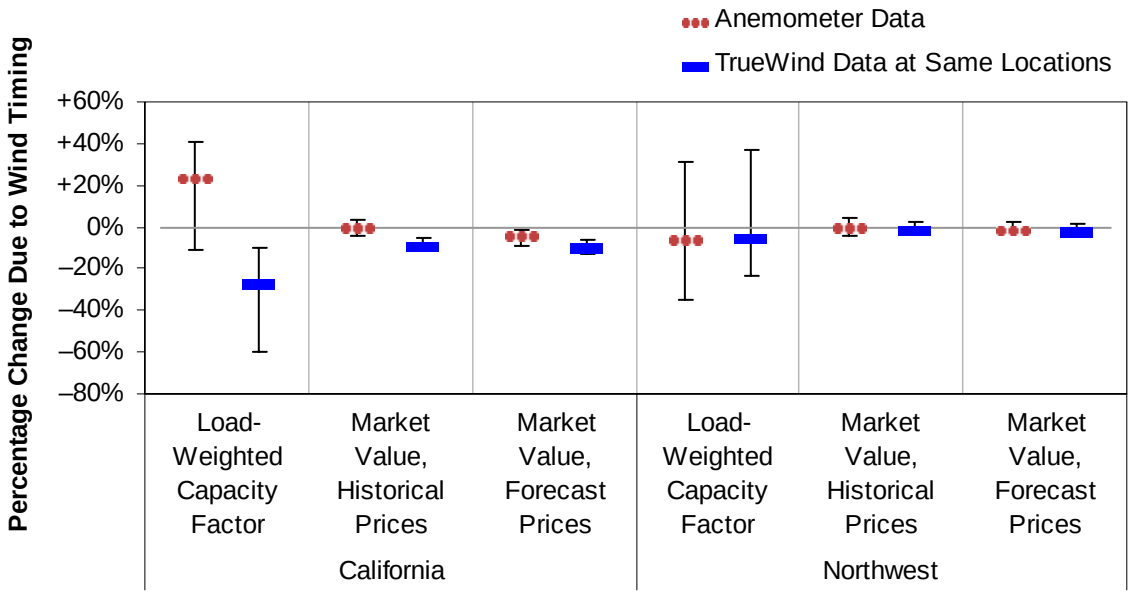

Figure 29. Comparison Between Wind-Value Measures Derived from Anemometer Measurements and Measures Derived from TrueWind Data for the Same Locations (Median and 10th–90th Percentile Range)

Table 12. Comparison Between Wind-Value Measures Derived from Anemometer Measurements and Measures Derived from TrueWind Data for the Same Location

Percentage Change in Value Measures Due to Wind Timing	California			Northwest		
	Load-Weighted Capacity Factor	Market Value, Historical Prices	Market Value, Forecast Prices	Load-Weighted Capacity Factor	Market Value, Historical Prices	Market Value, Forecast Prices
Anemometer Measurements						
10th Percentile	–11.3%	–4.3%	–9.1%	–35.4%	–4.2%	–3.6%
Median	+23.5%	–0.5%	–4.6%	–6.4%	–0.6%	–0.9%
90th Percentile	+40.7%	+3.1%	–1.2%	+31.0%	+4.0%	+2.4%
TrueWind Estimates at the Same Location						
10th Percentile	–60.0%	–11.3%	–12.9%	–23.1%	–1.9%	–2.6%
Median	–27.4%	–8.7%	–10.4%	–5.6%	–1.1%	–1.9%
90th Percentile	–9.7%	–4.9%	–6.3%	+37.0%	+2.6%	+1.3%

Difference Between Best and Worst Timed Locations. These data show that the TrueWind and anemometer data produce similar estimates of the *difference* in wind power value between the best and worst-timed wind sites for all wind-value measures, in both regions. For example, using historical prices, power from the ninetieth percentile of California sites is worth more than power from the tenth percentile by about 7.4 percent of the average market price according to the anemometer data, or about 6.4 percent of the average market price according to the TrueWind data.

Magnitude of Effects. In the Northwest, the TrueWind and anemometer-based data yielded approximately equal estimates of the *median* effect of timing on the load-weighted capacity factor or market value of wind power, in addition to the *difference* between the best- and worst-timed sites, discussed in the previous paragraph. In California, however, the TrueWind data yielded estimates of the effect of timing that were far more pessimistic than those derived from the anemometer data for the same sites; the top of the TrueWind ranges in California were roughly equal to the bottom of the anemometer ranges. Most of the discrepancy in the California results is due to the fact that the TrueWind wind-speed estimates in California dip deeper and longer during summer daytime hours than the anemometer wind speeds, making them a poorer match to California's summer-afternoon-peaking electricity loads and prices. This difference may be due to time-varying wind shear (which could boost low-elevation wind speeds during the day due to thermal instability or local terrain features), or it may be due to inaccuracy in the TrueWind model (e.g., limited ability to resolve the terrain features that drive the wind in these areas). This issue and other factors affecting the match between the two datasets are discussed further in Sections 2.5 and A.3. When the effects of timing in the San Gorgonio, Tehachapi and Altamont areas are estimated from historical wind power production (Section 4.4) the results fall between the TrueWind and anemometer estimates; this is consistent with the wind shear explanation because turbine hub-heights from the existing wind resource areas in California fall between the average height of the anemometers and the average height of TrueWind's wind-speed estimates.

To summarize, the TrueWind and anemometer datasets differ in the estimates they yield for the median effect of wind timing on the value of power, at least in California. However, they appear to agree in their estimate of the difference in value between the best- and worst-timed anemometer locations.

4.3 Effects of Wind Timing at Individual Anemometer Sites

We also investigated whether the TrueWind and anemometer data agreed about the relative impact of wind timing at individual locations (rather than the range of effects at all locations, shown above). We first calculated the correlation coefficient between the TrueWind and anemometer estimates of each wind-value measure, across all anemometer locations. Table 13 shows the correlation coefficient between the two datasets' estimates of the fractional change in each value measure due to wind timing.

Table 13. Correlation Between Wind-Value Measures Derived from Anemometer Measurements and Measures Derived from TrueWind Data for the Same Location

	Correlation Coefficient Between TrueWind and Anemometer Estimates	
	California	**Northwest**
Effect of Timing on Load-Weighted Capacity Factor	0.450	0.851
Effect of Timing on Market Value, Historical Prices	0.363	0.853
Effect of Timing on Market Value, Forecast Prices	0.562	0.843

The two data sources have high correlation coefficients for the effect of timing on all three value measures in the Northwest, indicating that they generally agree on the relative standing of

different sites, and on the relative variation in the effects of wind timing between sites. However, the agreement is worse for all three value measures at California sites, indicating that they are in poor to moderate agreement about the relative standing of wind sites there.

4.4 Effects of Wind Timing in Each Wind Resource Area

Figures 30–35 show the effects of wind timing in individual resource areas, as calculated using data from the anemometers, TrueWind, and historical wind power production (where available). In order to make the comparison of the datasets as consistent as possible, we used a single wind-value series in each figure to calculate the effect of wind timing in all resource areas; the first three figures use California loads and prices, and the next three figures use Northwestern loads and prices.

Figure 30 shows the median effect of wind timing on the load-weighted capacity factor, among anemometer sites in the key potential wind resource areas in California and the Northwest, based on historical California loads. The circular markers indicate the median effect among all anemometer sites in each area, and the rectangular markers indicate the median effect calculated via TrueWind modeled data at the same locations as the anemometers.[22] The pinwheel-shaped markers show the effect calculated from the actual hourly wind power production in Altamont Pass, Tehachapi and San Gorgonio. The anemometers generally provide more optimistic estimates than the TrueWind data of the correspondence between wind timing and California's power demand. The results from the two datasets are in better agreement in the Northwest than they are in California, where they often differ on both the magnitude and sign of the median effects of wind timing.[23] Despite these differences, the two datasets appear to generally agree on the relative standing of different resource areas, and the amount of difference between resource areas, with the exception of the Bear River Ridge, Columbia Hills and Tehachapi areas (*i.e.,* the anemometer results are approximately the same distance above the TrueWind results at all resource areas in the Northwest or in California). The historical actual wind power production data for Altamont Pass, Tehachapi and San Gorgonio yield estimates that fall between those from the TrueWind and anemometer datasets.

[22] The circular and rectangular markers do not necessarily show values for the same individual anemometer site. They show the median among all anemometer sites in each resource area, as calculated separately using either the anemometer data or TrueWind data.

[23] Where the circular anemometer markers appear to be missing in Figures 30–35, they are actually plotted exactly behind the rectangular TrueWind markers.

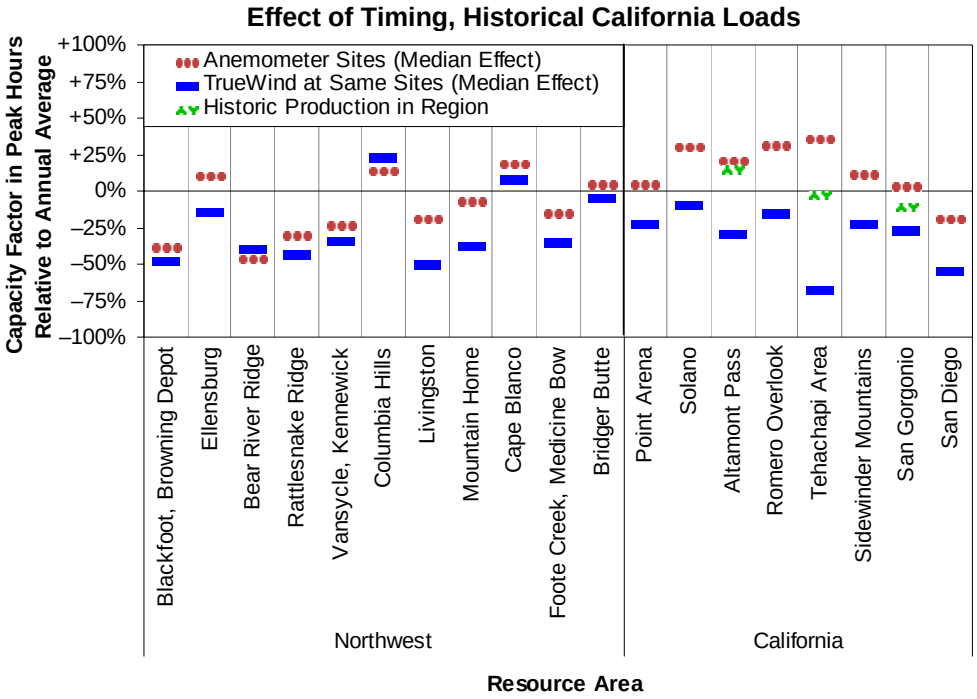

Figure 30. Median Effect of Timing on Load-Weighted Capacity Factor at Anemometer Sites in Each Resource Area, Based on Historical California Load

Figure 31 shows the median effect of wind timing on wholesale market value in each resource area using historical California power prices, and Figure 32 shows the same information using forecast California prices. With historical prices, the pattern is similar to what was shown for the load-weighted capacity factor: TrueWind and the anemometers are in somewhat better agreement about the size of the effect in individual resource areas in the Northwest; in California, they disagree on the typical size of the effect, but agree on the differences from one resource area to the next, with the exception of the south-central parts of the state. When California's forecast prices are used (Figure 32), there is better agreement between the anemometers and TrueWind on the effect of wind timing on market value in the Northwestern resource areas, but there is poor agreement about the relative standing of the areas. In the California areas, agreement on both the size of the effect in each area and the relative standing of individual areas is better with the forecast prices than with historical prices. In both cases, the production data produce estimates that fall between those from the other two datasets, with the exception of forecast prices applied to power output at San Gorgonio, where the anemometers and TrueWind are in good agreement, and the production data fall a little above both.

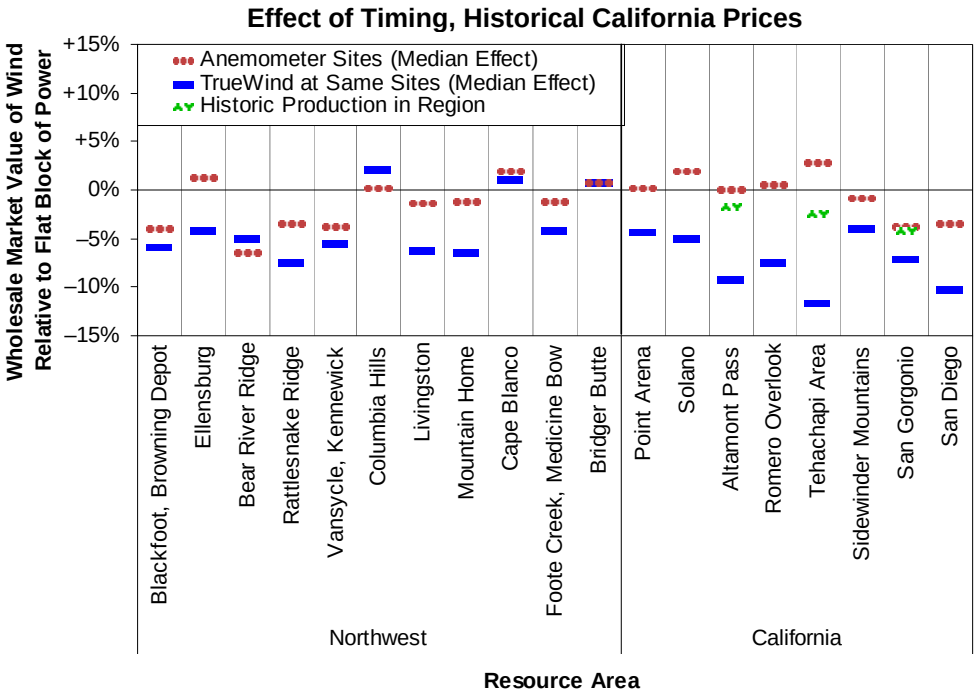

Figure 31. Median Effect of Timing on Market Value at Anemometer Sites in Each Resource Area, Based on Historical California Prices

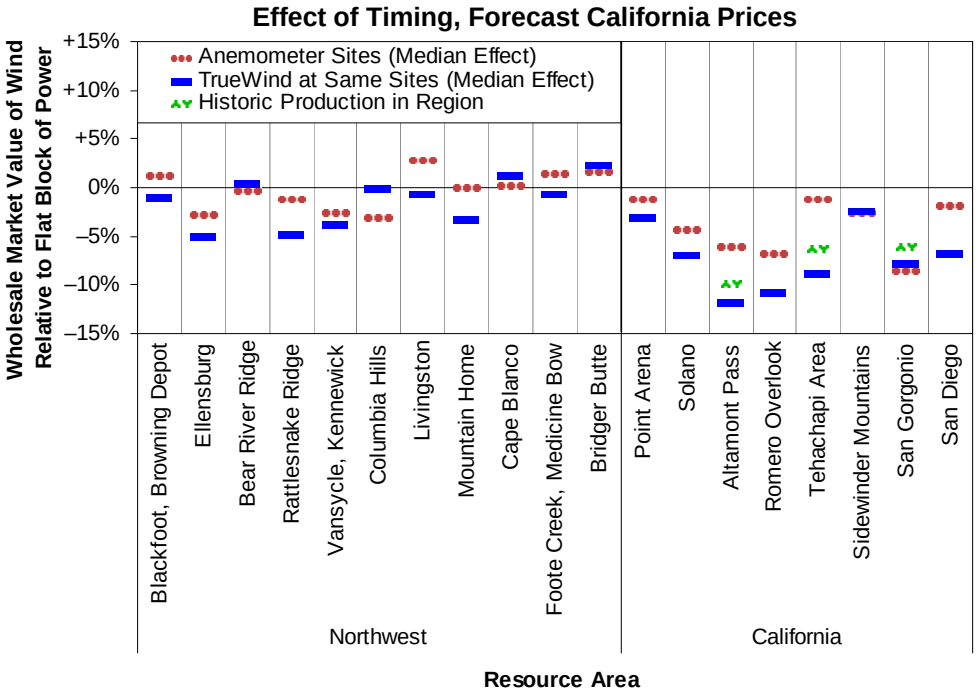

Figure 32. Median Effect of Timing on Market Value at Anemometer Sites in Each Resource Area, Based on Forecast California Prices

Figures 33–35 show the same measures as the previous three figures, but use loads and prices from the Northwest instead of California. There is very good agreement between TrueWind and the anemometers on the effects of wind timing in both California and the Northwest for all three Northwestern value measures. This improvement relative to the California metrics probably reflects the strong temporal pattern in the disagreement between the anemometer and TrueWind wind speed datasets. As will be discussed in Sections 5 and A.3, the two datasets have the greatest disagreement on summer days, especially in California. California loads and prices peak strongly on summer afternoons, so estimates of the value of power based on these measures are especially sensitive to power output at these times. Since the TrueWind and anemometer datasets disagree most sharply at precisely these times, it is not surprising that they also produce widely differing estimates of the effects of wind timing on the value of power when these measures are used. On the other hand, there is relatively good agreement between the TrueWind and anemometer datasets at other times of year, so there is also good agreement on the effects of wind timing on the value of power when historical Northwestern load and price series are used, since they do not place a strong emphasis on summer days.

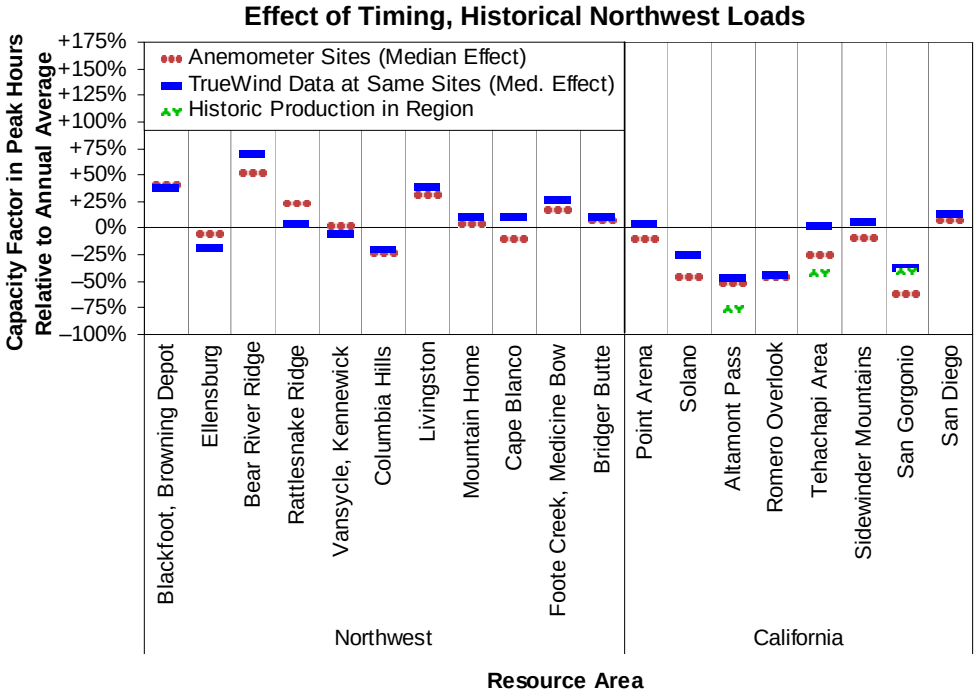

Figure 33. Median Effect of Timing on Load-Weighted Capacity Factor at Anemometer Sites in Each Resource Area, Based on Historical Northwestern Load

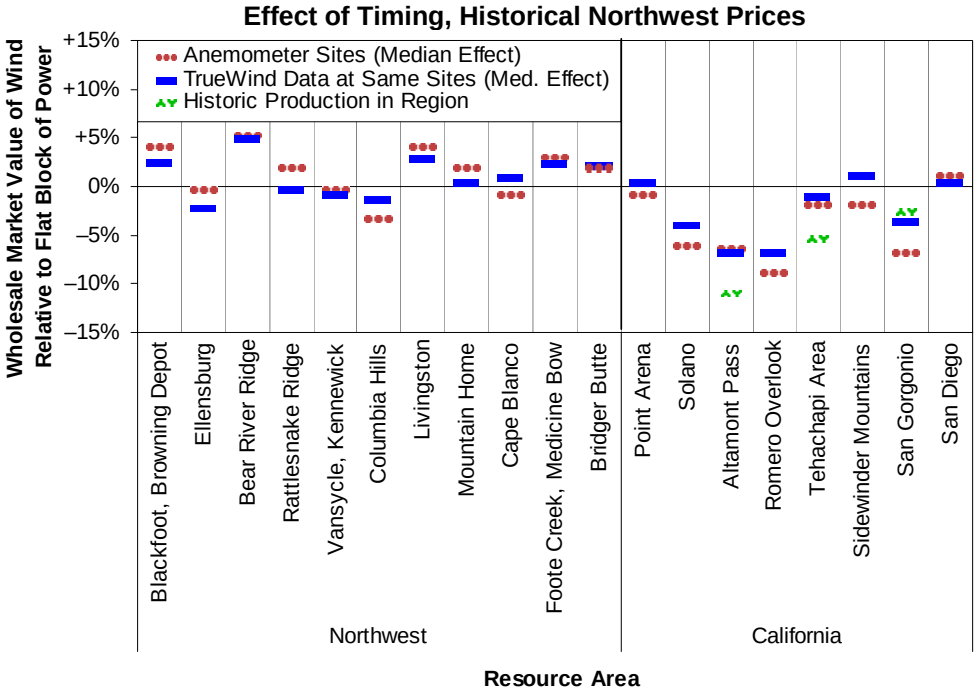

Figure 34. Median Effect of Timing on Market Value at Anemometer Sites in Each Resource Area, Based on Historical Northwestern Prices

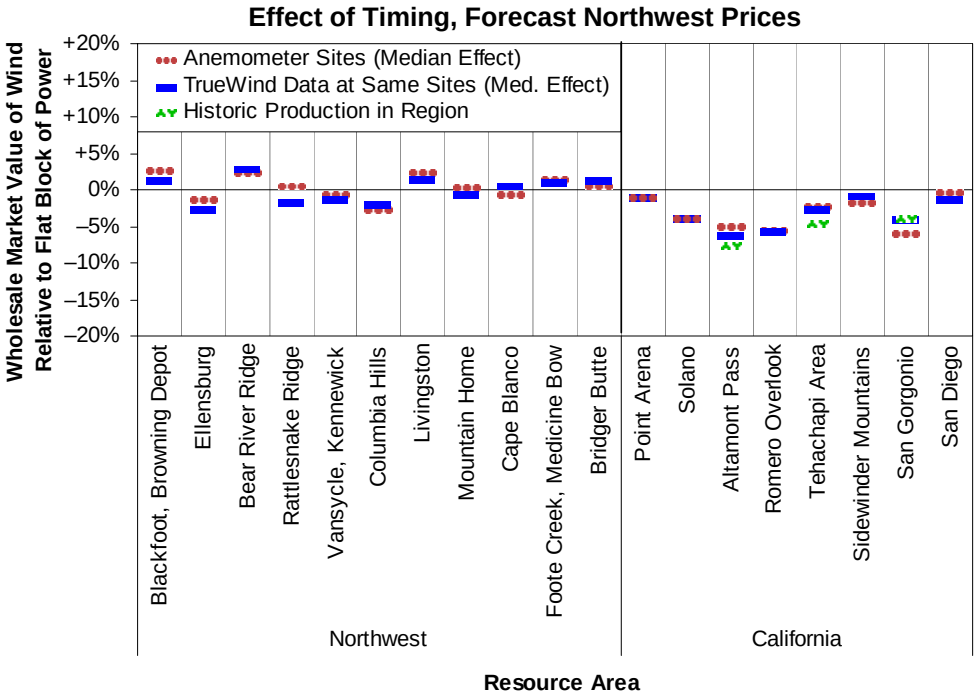

Figure 35. Median Effect of Timing on Market Value at Anemometer Sites in Each Resource Area, Based on Forecast Northwestern Prices

4.5 Discussion

Broadly, TrueWind and the anemometers are in good agreement on the amount of difference between the best-timed and worst-timed wind sites, which suggests that we can place some confidence in using the TrueWind data to estimate how wide a range of impacts wind timing could have within a state or region. The TrueWind data also match observational data reasonably well in identifying which locations have well-timed wind or poorly-timed wind, as compared to other locations in California or the Northwest. However, the two approaches disagree about the typical magnitude of the effects of wind timing, especially in California, and it is not possible to identify which approach is more accurate without more hub-height data from tall-tower anemometers or operating wind farms. Consequently, further work may be needed to obtain reliable estimates of the effects of timing on wholesale market value or peak-hour capacity factor at individual locations.

5 Effects of Monthly and Diurnal Timing on the Value of Wind Power

In this section we divide the temporal variation of wind speeds into monthly and diurnal components to explore the effects of each of these components on the value of wind power in each wind resource area. For simplicity, we consider the effects of these components only on the wholesale market value of power, using only the historical and forecast price series for California. We perform this analysis using estimated power production from TrueWind and anemometer data, so that we can assess whether disagreements about the effects of wind timing on the value of power stem from differences in these datasets' estimation of monthly or diurnal wind speeds. We also use data from operating wind farms, where available, which allows us to see which dataset matches more closely to actual historical production experience. The actual historical production data from California used here, however, derive primarily from older turbines with relatively low hub-heights; these data therefore offer an imperfect comparison to the TrueWind estimates. The wind production data from the Northwest used here are superior, because they represent output from newer commercial wind turbines at higher hub-heights, but those data were only available on a monthly (not hourly) basis, therefore not allowing a full range of comparisons.

To summarize, we find that the TrueWind and anemometer datasets disagree most about the diurnal timing of wind power production in California, and least about the monthly timing of power production in the Northwest. In particular, the TrueWind data show power production in California peaking less sharply in summer months and dipping lower and longer during summer afternoons than the anemometer data. The anemometers suggest that monthly wind timing significantly enhances the value of power from most California resource areas (considering summer-peaking wholesale prices), and that diurnal timing in the summer reduces this effect nearly to zero. The TrueWind data are more pessimistic, suggesting that monthly timing has a weaker positive effect than the anemometer data, and that diurnal timing is more negative than the anemometer data, so that both effects together produce a net negative effect in all California resource areas, relative to an unvarying block of power. The results based on historical production data from operating wind farms, where available, generally fall between the anemometer and TrueWind results.

5.1 Power Production in Each Resource Area on a Monthly and Hourly Basis

Figures 36 and 37 show the *monthly* average capacity factors in each of the wind resource areas used in our analysis. We show three data series:

- averages of data from all anemometer towers in each resource area,
- averages of TrueWind data from the same positions as the anemometer towers, and
- average historical power production by wind farms in that resource area, where available.

Monthly average winds in most major California resource areas show a strong seasonal pattern, peaking in spring or summer. Monthly average winds in Northwestern resource areas peak more weakly and show a less consistent pattern than California – some peak in spring and summer months, some peak in winter, and others are nearly uniform throughout the year.

By inspection of Figures 36 and 37, there appears to be generally good agreement between TrueWind and the anemometers about monthly or seasonal average power production, particularly in the Northwest. However, in California's Solano, Altamont and San Gorgonio resource areas, the TrueWind monthly wind speeds show weaker seasonal variation than the anemometer data, and the center of the high-wind season appears to be about a month earlier than the anemometer based-wind speeds. In the Tehachapi and Sidewinder areas, the TrueWind wind speeds drop in August and September, while the anemometer wind speeds remain relatively strong.

Where the TrueWind and anemometer datasets disagree about the seasonal timing of power production, the actual wind production data do not clearly agree more with one or the other. In Tehachapi, the anemometers appear to give a better estimate of historical monthly production, while in San Gorgonio, the TrueWind data appears to provide a better match to the wind farm production data. In Solano and Altamont Pass, the actual production data seem to agree a little better with the anemometer data, but peak in June instead of July. In the Northwest, the actual production data appear to match the anemometer and TrueWind data equally well, and about as well as these two datasets match each other.

It should be noted that the three data series plotted in these figures come from different years. As discussed in Section 2.2, most anemometer data were collected in the early 1990s, while the production data were collected in 2002, and the TrueWind data were based on weather conditions sampled from a 15-year period. Differences in weather conditions during these periods could contribute to the mismatches shown in these plots. This and other factors affecting these comparisons are discussed in Section 2.5. We also note that the TrueWind data appear to show too much variability in wind speeds on summer nights in San Gorgonio (see Section 2.2.1). This factor reduces the TrueWind estimate of power production on summer nights, and during summer months overall, even though there is actually good agreement between TrueWind and the anemometers about *average* wind speeds in San Gorgonio at these times. In all other places and times, disagreements about power production are due primarily to disagreement about average wind speeds, rather than the variability of wind speeds around the average.

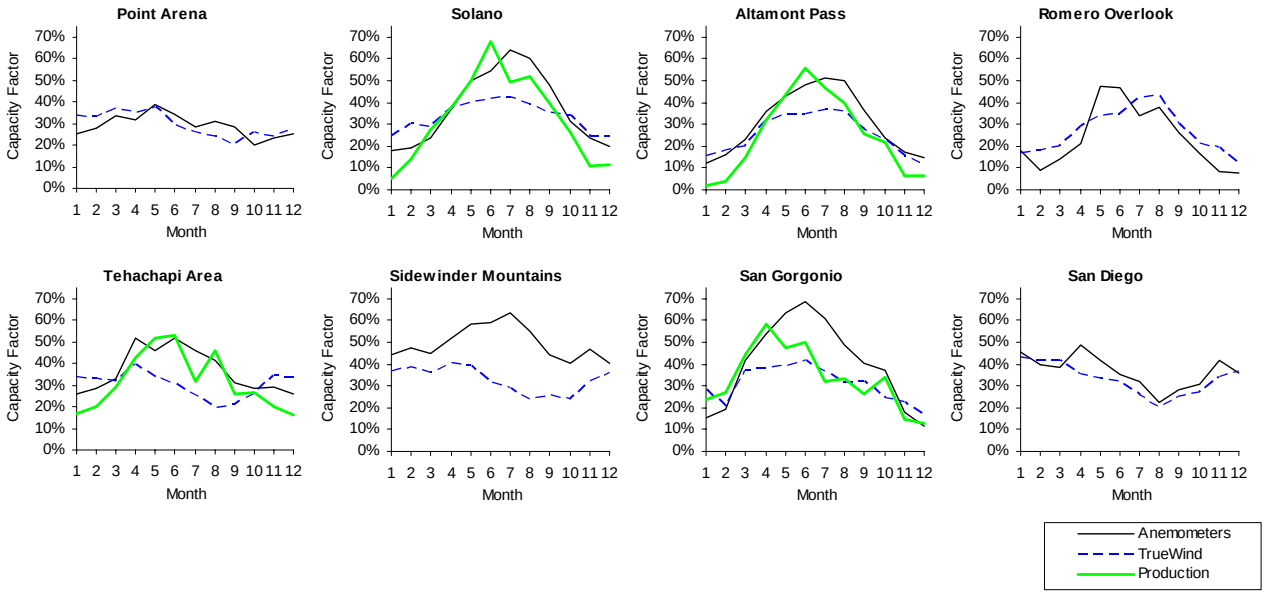

Figure 36. Monthly Average Capacity Factor for Each Resource Area from Anemometers and TrueWind Data at the Same Grid Cell, and Production Turbines in the Same Region (California)

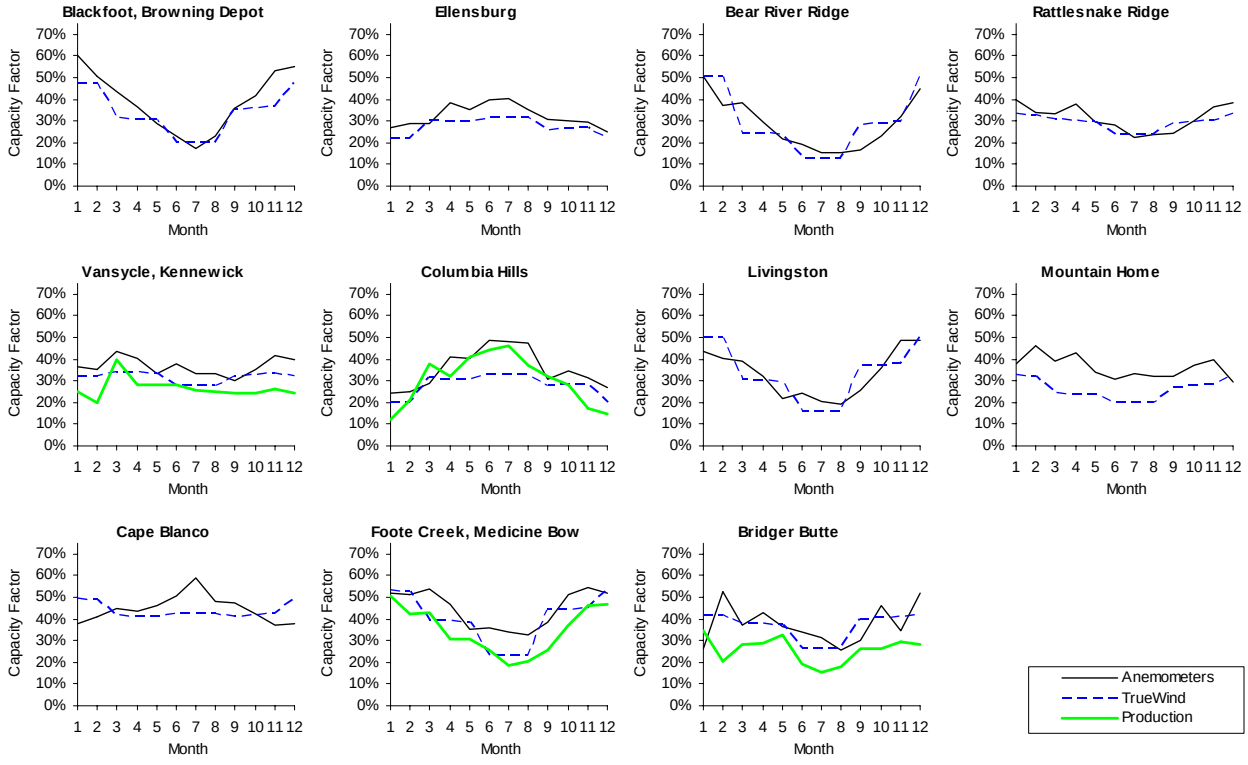

Figure 37. Monthly Average Capacity Factor For Each Resource Area from Anemometers and TrueWind Data at the Same Grid Cell, and Production Turbines in the Same Region (Northwest)

Figures 38 and 39 show average *hourly* production in each wind resource area for the months of January and July. Winter diurnal patterns are weak or non-existent in both California and Northwest resource areas. However, summer winds in most California resource areas and some

Northwestern areas drop off during the day and peak strongly in the evening or night. Summer winds at other Northwestern areas show little diurnal pattern.

The hourly power production values from the TrueWind and anemometer datasets are more divergent than the monthly averages, particularly in California. In almost every case, the chief disagreement appears to be over summer daytime power output, with the TrueWind data set yielding lower estimates than the anemometer data. In most cases, the biggest difference between the two datasets occurs around noontime, but in some cases it occurs later in the afternoon. This difference could be due to inaccuracy in our treatment of wind shear for the anemometer data (see Sections 2.3, 2.5 and A.3), or could be due to some other inaccuracy in the TrueWind or anemometer data. This disagreement manifests in three forms:

1) In a number of resource areas, the TrueWind data show a deeper, longer dip in summer daytime wind speeds than the anemometer data. In these areas, the biggest disagreement between the TrueWind and anemometer data occurs around noon, but the disagreement remains substantial throughout the day. We observed this effect in four of the eight California resource areas (Solano, Altamont Pass, Romero Overlook and San Gorgonio) and two of the eleven Northwestern resource areas (Ellensburg and Rattlesnake Ridge)[24].
2) In several resource areas, the TrueWind data show summer winds rising steadily from early afternoon until they peak at midnight, while the anemometer data show winds rising from late morning and peaking around 6 pm. In this case, the biggest disagreement between the two datasets occurs late in the afternoon. We noted this effect in the Ellensburg and Rattlesnake Ridge areas in Washington, and in the Tehachapi, Sidewinder and San Diego areas in California.
3) In the Blackfoot and Livingston areas in Montana and the Mountain Home area in Idaho, the weak summertime diurnal profiles from TrueWind and the anemometers are nearly reversed. In these areas, anemometers show morning lulls and afternoon peaks, while the TrueWind data show morning peaks and afternoon lulls. Again, the TrueWind data show less wind power available on summer afternoons than the anemometer data, with the biggest difference occurring in late afternoon.

Summertime diurnal power profiles are highly variable at many locations, with hour-to-hour variations often exceeding the month-to-month variability at the same site. We also note that the disagreements between the TrueWind and anemometer diurnal profiles are greatest in midsummer, and that the two datasets sometimes agree about summer nighttime wind power, even when they disagree about daytime power. Consequently, the relatively weak disagreements about monthly average wind speeds noted above (Figures 36–37) may reasonably be interpreted as a symptom of the diurnal disagreement, rather than a separate issue.

The diurnal profiles from the actual production data appear to be closer to the TrueWind data in Tehachapi and San Gorgonio, and closer to the anemometers in Altamont. Hourly historical wind power production data for wind farms in other resource areas would enable more robust comparisons, but are not publicly available.

[24] This effect would be even more pronounced if we used a constant wind shear factor, instead of the 0.09/0.20 day/night approach that we took.

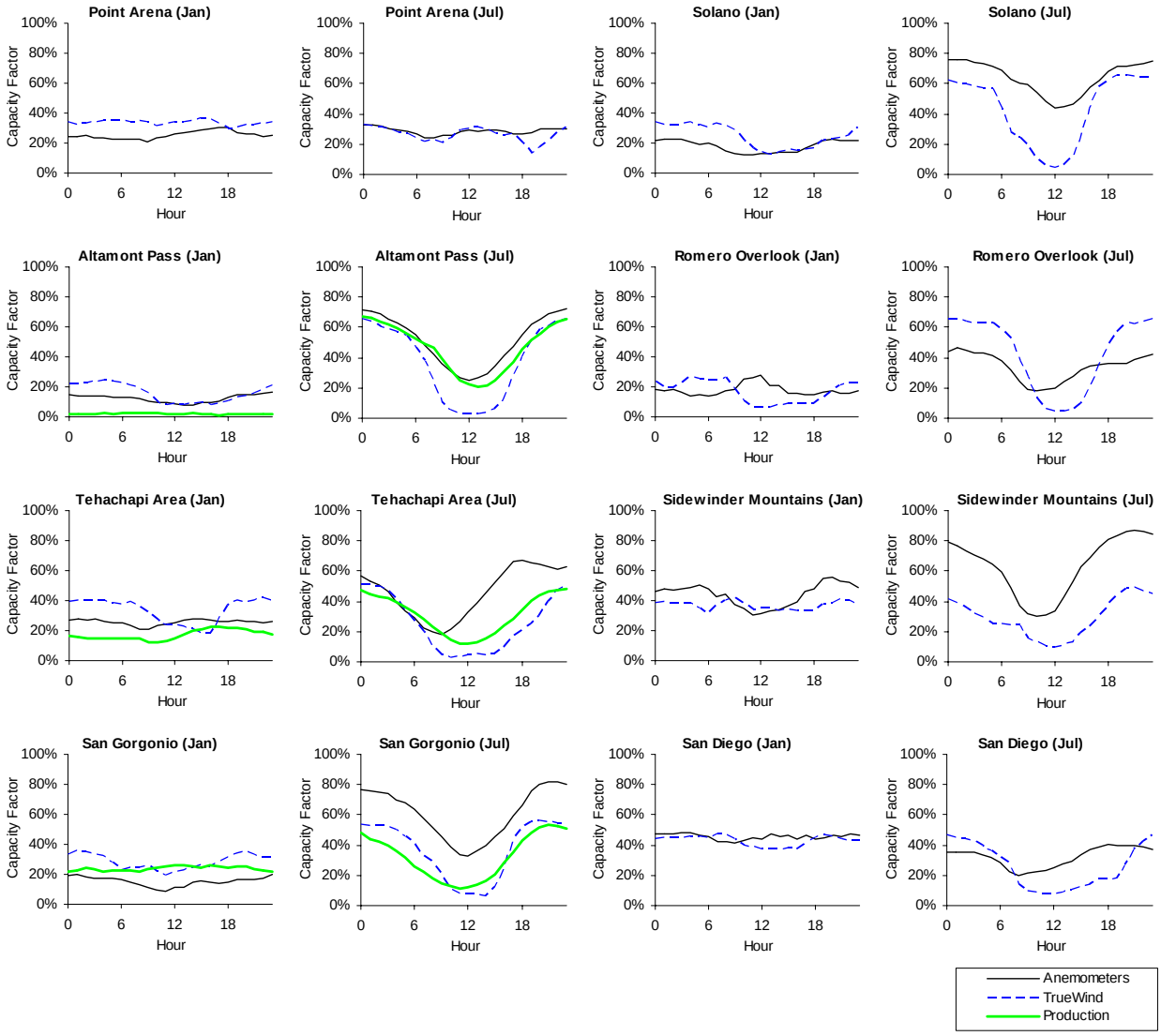

Figure 38. Diurnal Average Capacity Factor for Each Resource Area from Anemometers and TrueWind Data at the Same Grid Cell, and Production Turbines in the Same Region (California)

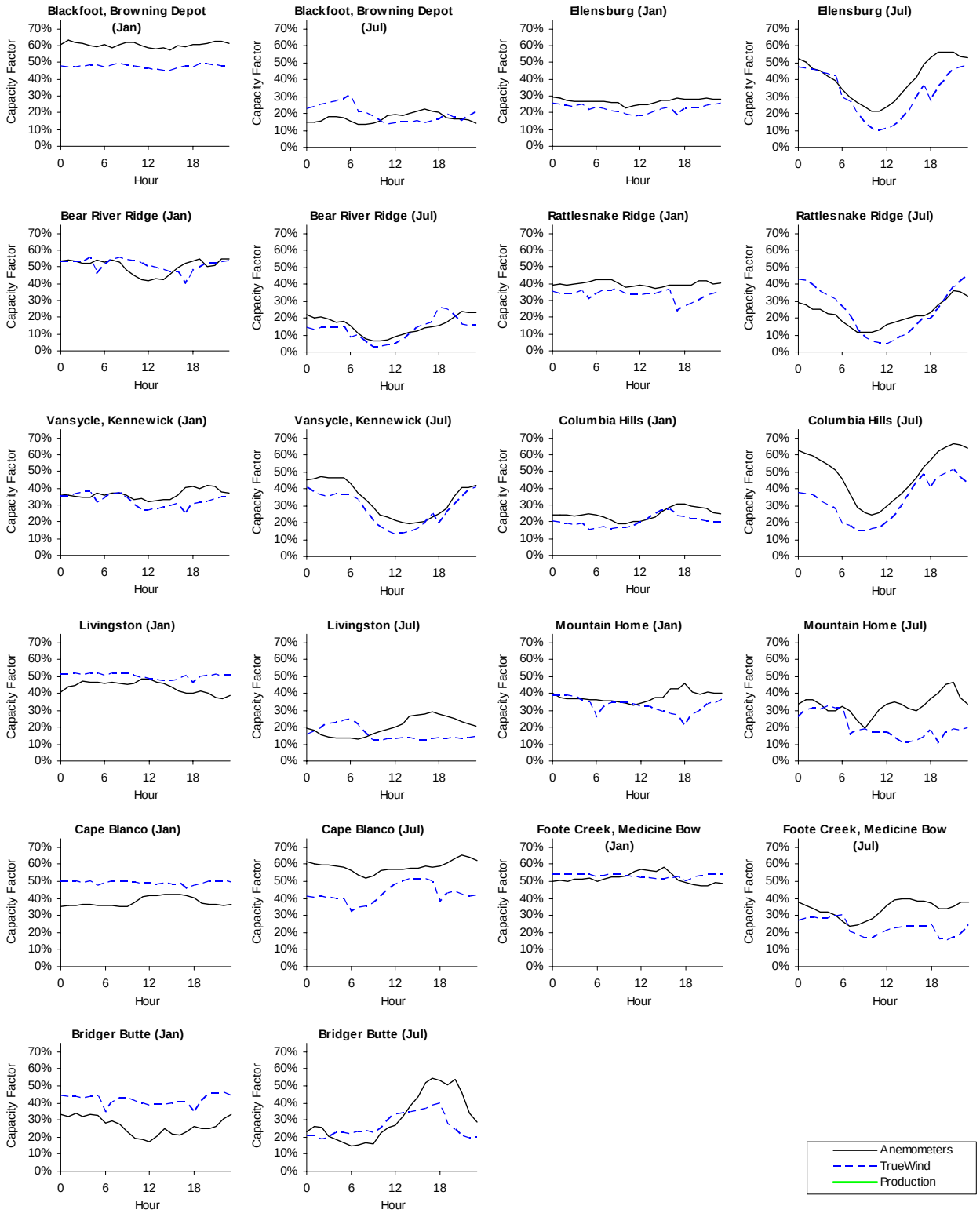

Figure 39. Diurnal Average Capacity Factor For Each Resource Area from Anemometers and TrueWind Data at the Same Grid Cell, and Production Turbines in the Same Region (Northwest)

5.2 Effects of Wind Timing on Value of Power, on a Monthly and Hourly Basis

To estimate the separable effects of diurnal and monthly variation in wind production on the value of electricity from wind farms in each wind resource area, we first assumed that power production varied on *only* a monthly basis and was constant for the whole month. We then compared these estimates to those found in Section 3, based on power production that varied on both a monthly and hourly basis. This allowed us to assess the effects on the value of wind power from monthly variations in wind speed. By comparing these to the values based on hourly-varying power, we can also see how diurnal variations affect the value of wind power.

Figures 40 and 41 show several measures of the effect of wind timing on the market value of wind power from all of the resource areas we studied, using historical California power prices. In these figures, hollow markers indicate results using only monthly average power output, and solid markers indicate results from month-hour average output.

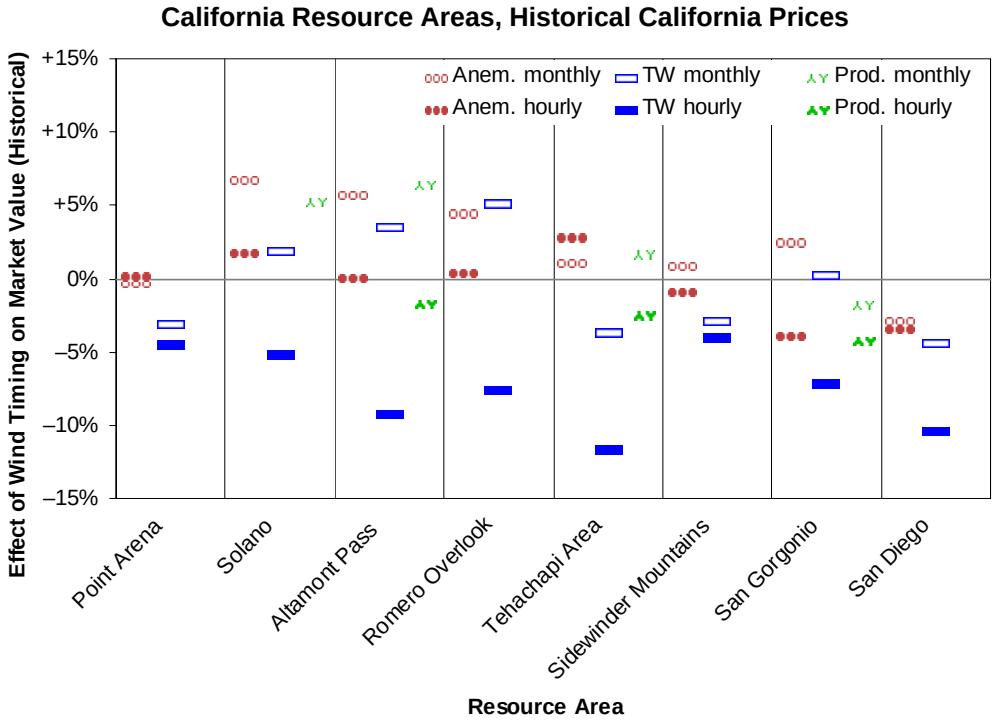

Figure 40. Effect of Wind Timing in Each California Resource Area, Using Monthly and Hourly Data from TrueWind, Anemometers and Production Records, with Historical California Power Prices

The hollow rectangular markers show the effect of wind timing when only monthly variations in the *TrueWind* power production are considered. As might be expected from the comparison of monthly power production estimates in the previous section, these markers often fall relatively close to the markers for the effect of timing found using the monthly average *anemometer* data (hollow circles). When the anemometers' monthly average wind speeds are used, most California resource areas are estimated to have a positive match to historical California prices, reflecting the strong summer peaks in both data series. However, when TrueWind's monthly wind speeds are used, the timing of wind has a weaker positive effect (reflecting the earlier and weaker peaks in

wind speeds in Solano, Altamont and San Gorgonio), or even a negative effect (due to the lull in August and September in the Tehachapi and Sidewinder Mountains areas).

We noted in the previous section that actual historical monthly wind power production in Tehachapi appeared to be similar to the values estimated from anemometer data, while the actual historical monthly production in San Gorgonio, Altamont Pass and Solano appeared more similar to the TrueWind data. This is also reflected in Figure 40, where the effect of timing based on actual monthly average wind production (thin pinwheels) falls closer to the estimate from anemometer data in Tehachapi and closer to the estimate from TrueWind data in San Gorgonio, Altamont and Solano.

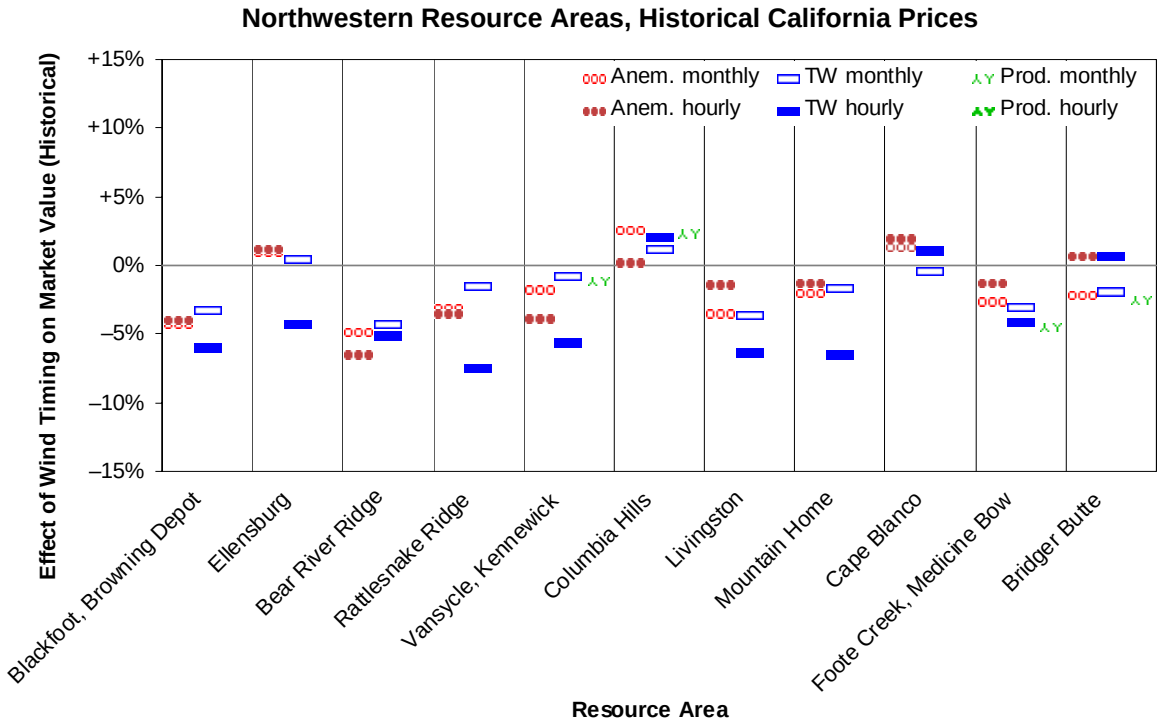

Figure 41. Effect of Wind Timing in Each Northwestern Resource Area, Using Monthly and Hourly Data from TrueWind, Anemometers and Production Records, with Historical California Power Prices

In the Northwest (Figure 41), the monthly anemometer and TrueWind markers are generally closer together than in California, and the monthly production data are in approximately equal agreement with both.

The darker markers in Figures 40 and 41 show the effect of timing on the value of wind power, calculated from the full month-hour data series, instead of only the monthly averages. These are similar to the median estimates shown for each resource area in Section 3.3.2.3, and identical to the values shown in Figures 31 and 32.

In both California and the Northwest, the hourly markers for the TrueWind and anemometer data are generally further apart than the monthly markers, indicating that the two data sets have some disagreement about the effect of the hourly timing of wind in addition to any disagreement about

the monthly timing. We also note that the two datasets frequently disagree about whether the effect of timing is better or worse when both monthly and hourly patterns are considered (solid markers) than when only monthly patterns of wind speeds are considered (hollow markers). The TrueWind data suggest that hourly wind timing almost always reduces the value of wind power relative to the monthly timing, especially in California (*i.e.,* the solid markers, which reflect the influence of both monthly and diurnal patterns, fall below the hollow markers, which reflect the influence of monthly patterns alone). On the other hand, the anemometer data indicate that diurnal timing improves the value of wind power in two of the California resource areas and many of the Northwestern resource areas.[25] This probably reflects the deeper and longer dips in power production on summer afternoons shown in the TrueWind data; California's historical prices peak on summer afternoons, so the values shown in Figures 40 and 41 are quite sensitive to any disagreement about wind speeds at those times.

The hourly production data from wind farms in Altamont, Tehachapi and San Gorgonio suggest that diurnal timing reduces the value of wind power in all three areas, relative to the value derived from monthly average power production. This finding agrees with both the anemometer and TrueWind data in Altamont and San Gorgonio, but contradicts the anemometer results in Tehachapi. No diurnal anemometer data are publicly available for the Northwest.

Figures 42 and 43 use forecast California prices instead of historical California prices to estimate the effect of monthly and month-hourly wind timing on the value of power in each resource area. As with historical prices, there is better agreement between the anemometer and TrueWind data about the effect of monthly wind timing than about the effect of month-hourly wind timing, and the anemometers suggest that diurnal timing often improves the value of wind power, while the TrueWind data suggest the opposite. However, the agreement between the two datasets on both monthly and month-hourly effects is generally improved relative to the estimates made using California's historical power prices; this probably reflects the reduced emphasis on summer months in the forecast price series. As with the historical prices, all three datasets agree that diurnal timing reduces the value of power in Altamont, Tehachapi and San Gorgonio, except for the anemometers in Tehachapi, which suggest that diurnal timing improves the value of power there.

[25] If a constant wind shear factor were used, instead of one which is low in the day and high at night, then the anemometer data would suggest an even more positive diurnal timing.

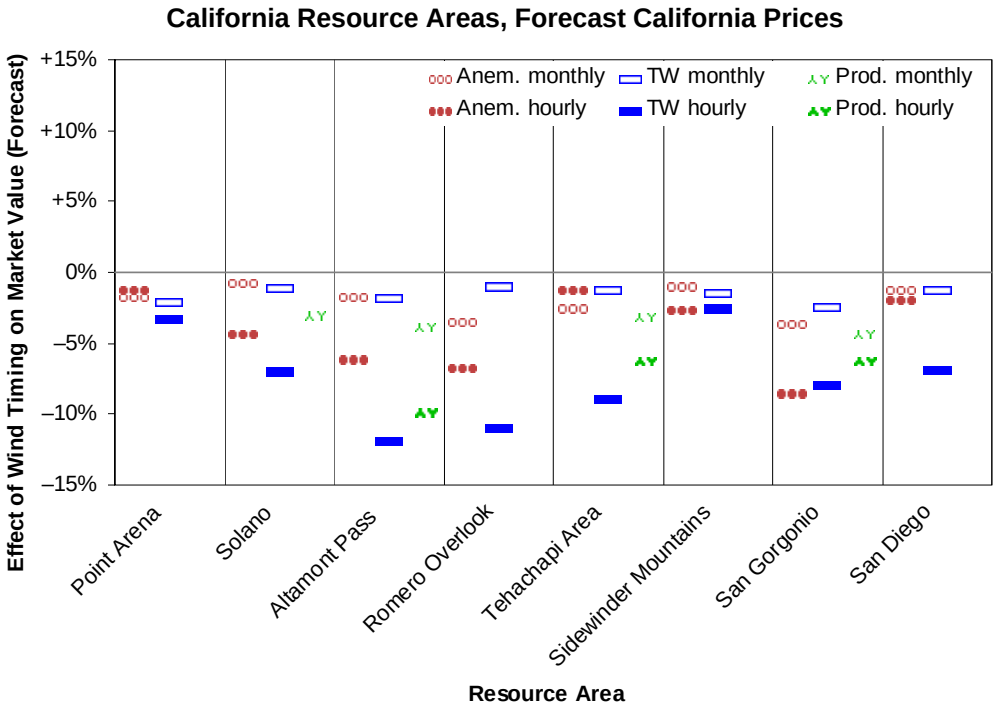

Figure 42. Effect of Wind Timing in Each California Resource Area, Using Monthly and Hourly Data from TrueWind, Anemometers and Production Records, with Forecast California Power Prices

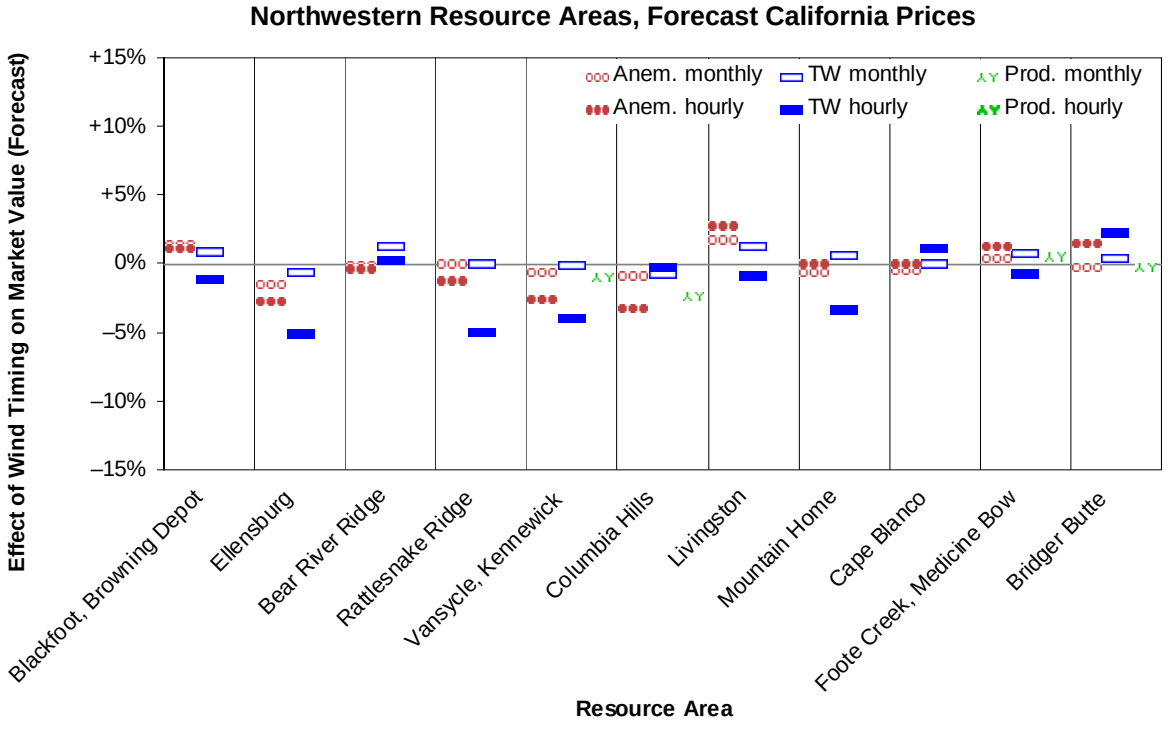

Figure 43. Effect of Wind Timing in Each Northwestern Resource Area, Using Monthly and Hourly Data from TrueWind, Anemometers and Production Records, with Forecast California Power Prices

5.3 Summary

Both monthly and diurnal timing of power production appear to be important in estimating the value of wind power from resource areas in California and the Northwest. There is some disagreement between the TrueWind and anemometer datasets on both of these, particularly about diurnal power production in California. As a result, the two datasets disagree on the effect of monthly wind timing on the value of wind power from resource areas in California, especially when historically summer-peaking prices are used. They also disagree on whether the diurnal timing of wind power reduces or increases the value of the power, relative to monthly average production. Historical data from operating wind farms does not appear to better match either dataset in estimating monthly power production, but it does seem to agree somewhat more with the TrueWind data about the effect of diurnal timing relative to monthly timing.

Some of the difference in temporal wind speed patterns between the anemometers and TrueWind data may be due to temporal variations in wind shear that result from surface heating or local terrain features. This process could increase power production at lower levels during the day and reduce it at night, relative to the upper-level winds. The height of the turbines at wind farms in California is often between the anemometer heights (around 20 meters) and the TrueWind reference height (70 meters), so the intermediate estimates of the effect of wind timing from the wind farm production data are consistent with this hypothesis. However, much of this disagreement could also be due to errors in the TrueWind or anemometer datasets. More anemometer or production data from tall towers are needed before we can judge whether the TrueWind data provide an accurate picture of the effects of wind timing on the value of power.

Using either the TrueWind or anemometer estimates of wind speeds at the tower locations studied in this section, the effects of temporal wind patterns are modest, at most a difference of about 10 percent of market value between the best and worst timed resource areas. By either measure, even the worst-timed resource areas have wholesale values close to the value for a flat block of power.

6 Conclusions

In this report, we have estimated the effects of temporal wind patterns on the value of wind power at different locations in California and the Northwest, using modeled wind speed data from TrueWind Solutions, LLC (now AWS Truewind). We have also made several comparisons between the TrueWind datasets and sets of anemometer and historical wind production data, both in terms of the time-varying wind speed or power output, and in terms of the overall effects of timing on the value of wind power from each location.

We found partial agreement between the TrueWind, anemometer and production datasets: they were quite close in their assessment of wind conditions in the Northwest, and they agreed somewhat on the timing of winds in California as well. However, the TrueWind dataset shows lower wind speeds than the anemometers during summer days in mountain passes in West Coast states, and so the TrueWind data reports more pessimistic wind timing than anemometers at the same locations.

This difference may be due to differences in wind patterns at the lower anemometer heights (around 20-25 meters) as compared to the higher TrueWind reference height (50 meters in the Northwest and 70 meters in California), or it may be due to other inaccuracies in the TrueWind or anemometer estimates of turbine-height wind speeds. It is not possible to definitely state which of these explanations is correct without more tall-tower anemometer data or actual production data from operating wind farms in the West. Results derived from the limited production data available from actual wind farms generally fall between the anemometer and TrueWind data, which may be because the turbines at these older wind farms fall at an intermediate height between the anemometer and TrueWind data. If this is true, then it is plausible to think that TrueWind's wind-speed estimates may more accurately represent hub-height temporal wind patterns than a simple scaling of publicly available anemometer data.

Both the modeled TrueWind data and the anemometer data indicate that many Northwestern wind resource areas are well matched to the Northwest's historically winter-peaking wholesale electricity prices, while most California areas are poorly matched to these prices. However, the TrueWind data indicate that most California and Northwestern resource areas are poorly matched to California's summer-afternoon-peaking prices, while the anemometer data suggest that many California sites and one additional Northwestern area are well matched to California's historical wholesale prices.

Tables 14 and 15 summarize our findings for the effect of wind timing on the peak-hours capacity factor and market value of wind power, as estimated at anemometer tower locations and class 4 or better grid cells, using either anemometer or TrueWind data. It appears that the best-timed wind sites could produce as much as 30–40 percent more power during peak hours than they do on average during the year, while the worst timed sites may produce 30–60 percent less power during peak hours. This could have a substantial impact on the capacity contribution available from wind farms at these locations, though we again note the imprecise nature of our metric (production during the top 10 percent of load hours) relative to the effective load carrying capacity.

The effects of temporal wind patterns on the wholesale value of power from these sites are less pronounced but still somewhat significant: The best-timed wind power sites appear to have a wholesale market value that is up to 4 percent higher than the average market price, while the most poorly timed wind sites are found to have a wholesale market value that is about 11 percent below that of a flat, baseload block of power.

Region	California			Northwest		
Scope	All Anemometer Towers		All Class 4+ Cells	All Anemometer Towers		All Class 4+ Cells
Dataset	Anemometers	TrueWind	TrueWind	Anemometers	TrueWind	TrueWind
10th Perc.	–11.3%	–60.0%	–30.2%	–35.4%	–23.1%	+6.0%
Median	+23.5%	–27.4%	–14.8%	–6.4%	–5.6%	+19.7%
90th Perc.	+40.7%	–9.7%	+7.0%	+31.0%	+37.0%	+34.3%

Table 14. Effects of Wind Timing on Peak-Hours Capacity Factor in California and the Northwest, Using Historical Loads

Region	California			Northwest		
Scope	All Anemometer Towers		All Class 4+ Cells	All Anemometer Towers		All Class 4+ Cells
Dataset	Anemometers	TrueWind	TrueWind	Anemometers	TrueWind	TrueWind
10th Perc.	–4.3%	–11.3%	–5.7%	–4.2%	–1.9%	+0.3%
Median	–0.5%	–8.7%	–3.2%	–0.6%	–1.1%	+1.5%
90th Perc.	+3.1%	–4.9%	+0.3%	+4.0%	+2.6%	+2.9%

Table 15. Effects of Wind Timing on Market Value of Wind Power, in California and the Northwest, Using Historical Wholesale Prices

The anemometer and TrueWind datasets disagree most on wind speeds at California sites on summer afternoons, so they also disagree on the effects of wind timing when these times are important, such as when California's historically summer-peaking load and price series are considered. The disagreement is less significant at other times and locations, so there is better agreement on the effects of wind timing in the Northwest, or when flatter or winter-peaking power values are used (*e.g.,* historical Northwest loads or forecast California prices).

Although the estimated effect of timing for each location varies depending on the wind dataset or electricity value series that is used, the difference in value between the best-timed and worst-timed wind sites is consistent when different wind resource datasets or power value series are used. Based on the TrueWind, anemometer, and actual production data, it appears that the best-timed wind sites have power output during hours of peak electricity demand that is about 40–50 percent higher than the worst-timed sites. The timing of wind appears to produce a spread of 3–8 percent between the market value of well timed and poorly timed wind sites.

Appendix A. Validation of TrueWind Temporal Wind Speed Estimates

A.1 Introduction and Summary

As noted in the introduction to this report, model results from TrueWind allow us to analyze wind resources on a more comprehensive spatial scale than the available anemometer wind speed measurements. However, the only validation of the TrueWind estimates that we are aware of has been on an annual basis.[26] Our use of TrueWind's monthly and seasonal diurnal profiles is therefore novel (or, at a minimum, novel for public domain research). So the first step of our analysis was to investigate whether the temporal and spatial variations in the TrueWind data are similar to the variations in the wind speed observations dataset.

Because the TrueWind wind speeds had already been validated on an annual basis, we focused most of our effort on checking whether the TrueWind data accurately reflected the intra-annual wind speed variations at each site and between sites.

We used three techniques for this comparison, which are described in more detail later in this section:

- First, we directly compared TrueWind wind speeds to measured wind speeds at individual sites and across the whole dataset, using several statistical measures, to determine the general quality of match between these two datasets (Section A.4).
- Second, we compared coarser spatial and temporal averages of the observed wind speeds to the full observation dataset (as well as to the TrueWind estimates), to see the amount of "blurring" of the observation dataset that would give it an equivalent accuracy to the TrueWind dataset (Section A.5).
- Finally, we compared coarser averages of the TrueWind model results to the full observation dataset, to see whether TrueWind's finer time and spatial scales accurately reflect variations in observed wind speeds on the same time scales (Section A.6).

In making these comparisons, it was necessary to make a number of adjustments to the anemometer data in order to compare it to TrueWind data; these included estimating "typical" month-hour wind speed profiles from the hourly data, estimating wind speeds at our reference elevation from wind speeds at the lower anemometer heights, and identifying the appropriate cells on the TrueWind grid to which to compare the anemometer data. Each of these steps introduces some uncertainty in our estimates of turbine-height wind speeds from the anemometer data. As a result, disagreements between the anemometer and TrueWind data may reflect

[26] TrueWind used meteorological observations and worked with NREL and several consulting meteorologists to identify regions where their annual average wind speed estimates were generally too high or low. In a few cases, this yielded insights that were used to change the internal calculations of the wind speed model. However, most corrections were applied using a post-model map of correction factors, which were used to scale the model outputs to better match observed wind speeds. No validation was done on a finer-than-annual time scale. TrueWind assumed for simplicity that seasonal average wind speeds would scale using the same correction factor as annual wind speeds, and we have assumed the same about monthly and diurnal average wind speeds. The finer time-scale validation described in this paper was used only to assess whether we could rely on the TrueWind data for our analysis, and not to correct or improve the TrueWind estimates.

inaccuracy in our estimates of hub-height wind speeds from the anemometer data, rather than inaccuracy in the TrueWind estimates. Limitations to our comparisons are discussed further in Sections 2.5 and A.3.

In Section A.7 we investigate factors that are associated with better or worse fits between the TrueWind and anemometer data. Key findings from this section are that the disagreement between the datasets is reduced at sites where anemometers were placed close to the TrueWind reference height, at sites with strong temporal wind patterns, and at sites further inland, most of which have winter-peaking winds. The first and third of these factors improve the fit at Northwestern sites, and the second factor improves the fit at California sites.

As we show in the pages that follow, the TrueWind model does not provide a perfect fit to the measured wind speeds, but nonetheless does appear to be a useful source of data. In California, the variations in the TrueWind dataset had a correlation coefficient of about 0.71 with the observations, indicating that they matched about 51 percent of the wind speed variation in the anemometer dataset at all sites and times.[27] In the Northwest, the TrueWind estimates matched the anemometer dataset a little more closely, achieving a correlation coefficient of 0.75 (capturing about 56 percent of the variation in observations).

In California, the TrueWind data match the observed wind speeds about as closely as could be done by using a data series consisting of 12x24 month-hourly averages of observed wind speeds for the entire state, or 12 monthly average wind speeds for the local resource area. In the Northwest, TrueWind improved on these measures, but did not give as close a match as could be achieved with 4x24 season-hourly averages for the local resource area, or 4 seasonal averages for the individual anemometer tower.

The TrueWind estimates also generally come closer to the anemometer measurements as they approach finer levels of resolution; the extra detail does not appear to be simply "noise" in most cases. Since the finer scale TrueWind forecasts are better than coarser averages of the forecasts, we assume that the TrueWind data must be incorporating at least some of the real fine-scale variation, which is what our analysis depends on.

Given that the TrueWind model appears to accurately reflect much of the variation in the available wind speed observations, and that it appears to capture at least some of the spatial variation in wind timing, we decided that it would be worth using the TrueWind wind speed estimates for our analysis. At sites where direct measurements are available, the TrueWind data may not provide as accurate an estimate of wind speeds as the direct observations do. However, at sites where direct observations are not available (*i.e.,* most of the area that would be covered by a comprehensive wind resource map), the TrueWind data are the best estimator available to us, and based on our validation efforts, it appears likely that they are a reasonably good proxy for the true average wind speeds.

[27] The correlation coefficient (r) between two data series measures the strength and direction of their linear relationship (assuming they are linearly related). The coefficient of determination (r^2) measures the percentage of the variation in one variable that can be explained by variation in the other, assuming they are linearly related.

A.2 Data Series Used for Validation

We derived expected wind speeds for each hour of the day, for each month or season of the year, from both the TrueWind data and the wind observations dataset, following the approaches discussed in Sections 2.2 and 2.3. We then compared these two datasets, using the techniques described below, to try to determine how well the TrueWind wind speed estimates matched the mean observed wind speeds for each location and time interval.

We performed our validation analysis separately for California and the Northwest, since the TrueWind data for these regions were provided as separate datasets with different averaging intervals. As discussed earlier, the TrueWind model results for the Northwest states showed hourly average speeds on a seasonal basis, while the TrueWind data for California showed hourly average wind speeds on a monthly basis.

We averaged the wind speeds at each observation site on the same temporal basis as the corresponding TrueWind data before making any comparisons. That is, all of our comparisons were between the TrueWind month-hour or season-hour wind speeds and the 12x24 month-hour or 4x24 season-hour averages of the observed wind speeds; whenever we refer to the "observed wind speeds" below, we mean the averages taken over these intervals. We did not compare the TrueWind data directly to hour-by-hour observations at each site, which are more volatile, but also more irregular in their availability, and less useful for our analysis than the month-hour or season-hour averages.

For these comparisons, we used a subset of the full TrueWind dataset, consisting only of the wind speeds for the closest point on the TrueWind grid to each of the observation towers for which we had data. So, for each observation site, we used the month-hour or season-hour averages of the observed wind speeds for that site, and the TrueWind estimates of the average wind speed for the same location and time scale. When averaging to coarser time or spatial scales for further comparisons, we used the same techniques on the observed mean wind speeds and corresponding TrueWind mean wind speeds, rather than retrieving coarser averages from the full TrueWind dataset.[28]

A.3 Limitations to Our Validation Efforts

Before describing our comparison of the TrueWind and observation datasets, we note that the conclusions that can be drawn from this comparison are restricted by the scope of the anemometer dataset. In Section 2.5 we discuss a number of factors that impair our ability to use the anemometer data to estimate accurate average wind speeds at the TrueWind reference height. Because of these limitations, lack-of-fit between the TrueWind and anemometer data could reflect inaccuracy in either the anemometer or TrueWind datasets' representation of typical wind conditions.

[28] For example, when averaging wind speeds for a local resource area, we averaged all the data from observation sites within that area, and, correspondingly, from TrueWind's 200 m cells matching those observation sites; we did not average *all* the 200 m cells within the region.

In particular, we note in Section 2.5 that much of the disagreement between the TrueWind and anemometer data may be due to limitations in our ability to estimate time-varying wind shear between the anemometer and turbine heights. With time-varying wind shear, the two datasets could disagree even if the anemometers give an accurate estimate of low-level winds and the TrueWind data give an accurate estimate of higher-level winds. This possibility is suggested by several findings from our validation work:

- We repeated our validation analysis using hourly wind shear values estimated from towers with multiple anemometers, or anemometers within a few meters of TrueWind's reported elevation, at 80 sites in the Northwest and 8 sites in California. The goodness of fit between the TrueWind and anemometer data when using this technique was nearly identical to what we found using our fixed day/night wind shear algorithm (Section 2.3), in either region. However, at the California sites, the match between the datasets when using either of these time-varying techniques was significantly better than we obtained when using a fixed wind shear exponent of 0.14 at all times. This suggests that time-varying wind shear can be an important factor in comparing the TrueWind and anemometer datasets, at least in California.[29]
- The quality of fit between TrueWind and anemometer data was generally higher at locations where the anemometer height was close to the reference height of the TrueWind data, and lower at locations where the anemometer height was far from the TrueWind height. This relationship also suggests that wind shear could be an important source of disagreement between the two datasets. This factor is discussed in more detail in Section A.7.
- The mismatch between TrueWind and anemometer data had a strong temporal pattern. TrueWind estimates of wind speeds were generally lower relative to anemometer measurements during summer months and daytime hours, particularly in California. It is possible that both datasets are accurate and that this difference is caused by a reduction in wind shear during hot hours, as turbulent mixing transfers momentum from upper levels closer to the ground, or as local terrain features cause strong near-surface flows. This temporal pattern also appeared in the wind shear estimated from anemometers at multiple levels, although it was not as sharp as the temporal pattern in the difference between the TrueWind and anemometer data.

However, as discussed in Section A.7, not all of the mismatch between the TrueWind and anemometer data can be attributed to our treatment of wind shear, and some is likely due to errors in the TrueWind model results.

A.4 Comparison Between Observed Wind Speeds and TrueWind Model Results

A.4.1 Comparative Statistics for Individual Sites

We first made a direct comparison between the TrueWind and observed wind data for each observation site. We calculated comparative statistics for each individual site, matching up the

[29] Results in the Northwest were little changed by either time-varying wind shear technique, but this could be because the Northwestern anemometers were on average only about 25m below the TrueWind reference height of 50m, as compared to California anemometers, which were on average about 50m below the TrueWind reference height of 70m.

TrueWind wind speed with the observed wind speed for that site for the same month or season, at the same hour of the day.

Table A-1 shows the median value of the error statistics calculated for the 78 anemometer sites in California and 102 sites in the Northwest. The TrueWind temporal data appear to match observed wind speeds fairly well, although certainly not perfectly. The median correlation coefficient indicates that the TrueWind data reflect 62 percent (R=0.786) or more of the temporal variation in wind speeds at half of the sites in California for which we have data. In the Northwest, the TrueWind data appear to match our observational data set a little more closely, capturing 68 percent (R=0.823) or more of the variation at half of the sites. However, the TrueWind data do disagree with the anemometer measurements by an average of 1.5 m/s or more at half of the California sites and 1.2 m/s or more at half of the Northwest sites.

Table A-1. Comparison Statistics Between TrueWind Modeled Wind Speeds and Measured Wind Speeds at Individual Sites

	Median Among Sites	
	California	**Northwest**
Mean Absolute Error	1.50 m/s	1.20 m/s
Root Mean Squared Error	1.85 m/s	1.43 m/s
Correlation Coefficient	0.786	0.823

The range of correlation coefficients found at different sites are shown in Figures A-1 and A-2. Figure A-1 shows the range of correlation statistics found at individual sites in California. Seventy of the 78 sites (90 percent) have correlation coefficients greater than 0.50. Figure A-2 shows the same information for the Northwest, where 92 of the 102 sites (90 percent) have correlation coefficients greater than 0.50.

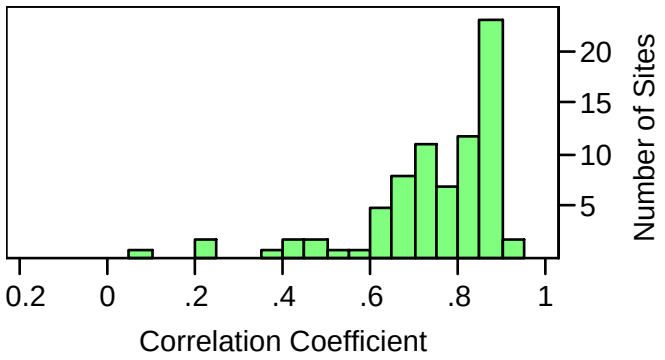

Figure A-1. Correlation Between TrueWind Wind Speeds and Measured Wind Speeds at Each Site in California

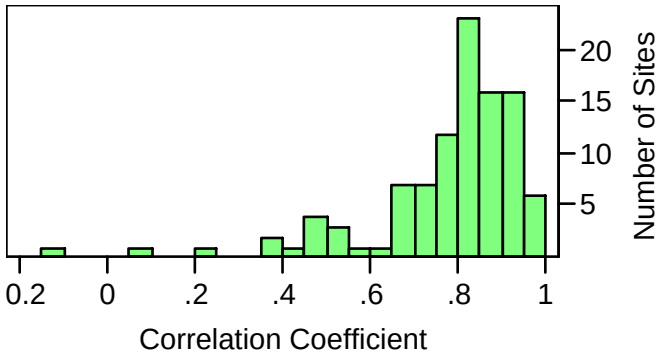

Figure A-2. Correlation Between TrueWind Wind Speeds and Measured Wind Speeds at Each Site in the Northwest

A.4.1.1 Variation in TrueWind Goodness of Fit at Different Locations

We also analyzed how the quality of TrueWind's fit to the anemometer data varied geographically, between different major wind resource areas. Table A-2 and Figure A-4 show the correlation coefficient between the TrueWind data and wind speed measurements for each resource area in California where measurements were available. The TrueWind data appear to fit the observations best in Altamont Pass and San Gorgonio, and worst in the area around Tehachapi Pass. Results were intermediate in Solano County and east of San Diego.

It should be noted that regions where high correlation was found between TrueWind and anemometer wind speeds may or may not also have good agreement on the effect of wind timing on the market value or peak-hours capacity factor of wind power, discussed in the main body of this report. This is because some sites may have good year-round correlation of wind speeds, but have their largest errors at times that are most important for assessing the value of power. For example, the TrueWind and anemometer data agree fairly well about the general timing of wind at Altamont Pass and San Gorgonio, but their disagreement on summer afternoons causes them to disagree about the value of power from these resource areas for serving California power markets and loads. In some cases, the TrueWind and anemometer data may disagree generally about the timing of wind speeds, but agree during critical periods, or have disagreements that randomly offset each other, yielding good agreement on the value of wind power. For example, the anemometer and TrueWind datasets produce similar estimates of the effect of wind timing on the market value of power from Tehachapi, Mountain Home and Rattlesnake Ridge when historical Northwestern power prices are used, despite their general disagreement on year-round variation in wind speeds at these sites. The apparent agreement disappears when we use historical California power prices, which give more weight to summer afternoon hours.

Table A-2. Median Correlation Coefficient Between TrueWind Modeled Wind Speeds and Measured Wind Speeds in Each Wind Resource Area in California

Description	Median Correlation	Number of Observation Sites
Point Arena	0.434	1
Altamont Pass	0.855	40
Solano	0.718	16
Romero Overlook	0.677	1
Tehachapi Area	0.298	6
Sidewinder Mountains	0.619	1
San Gorgonio	0.872	5
San Diego Area	0.634	8

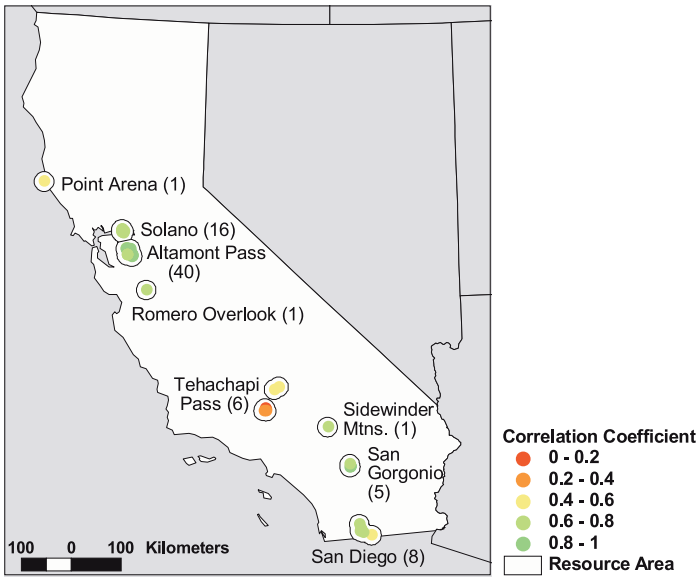

Figure A-3. Correlation between TrueWind and Anemometer Data in California Wind Resource Areas

In the Northwest, TrueWind matches observed wind speeds somewhat more closely than in California. The correlation between TrueWind and observed wind speeds is high (median > 0.80) in most of the resource areas where more than one observation site was established: at Bear River Ridge near the Pacific coast; in the Columbia Hills along the Columbia River; at Browning Depot and Blackfoot, Montana; near Livingston, Montana; and near Foote Creek Rim, Wyoming. However, TrueWind's results did not match available anemometer data quite as well further inland along the Colombia River (Vansycle/Kennewick, Rattlesnake Ridge and Ellensburg).

Table A-3. Median Correlation Coefficient Between TrueWind Modeled Wind Speeds and Measured Wind Speeds in Each Wind Resource Area in the Northwest

Description	Median Correlation	Number of Observation Sites
Blackfoot / Browning Depot, MT	0.924	6
Ellensburg, WA	0.621	10
Bear River Ridge, WA	0.869	2
Columbia Hills, WA/OR	0.817	43
Rattlesnake Ridge, WA	0.556	8
Vansycle, OR / Kennewick, WA	0.625	3
Livingston, MT	0.841	6
Cape Blanco, OR	0.795	1
Mountain Home, ID	0.081	1
Foote Creek / Medicine Bow, WY	0.931	21
Bridger Butte, WY	0.668	1

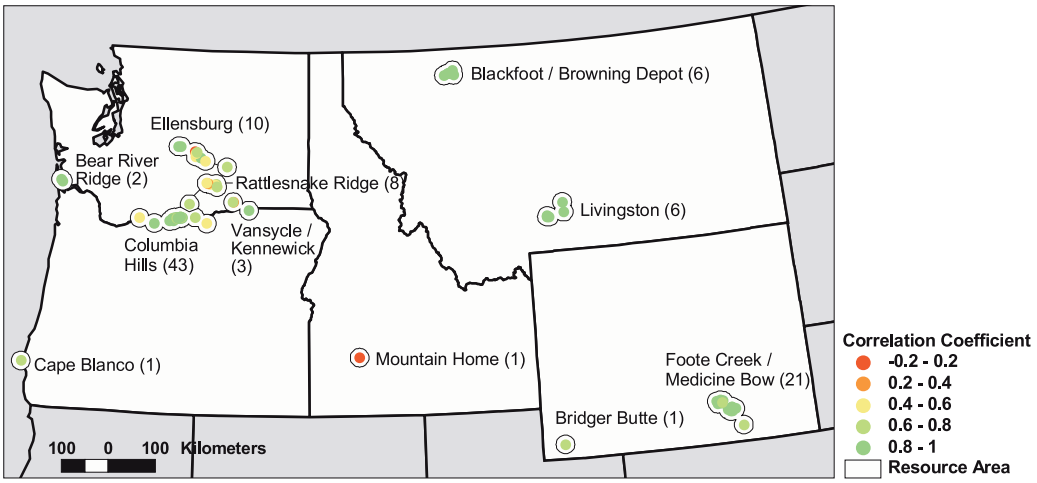

Figure A-4. Correlation between TrueWind and Anemometer Data in Northwest Wind Resource Areas

A.4.1.2 Variation in TrueWind Goodness of Fit on Different Time Scales

Many wind sites have both seasonal and diurnal wind speed patterns, either or both of which could be important in determining how well wind power from the site will match electricity load and prices. We therefore investigated whether the TrueWind model better matched the anemometer data on a monthly timescale or on a diurnal timescale. To do this, we divided the TrueWind and observation data series into two components. The first component was simply the average wind speed for each site for each month or season (four or twelve means per site). The second component was the residual variation, calculated by dividing the wind speed for each month-hour or season-hour by the average speed for that month or season. This second series consisted of 4x24 or 12x24 diurnal weights for each site, which show how wind speeds vary with time of day, and how this pattern changes during the year. We then calculated correlation coefficients between the respective TrueWind and observation data series. The results of this comparison are shown in Table A-4.

Table A-4. Correlation Between TrueWind Modeled Wind Speeds and Measured Wind Speeds on Seasonal and Diurnal Bases

	Correlation Coefficient, Median Among Sites	
	California	**Northwest**
Monthly or Seasonal Variation	0.936	0.938
Residual (Diurnal) Variation	0.814	0.695

The TrueWind data closely match the observed wind speeds on a month-to-month or season-to-season basis at sites in both California and the Northwest, achieving a median correlation coefficient of about 0.94 (r^2=88 percent) in both cases.[30] However, they are not as close a match to the diurnal variation in either region.

It may also be worth noting that variations in the monthly mean wind speed contribute most of the variance in month-hour wind speeds at sites in both California and the Northwest. In California, the monthly means contribute 27–90 percent of the total variance in month-hour wind speeds at individual sites, with a median value of 76 percent. In the Northwest, the seasonal means contribute 16–97 percent of the total variance, with a median value of 65 percent.[31]

Wind speeds appear to match as well or better in California as in the Northwest. This contrasts to the greater disagreement we found in California when we estimated the market value or peak-hours capacity factor of wind power, discussed in the main body of the text. The greater disagreement on the "value" of wind power in California may be because disagreements about wind speeds are concentrated in summer afternoons, so that they have a stronger effect when summer-peaking California loads and market prices are used, and have less influence when the Northwest's winter-peaking loads and prices are used.

[30] This indicates good agreement on the seasonal timing of peak wind speeds, but not necessarily the magnitude of the seasonal peaks. The monthly or seasonal correlation statistics for individual sites are the result of a linear fit of 4 or 12 modeled datapoints to 4 or 12 observed ones. The shapes of the curves defined by these datapoints are relatively simple, so with the scaling and translation available in a linear fit, it is easy to achieve a good fit between the two sets of datapoints for each site, provided the basic timing matches. This issue is discussed further in section A.4.2.

[31] As discussed above, we separated monthly/seasonal and residual wind speeds by assuming that the wind speed in any month-hour for a given site ($v_{s,m,h}$) was the product of the monthly/seasonal average wind speed for that site ($v_{s,m}$) and a weight for the residual wind speed for that month-hour ($w_{s,m,h}$). For such a model, the fractional variance in the wind speed ($\sigma^2_{v_{s,m,h}} \Big/ \overline{v_{s,m,h}}^2$) should be the sum of the fractional variance in the individual components: $\left(\frac{\sigma_{v_{s,m,h}}}{\overline{v_{s,m,h}}}\right)^2 = \left(\frac{\sigma_{v_{s,m}}}{\overline{v_{s,m}}}\right)^2 + \left(\frac{\sigma_{w_{s,m,h}}}{\overline{w_{s,m,h}}}\right)^2$. Then, the share of variance that can be attributed to the monthly/seasonal variation is $\left(\frac{\sigma_{v_{s,m}}}{\overline{v_{s,m}}}\right)^2 \Bigg/ \left(\frac{\sigma_{v_{s,m,h}}}{\overline{v_{s,m,h}}}\right)^2 = \left(\frac{\sigma_{v_{s,m}}}{\overline{v_{s,m}}}\right)^2 \Bigg/ \left[\left(\frac{\sigma_{v_{s,m}}}{\overline{v_{s,m}}}\right)^2 + \left(\frac{\sigma_{w_{s,m,h}}}{\overline{w_{s,m,h}}}\right)^2\right]$.

A.4.2 Comparative Statistics Among All Sites and Times

We also computed comparative statistics between the full TrueWind and observation datasets, for all sites together, rather than for individual sites. For the mean absolute error statistic, this approach is equivalent to taking the mean of the MAEs for all of the individual sites, and would not be expected to produce results that are more informative than the median of the site-by-site MAEs, already shown earlier. The root mean squared error (RMSE) calculated for the full dataset also does not appear to be more useful than the median RMSE for individual sites; the RMSE calculated for all sites will generally overemphasize the sites with the largest errors, and so would be expected to be somewhat larger than the mean or median RMSE for the individual sites.

However, the correlation statistic for the whole TrueWind and observation datasets, across all times and locations, may be more useful than the median of the correlations calculated for individual sites in Section A.4.1. A correlation coefficient is calculated by mapping the closest possible linear relationship between two data series. This is mathematically similar to scaling and vertically shifting the modeled, predictive series to obtain the closest possible match to the observation series being predicted. Then, the correlation coefficient indicates how much variation in the observations is explained by the model. The correlation coefficient ignores the magnitude of both the scaling and shifting required to create this optimal match, and simply measures how good the final match is. If correlation coefficients are calculated separately for each of the sites, as in Section A.4.1, then different adjustment factors may be used for the linear transformation for each site. The model series can in effect be custom-tailored to each individual site as the correlation statistics are calculated, possibly improving the model's apparent fit to the site-to-site variations in average wind speed and timing. On the other hand, if a single correlation coefficient is calculated for all sites and times together, then the same scaling and shifting factors are used for all sites, and the correlation statistic will more accurately reflect the model's match to the wind speeds as both time and location are varied.[32]

The statistics shown in Table A-5 were calculated by comparing the full series of California or Northwest TrueWind wind speeds for all locations and times with the full set of anemometer measurements at the same locations and times. The full-dataset correlation statistic indicates that the TrueWind data reflect about 51 percent ($r=0.713$, $r^2=0.51$) of the variation in California wind

[32] The regression coefficients for the best linear fit of observed wind speeds to TrueWind's modeled wind speeds are as follows:

	Across all Sites		At Individual Sites	
	California	Northwest	California	Northwest
Slope (ratio of observed speed to modeled)	0.62	0.57	+0.07 to +1.36	–0.15 to +1.40
Intercept (displacement of observed wind speeds relative to modeled)	2.36 m/s	2.77 m/s	–5.4 to +7.2 m/s	–2.8 to +8.2 m/s

Note: These coefficients do not match the average bias of the modeled dataset, which could be calculated by taking the difference of mean wind speeds and the ratio of standard deviations of the two sets. The values in this table are simply the parameters of the linear transformation of the modeled dataset that produces the smallest root mean squared error relative to the observation dataset.

speeds due to differences in location and time. For the Northwest, the TrueWind data match about 56 percent ($r=0.748$, $r^2=0.56$) of the variation in wind speed across locations and season-hours.

Table A-5. Comparison Statistics Between TrueWind Modeled Wind Speeds and Observed Wind Speeds

	Across all Sites	
	California	**Northwest**
Mean Absolute Error	1.63 m/s	1.56 m/s
Root Mean Squared Error	2.12 m/s	2.17 m/s
Correlation Coefficient	0.713	0.748

A.4.2.1 Variation in TrueWind Goodness of Fit on Different Time Scales

We also analyzed separately how TrueWind reflected the monthly or seasonal variation and diurnal variation relative to all anemometer sites. This is identical to the technique described in Section A.4.1.2 and presented in Table A-4, but correlation coefficients were now calculated for all sites together, instead of site-by-site. Table A-6 shows these correlation statistics. These statistics indicate how the TrueWind data matched the shape of the monthly/seasonal wind speed distribution as it varied from site to site, or the shape of the residual (mostly diurnal) distribution as it varied from site to site. To calculate these statistics, we first broke the full wind speed series into three components: the annual average wind speed for each site, the monthly or seasonal variation (consisting of the average wind speed for that site for that month or season, divided by the annual average for that site), and the residual variation (the average wind speed for each site, month/season and hour, divided by the previous two factors). We then compared the observed values and TrueWind's estimated values for each of these components, across the full dataset.

From Table A-6, we see that the TrueWind and anemometer datasets remain more closely matched on a seasonal or monthly basis than on a diurnal basis, even when all sites are considered together. However, when using this technique, the quality of fit for these monthly and seasonal means is reduced in both California and the Northwest, as compared to the results in Section A.4.1.2. This decrease in the quality of fit may be explained by the fact that this approach uses common fitting parameters for all the sites in each region, rather than allowing for an optimal fit at each site. There are only 12 months or 4 seasons to fit at each site, and these tend to have a fairly simple flat or single-humped shape for the year, so site-by-site fitting of the observations to even the simplest modeled curve could be expected to produce strong correlations, as it did in Section A.4.1.2. However, when the same linear fitting parameters must be used for all 78 or 102 sites, as was the case for Table A-6, then the correlation statistic shows how the TrueWind data reflect both the general shape of seasonal variation at each site, as well as the relative magnitude of this variation at different sites. There are more datapoints for the residual (diurnal) wind speed variation at each site than there are for the monthly or seasonal variation, but similar effects also apply for these data.

Table A-6. Correlation Between TrueWind Modeled Wind Speeds and Observed Wind Speeds on Seasonal and Diurnal Bases, for All Sites

	Correlation Coefficient, Across All Sites	
	California	**Northwest**
Per-Site Annual Wind Speed	0.510	0.713
Monthly or Seasonal Variation	0.872	0.860
Residual (Diurnal) Variation	0.736	0.606

A.5 Predictive Ability of Simple Averages of Observed Wind Speeds

To get a better idea of how well the TrueWind data match the anemometer-based variation in wind speeds between sites and times, we calculated some additional statistics on the dataset. These statistics were designed to show how much spatial and temporal "blurring" – or averaging – of the anemometer-based observation dataset it would take to produce wind speed estimates with the same quality of fit as the TrueWind data. We first compared averages of the wind speed observations over coarser time and space scales to the full observation dataset, to establish benchmarks for how much of the variation in the full dataset could be reflected in a more limited dataset. We then compared these benchmarks to TrueWind's estimation scores, to find out what level of averaging produced estimates with a similar fit to TrueWind's.

Table A-7 shows the correlation between the observed wind speeds and averages of those wind speeds taken at a coarser scale. The spatial scales used for these averages are listed in the leftmost column, and the time scales are shown in the top row. The value at the intersection of two scales is the correlation coefficient between the average wind speed observed at that temporal and spatial scale and the average wind speed observed for each site on a month-hour (or season-hour) basis (*i.e.,* the full dataset). So, for example, this table indicates that a simpler wind speed series consisting of only the 12 monthly means for each of the 78 sites in California achieved a correlation coefficient of 0.856 with the (12x24) month-hour means for those sites.

We also used the local area in which each anemometer was located (see Section 2.2.2) as an intermediate spatial scale for this averaging process. Table A-7 indicates, for example, that a wind speed series consisting of 12 monthly average wind speeds for each of the resource areas we identified in California was able to achieve a correlation coefficient of 0.752 when compared to the wind speeds for all sites and hours.

We calculated the average wind speed for the state or region for any time interval as the average of the wind speeds for all resource areas within that state or region during the same interval. This approach gives equal weight to each major wind resource area, rather than giving equal weight to each anemometer tower, which would have created a statewide average that was strongly influenced by the resource areas that happened to have the most measurement sites (*e.g.,* the Altamont Pass area near San Francisco or the Columbia Hills area on the Washington/Oregon border).

As discussed above (see Table A-5), the TrueWind wind speeds for each site and month-hour in California had a correlation coefficient of 0.713 with the observed wind speeds for the same sites and month-hours. From Table A-7, we can see that the TrueWind estimates are a closer fit than a

simple average of the measured wind speed for the whole year at each site (0.424), or a month-hour series averaged over the whole state (0.701), but fall short of what could be predicted by a set of monthly mean wind speeds for each resource area (0.752). For the Northwest, the TrueWind dataset had a correlation coefficient of 0.747 with the observation dataset, which is higher than could be achieved by any averaged series other than the seasonal average wind speeds for each site, or the season-hour wind speeds for each resource area.

Put another way, most of the variation in wind speeds can be predicted using only the average wind speed for the month or season of the year, for the general geographic area where a wind site is located, and the TrueWind data match the measured wind speeds with approximately this level of closeness.[33]

Table A-7. Correlation Between Observed Wind Speeds and Averages of Those Wind Speeds Taken at a Coarser Time or Spatial Scale

	California			Northwest		
	Year	Month	Month-Hour	Year	Season	Season-Hour
Multi-State Region				n/a	0.080	0.235
State	n/a	0.579	0.701	0.461	0.587	0.661
Resource Area	0.266	0.752	0.881	0.329	0.635	0.794
Site	0.424	0.856	1.000	0.702	0.921	1.000

Note: Each cell shows the correlation between an average of the observations taken on a particular space and time scale and the full series of month-hour or season-hour averages at all sites.

We also calculated a special average, which we called the "simple estimate" of wind speeds at each site. This is a temporal wind speed estimator that might be used in lieu of the intra-annual TrueWind data. It consisted of the annual average TrueWind wind speed for each site, multiplied by a set of weights reflecting the average temporal wind speed observed for each month-hour or season-hour for the whole region (California or the five states of the Northwest). Comparing this "simple estimate" of wind speed to the observed wind speeds for the same sites at the same time interval yielded a correlation coefficient of 0.694 in California and 0.562 in the Northwest. The TrueWind correlation coefficients of 0.713 and 0.747 indicate that the TrueWind data match the observed wind speeds somewhat more closely than this simple estimator.[34]

[33] This test is stacked against TrueWind, since the averages used for Table A-7 are calculated from the observations to which they are being compared, and are therefore the best possible coarser-scale predictor of those observations. But this table at least gives a sense of the amount of "blurring" of the observation data that produces results with an equivalent match to the TrueWind dataset.

[34] We also created a more finely tuned "local simple estimate," which combined the TrueWind annual wind speed for each site with temporal weights based on the observed wind speed at all sites in the same resource area, rather than the whole state or region. The local simple estimate matched observed wind speeds better than the TrueWind estimate for each site, achieving a correlation coefficient of 0.857 in California and 0.791 in the Northwest. This could be taken as an indication that it would be better to use weights based on the average wind speeds measured in each resource area, rather than the seasonal and diurnal weights provided by TrueWind, to develop a forecast of wind speeds. Or, going one step further, Table A-7 seems to indicate that it would be even better to use simple averages of the observed wind speed for each resource area, month and hour, and dispense with the TrueWind data entirely. However, since observational data are only available for certain areas, either of these approaches would leave us unable to analyze the wind resources across most of the region. Further, the high correlation between local

Again, we note that a mismatch between the TrueWind estimates and the anemometer data does not necessarily indicate inaccuracy in the TrueWind estimates. To the contrary, it may indicate that our relatively simple power-law scaling of the anemometer data (Section 2.3) is problematic, and that TrueWind estimates of 50 m and 70 m temporal wind patterns are superior to those generated from the anemometer data that we use here.

A.6 Contribution to Goodness of Fit from Finer-Scale TrueWind Data

We performed one more set of calculations to further evaluate the ability of the TrueWind data to predict site-to-site or hour-to-hour variations in wind speeds estimated from anemometers. In principle, the TrueWind wind speed estimates for each site for each month-hour or season-hour can be thought of as a set of estimates that start on a much coarser scale – *e.g.,* the annual average wind speed for the entire region – and then add in finer and finer detail to produce estimates that are custom-tailored to each site and hour. These coarser estimates can be inferred from the TrueWind wind speeds by averaging the site-by-site hourly wind speeds at a coarser scale. If the TrueWind estimates are a good fit to the measurements, then coarser averages of them should come as close as possible to capturing the amount of variability that is captured by a simple average of the wind speed observations with the same temporal and spatial resolution, as shown in Table A-7. (The means of the observations on each time and space scale are the best possible non-varying estimator of the observations on a finer space and time scale, so these set the upper limit for how much variation could be predicted using a coarser time-space series.) Further, the TrueWind estimates should more closely match the full set of site-by-site month-hour or season-hour observations as they move to a finer resolution.

To build Table A-8, we first calculated the TrueWind estimates of wind speeds for each month-hour or season-hour at each site. Then we averaged them to coarser time and space scales, using the same techniques used for the observation values when building Table A-7. Finally, we compared these coarser TrueWind estimates to the full set of anemometer-based observations for all sites and hours, and recorded the correlation coefficient.

Table A-8. Correlation Between Observed Wind Speeds and Averages of the TrueWind Wind Speeds Taken at a Coarser Time or Spatial Scale

	California			Northwest		
	Year	**Month**	**Month-Hour**	**Year**	**Season**	**Season-Hour**
Multi-State Region				n/a	0.080	0.197
State	n/a	0.466	0.551	0.452	0.592	0.641
Resource Area	0.238	0.688	0.710	0.322	0.606	0.737
Site	0.216	0.639	0.713	0.501	0.720	0.748

Note: Each cell shows the correlation between an average of the TrueWind wind speeds taken on a particular space and time scale and the full series of month-hour or season-hour observations at all sites.

wind speeds and observations at individual sites is due in part to the fact that the local averages are made up from the wind speeds at the individual sites to which they are being compared. This approach is guaranteed to produce excellent correlation scores if it is taken to a fine enough spatial scale.

Comparing Table A-8 to Table A-7, we can see that the TrueWind data match fairly well to the state-wide monthly average of observed wind speeds in California. For example, it is only possible to attain a correlation coefficient of 0.579 to the full set of observations by using statewide monthly means of the observational dataset (see Table A-7). The statewide monthly means of the TrueWind wind speeds for each observational site had a correlation of 0.466 with the full set of observations, so they matched most of the variation that was possible at this scale. The TrueWind estimates are also close when taken to a finer spatial scale, with monthly estimates for each resource area attaining a correlation coefficient of 0.688 with the full observation dataset. The monthly means of the observations themselves for each resource area (Table A-7) had a correlation coefficient of only 0.752 with the whole dataset, so the TrueWind data reflected most of the variation that could be captured at this scale as well. However, the TrueWind estimates of the California wind speed then move further away when taken to a finer spatial scale. The site-by-site monthly average of the TrueWind wind speeds is actually a worse estimator of the observed wind speeds than the resource-area monthly average is. This seems to indicate that the extra data provided by the model to make site-by-site wind speed estimates does not match the measured data. Three possibly overlapping possibilities may explain this reduction in the quality of the fit: (1) the TrueWind profiles may be inaccurate on a fine spatial scale; (2) spatial variations in wind shear may invalidate our estimates of the "measured" upper level wind speeds at each anemometer site (since we assumed the same wind shear at all locations); or (3) mismatches in the location of anemometer sites in the two datasets may allow the TrueWind data to match the general picture given by all the anemometers in each region, but interfere with the agreement when it comes to individual sites.

The TrueWind estimates for the Northwest are less problematic. They seem to move closer as they are taken from each coarser scale to a finer spatial or temporal scale, reflecting most of the variation that is possible to capture at each resolution.

A.7 Factors Affecting the Fit Between TrueWind and Anemometer Data

Finally, we investigated the conditions under which the TrueWind and anemometer datasets match well or poorly . We first identified several factors that might affect the fit between these datasets, and then used a multiple linear regression model to identify which of them were associated with better or worse fits.

To measure the goodness-of-fit between the TrueWind and anemometer data at each site, we calculated the year-round correlation coefficient between the two datasets' estimate of 70-meter elevation wind speeds. This is the same correlation coefficient as we showed in Figures A-1 and A-2. We then tested the following factors as explanatory variables for this goodness-of-fit marker:

- ***d_height:*** absolute value of the difference between the anemometer height and the TrueWind reference height (50m in the Northwest and 70m in California);
- ***cv_obsspeed:*** coefficient of variance of the observed speeds, indicating the amount of temporal variation found in wind speeds at each site, defined as stddev(v)/mean(v);

- ***summer_peak:*** a flag which is greater than zero for sites with summer-peaking winds and less than zero for winter peaking winds (defined from the anemometer data as $(v_{summer}-v_{winter})/v_{year}$);
- ***longitude:*** used to distinguish between coastal and inland sites**;**
- ***latitude:*** used to distinguish between California and Northwestern sites**;**
- ***region:*** a flag which distinguishes explicitly between California and the Northwest;
- ***source:*** a flag which distinguishes between data from Kenetech (KT), the DOE Candidate Site program (DOE) and the BPA Long-Term Wind Database (BPA); and
- ***month_count:*** the number of months during which anemometer data was collected at each site.

Of these, only *d_height, cv_obsspeed, source* and *longitude* were useful predictors for the goodness of fit between the anemometer and TrueWind data at any site. *Latitude* and *region* produced similar effects to each other in the regression analysis, and neither of them added significantly to our model once the previous four variables were included. *Longitude* and *summer_peak* were also strongly associated with each other, because coastal-mountain sites in our study area tend to have summer peaking winds, while inland sites have winter-peaking winds. *Longitude* had greater explanatory power, so we omitted the *summer_peak* variable from our model.

We also found that the 24 towers with the worst fit (correlation coefficient < 0.60) were resistant to explanation by any of these variables. These included all of the towers in the Tehachapi area, about half of the Rattlesnake Ridge, Ellensburg and San Diego towers, the single towers at Point Arena and Mountain Home, two of the Columbia Hills towers and the Kenetech tower in Kennewick. We treated these towers as outliers, and omitted them from our final regression model. They are shown in red on the regression plots below but were not used to calculate the trendlines shown.

The poor fit in some of these regions may be due to the limited resolution of the main numerical weather model used by TrueWind. This model had a resolution of around 2.5 km, which is not enough to fully resolve the geographic features in Tehachapi, San Gorgonio, Livingston and Mountain Home (Schwartz 2006). We were not able to test for this specific problem in our validation work.

Some of the outliers also appear to be due to data collection problems at individual towers, since nearby towers had much better fits to the TrueWind data (*e.g.,* in Ellensburg, Columbia Hills and Vansycle/Kennewick).

Figure A-5 plots the skill score for the TrueWind data (indicated by the correlation coefficient between the TrueWind and anemometer data series) for each anemometer tower, against the *d_height, cv_obsspeed, source* and *longitude* variables. For the third plot, we converted the *source* flag into a number by using the mean correlation coefficient for all towers from each data source – 0.711 for towers in the Candidate Site program, 0.817 for Kenetech towers and 0.837 for BPA long-term wind towers.

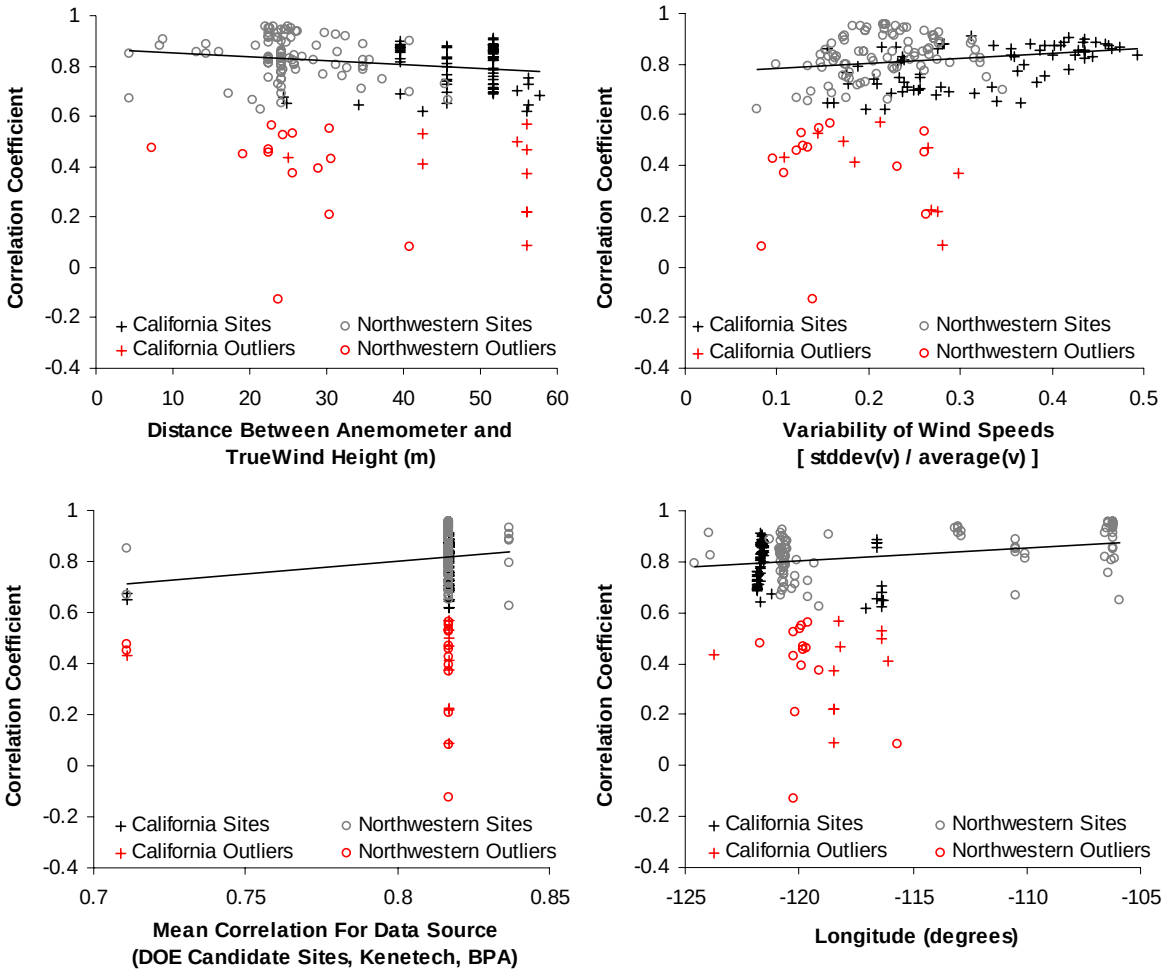

Figure A-5. Plots of TrueWind Skill Score Against Several Explanatory Variables

The TrueWind data match the anemometer data best at sites with anemometers close to the TrueWind height, sites with highly variable wind speeds, sites measured by the Kenetech or BPA anemometers, and sites further inland (with winter-peaking winds). These factors appear to produce counterbalancing differences between the California and Northwestern sites. In particular, California sites generally have anemometers further below the TrueWind reference height than in the Northwest[35], which would be expected to reduce the TrueWind skill score. However, the California sites also have stronger temporal wind patterns, and the TrueWind data

[35] As discussed in Section 2.2.1, TrueWind provided estimates of wind speeds at an elevation of 50 meters above effective ground level in the Northwest and 70 meters above effective ground level in California. The anemometers used for our validation were at an average height of 25.4 meters above ground level in the Northwest and only 21.8 meters above ground level in California. As a result, the California anemometers were typically about 50 meters below the elevation used for the TrueWind modeling, while the Northwestern anemometers were only about 25 meters below the TrueWind level.

appear to match these better. This effect seems to improve the TrueWind-anemometer correlation in California nearly to parity with the Northwest.[36]

The best fit of the TrueWind skill score (correlation coefficient) using all of these factors together is obtained by the model,

$$Cor = 1.35 - 0.00286 \cdot d\_height + 0.532 \cdot cv\_obsspeed + \begin{Bmatrix} source = BPA : +0.079 \\ source = KT : +0.047 \\ source = DOE : -0.126 \end{Bmatrix} + 0.00524 \cdot longitude \cdot$$

The predictions from this model are plotted against the actual TrueWind skill score in Figure A-6. In the final model, the p-value for each of these parameters was less than 0.0001. We found that this model explained about 41 percent of the variation in the TrueWind-anemometer correlation coefficients between different wind sites, after excluding outliers (i.e., $R^2 = 0.41$ for the best-fit line).

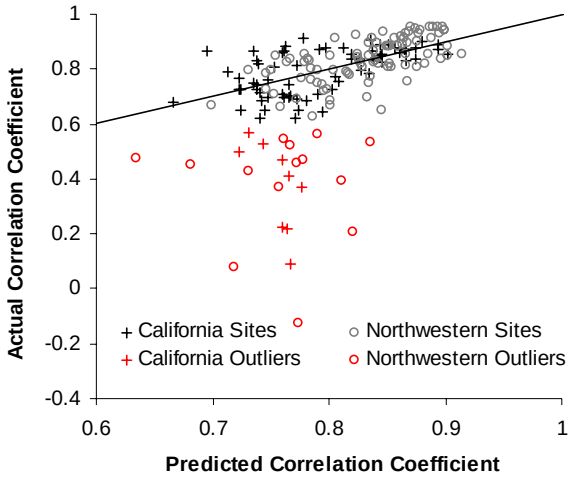

Figure A-6. Skill Score Predicted from *d_height, cv_obsspeed, source* and *longitude,* Excluding Outliers

From this analysis, we draw the following tentative conclusions:

- Anemometer measurements appear to converge toward the TrueWind values as the anemometer height approaches the TrueWind height. That is, the gap between the anemometer height and the TrueWind reference height has a significant effect on the match between TrueWind and anemometer data. In our anemometer dataset, this gap varies over a range of about 55m, which yields an expected variation in the TrueWind skill score of about 0.16. This suggests that much of the mismatch between these two datasets could be due to inaccuracy in our estimates of wind shear between the anemometer and reference height, and

[36] Earlier in our analysis, we tried using a constant wind shear exponent of 0.14 at all times. This appeared to introduce more shear-based mismatch than the 0.09/0.20 day/night approach we used for our final analysis, and as a result, TrueWind's skill score was distinctly lower for California sites than for Northwestern sites.

that the TrueWind data may provide a more accurate picture of upper-level wind speeds than the scaled anemometer data. Anemometers were placed further below the TrueWind height in California than in the Northwest, so this effect appears to reduce the quality of fit in California.

- TrueWind does well at matching the anemometer-based wind speed at sites with strong temporal patterns. The variation of about 0.4 in this parameter in our anemometer datasets yields an expected variation of about 0.21 between the most variable and least variable wind sites. California sites in our dataset have stronger temporal patterns than Northwestern sites, so this effect appears to improve the TrueWind skill score in California. This partly counterbalances the effect of the larger gap between anemometers and the TrueWind reference height in California. Wind variability does not appear to change significantly with longitude within California or the Northwest, so this effect does not mask the effect of longitude, discussed below.

- The TrueWind data match better to the BPA or Kenetech anemometers than to the DOE candidate site anemometers, even after controlling for tower height, variability of wind and other factors. There is a variation in skill score of about 0.21 between the Candidate Site and BPA anemometers, with the Kenetech anemometers falling in between. This effect may be due to some yet-unidentified geographic factor that makes the limited number of Candidate Site locations more difficult to model, or the BPA locations easier to model. Alternatively, it suggests that different data collections may have different quality, and some of the mismatch between TrueWind and anemometer data could be due to inconsistencies in the anemometer data.

- The TrueWind data matched the anemometer data more closely at sites further inland. Over the 20 degree longitude range of our datasets, this may explain skill score variation of about 0.10. This suggests that TrueWind is marginally better at matching the winter-peaking winds further inland, relative to the summer-peaking winds in coastal ranges.

- The TrueWind data were especially poorly matched to anemometer data in the Tehachapi, Rattlesnake Ridge and San Diego areas, even after controlling for other factors. This may be due to poor resolution in the TrueWind model, or some other form of modeling error. Unexplained poor fits were also found in Mountain Home and Point Arena, but with only one anemometer in each area, it is difficult to distinguish between modeling problems and bad anemometer data. Individual anemometers in some other resource areas were also poorly matched to the TrueWind data, but since neighboring anemometers were generally well-matched, this appears to be due to quality problems with the anemometer data.

References

Alawaji, S.H., N.N. Eugenio, U.A. Elani. 1996. "Wind Energy Resource Assessment in Saudi Arabia: Part II: Data Collection and Analysis." *World Renewable Energy Conference, 1996.*

Archer, C. and M. Jacobson. 2003. "Spatial and temporal distributions of U.S. winds and wind power at 80 m derived from measurements." *Journal of Geophysical Research,* 108 (D9), 4289.

Bolinger, M. 2005. Lawrence Berkeley National Laboratory. Personal communication, February 5, 2005.

Borenstein, S. 2005. *Valuing the Time-Varying Electricity Production of Solar Photovoltaic Cells.* Center for the Study of Energy Markets Working Paper #142, University of California Energy Institute, Berkeley. March.

BPA. 2005. Data supplied via e-mail from Bonneville Power Administration. January 19 and October 21.

Brower, M. 2002a. *New Wind Energy Resource Maps of California.* Contract #500-01-009, California Energy Commission, Sacramento. November.

Brower, M. 2002b. *Wind Resource Maps of the Northwest and Wyoming*. Agreement # NWCDC-2001-01 and Agreement # NWCDC-2001-02, Northwest Cooperative Development Center. October.

Brower, M. 2005. Personal communication. July 16.

Elliott, D. and M. Schwartz. 1993. *Wind Energy Potential in the United States*. PNL-SA-23109. NTIS no. DE94001667. Northwest Laboratory, Richland, WA. Available on-line at http://www.nrel.gov/wind/wind_potential.html.

Elliott, D., C. Holladay, W. Barchet, H. Foote, and W. Sandusky. 1986. *Wind Energy Resource Atlas of the United States.* DOE/CH 10093-4, Solar Energy Research Institute, Golden, Colorado. Available on-line at http://rredc.nrel.gov/wind/pubs/atlas/.

Emeis, S. 2001. "Vertical variation of frequency distributions of wind speed in and above the surface layer observed by sodar." *Meteorologische Zeitschrift,* 10 (2), 141-149 .

EPA. 2000. *Meteorological Monitoring Guidance for Regulatory Modeling Applications.* EPA-454/R-99-005. U.S. Environmental Protection Agency, Washington, DC.

Farrugia, R.N. 2003. "The wind shear exponent in a Mediterranean island climate." *Renewable Energy,* 28 (2003), 647–653

FERC. 2005. "Form 714 Data." Federal Energy Regulatory Commission, Washington, DC. Available on-line at http://www.ferc.gov/docs-filing/eforms/form-714/data.asp. Accessed September 29, 2005.

Gipe, P. 1995. *Wind Energy Comes of Age.* John Wiley and Sons, Inc., New York.

Gipe, P. 2004. *Wind Power: Renewable Energy for Home, Farm and Business.* Chelsea Green Publishing Company, White River Junction, VT.

Gopal, J., J. Grau, K. Kennedy, L. Marshall, J. McKinney, M. Rudman, R. Tavares, D. Vidaver. 2003. *Electricity and Natural Gas Assessment Report*. 100-03-014F, California Energy Commission, Sacramento, CA. Available on-line at http://energy.ca.gov/reports/100-03-014F.PDF.

Guey-Lee, L. 2001. "Forces Behind Wind Power," in *Renewable Energy 2000: Issues and Trends*. DOE/EIA-0628(2000), U.S. Department of Energy, Washington, DC. Available on-line at http://www.eia.doe.gov/cneaf/solar.renewables/rea_issues/.

Jackson, K.. 2002. *Wind Power Generation Trends.* Report Number CWEC-2003-01, California Wind Energy Collaborative, sponsored by the California Energy Commission.

Kahn, E. 1991. *Electric Utility Planning and Regulation*. American Council for an Energy-Efficient Economy. Washington, D.C.

Karl, T., C. Williams, Jr., F. Quinlan, and T. Boden. 1990. *United States Historical Climatology Network (HCN) Serial Temperature and Precipitation Data.* Publication No. 3404, Environmental Science Division, Carbon Dioxide Information and Analysis Center, Oak Ridge National Laboratory, Oak Ridge, TN. Data available online at http://lwf.ncdc.noaa.gov/oa/climate/research/ushcn/ushcn.html.

King, J. 2005. Northwest Power Planning and Conservation Council. Personal communication, September 8.

Kirby, B., M. Milligan, Y. Makarov, D. Hawkins, K. Jackson and H. Shiu. 2003. *California Renewables Portfolio Standard Renewable Generation Integration Cost Analysis, Phase 1.* CWEC-2003-06. Davis, California: California Wind Energy Collaborative.

Kirchhoff, R.H., and F.C. Kaminsky. 1983. "Wind Shear Measurements and Synoptic Weather Categories for Siting Large Wind Turbines." *Journal of Wind Engineering and Industrial Aerodynamics,* 15 (1983), 287-297.

Klein, J. 2004. California Energy Commission. Personal communication, March 2004.

Mahrt, L. 1981. "The Early Evening Boundary Layer Transition." *Quarterly Journal of the Royal Meteorological Society,* 107 (1981), 329-343.

Mainzer, E. 2003. Bonneville Power Administration. Personal communication, June 2003.

Martner, B.E., and J.D. Marwitz. 1982. "Wind Characteristics in Southern Wyoming." *Journal of Applied Meteorology,* 21, 1815-1827.

Meyer, T., and Luther, J. 2004. "On the correlation of electricity spot market prices and photovoltaic electricity generation," *Energy Conversion and Management,* 45, 2639-2644.

Milligan, M. 2002. *Modeling Utility-Scale Wind Power Plants Part 2: Capacity Credit*. NREL/TP-500-29701. Golden, Colorado: National Renewable Energy Laboratory.

Milligan, M. 2003. National Renewable Energy Laboratory. Personal communication, November 7, 2003.

Milligan, M. 2004. National Renewable Energy Laboratory. Personal communication, March 12, 2004.

Milligan, M. and K. Porter. 2005. "Determining the Capacity Value of Wind: A Survey of Methods and Implementation." WINDPOWER 2005. Denver, Colorado, May 15-18.

OWPI. 2003. "April 2002 to March 2003 Wind Summary: Hobart's KTJS Tower Sensors at 40, 70, and 100 m." Oklahoma Wind Power Initiative.

OWPI. 2004. "Annual Wind Summary: Fred Factory Tower (Blaine Co.) 10m and 20 m sensor heights." Oklahoma Wind Power Initiative.

Perez, I.A., M.A. Garcia, M.L. Sanchez, and B. de Torre. 2005. "Analysis and parameterisation of wind profiles in the low atmosphere." *Solar Energy* 78 (2005), 809–821.

Peterson, E.W., and J.P. Hennessey. 1978. "On the use of power laws for estimates of wind power potential." *Journal of Applied Meteorology,* 17 (3), 390-394.

Rehman, S., and N.M. Al-Abbadi. 2005. "Wind shear coefficients and their effect on energy production." *Energy Conversion and Management,* 46 (2005), 2578–2591.

Schwartz, M. 2006. National Renewable Energy Laboratory. Personal communication, January 23, 2006.

Sisterson, D.L. and P. Frenzen. 1978. "Nocturnal boundary-layer wind maxima and the problem of wind power assessment." *Environmental Science and Technology,* 12 (2), 218-221.

Sisterson, D.L., B.B. Hicks, R.L. Coulter, and M.L. Wesely. 1983. "Difficulties in Using Power Laws for Wind Energy Assessment." *Solar Energy,* 31 (2), 201-204.

Smith, K. and Jurotich, T. 2004. "Big Spring Wind Power Project Third- through Fifth-Year Operating Experience: 2001-2004." U.S. Department of Energy – EPRI Wind Turbine Verification Program.

Smith, K., G. Randall, and D. Malcolm. 2002. "Evaluation of Wind Shear Patterns at Midwest Wind Energy Facilities." *American Wind Energy Association (AWEA) WINDPOWER 2002 Conference*.

TrueWind Solutions, LLC. 2002. *TrueWinds: New York Wind Map.* Available on-line at http://truewind.teamcamelot.com/ny/.

UCEI. 2004. "Day-Ahead Zonal Prices." U.C. Energy Institute. Database available on-line at http://www.ucei.berkeley.edu/CSEM/datamine/datamine.htm. Accessed May 27, 2004.